A dissertation for the Degree of Doctor of Philosophy

The Molecular Mechanisms of c-MYC and REX1 for Proliferation and Differentiation in Adult Stem Cells

성체줄기세포의 분화와 증식에관한 c-MYC 과 REX1 의 분자 생물학적 메커니즘 연구

By

Dilli Ram Bhandari

August 2011

Department of Veterinary Public Health,

College of Veterinary Medicine,

Graduate School of Seoul National University

ABSTRACT

The Molecular Mechanisms of c-MYC and REX1 for Proliferation and Differentiation in Adult Stem Cells

Dilli Ram Bhandari, B.V.Sc. &A.H., MS

Department of Veterinary Public Health

College of Veterinary Medicine

Graduate School of Seoul National University

Supervisor: **Kyung-Sun, Kang, D.V.M., Ph.D.**

c-MYC and REX1, the transcription factors, are considered as pluripotent markers genes in embryonic stem cells. They have multiple functions in cell proliferation, differentiation and cellular transformations in stem cells including mesenchymal stem cells (MSCs). Molecular mechanistic studies through histone modification for c-MYC and p38 MAPK signal pathways for

REX1 are performed in MSCs. Lentiviral vector based gene knock-down studies were performed for c-MYC and REX1 as well as lenti-viral vector system based c-MYC over expression also done. Cell proliferation and differentiation status was dramatically decreased in c-MYC knocked-down cells; however it was improved in c-MYC over-expression cells. Cell proliferation status in REX1 inhibited cells was found to be similar as of c-MYC, but more adipogenic positive cells were found in REX1 inhibited cells. On the other hand, osteogenic differentiation was dramatically decreased in REX1 inhibited cells. The results of RT-PCR and Western blot showed the regulatory role of c-MYC over HDAC2 and polycomb group (PcG) genes. Similar studies of REX1 showed the inverse relation between the expressions of REX1 and MKK3, upstream activator of p38 MAPK. Finally, they were confirmed as cell fate determinants for proliferation and differentiation in human MSCs. Chromatin immuno-precipitation assay confirmed that c-MYC bound in *HDAC2* and REX1 bound in *MKK3* directly. From this study, it is concluded that c-MYC has influential role for cell proliferation and differentiation via chromosomal modification, and REX1 plays similar role through p38 MAPK signal pathways in human adult stem cells.

Keywords: c-MYC, Differentiation, HDAC2, Proliferation, REX1, Stem cells

Student number: 2007-30701

Table of Contents

List of Figures

List of Tables

ABBREVIATION

AD-MSC: adipose tissue derived mesenchymal stem cell

AE-SC: amniotic epithelial stem cell

ASC: adult stem cell

BM-MSC: bone marrow derived mesenchymal stem cell

CPDL: cumulative population doubling level

CX36:   connexin 36

EBM2:   endothelial cell basal medium-2

GVDH: graft-versus-host-diseases

HDAC: histone deacetylase

hUCB-MSC: human umbilical cord blood derived mesenchymal stem cells

IPCs: insulin producing cells

MAPK: mitogen activated protein kinase

PcG: polycombcomb group

UC-MSC: umbilical cord derived mesenchymal stem cell

VC: vector control

WJ-MSC: wharton's jelly derived mesenchymal stem cell

LITERATURE REVIEW

Cell proliferation and differentiation determine the expression level of c-MYC and REX1 in Adult stem cells

Introduction

Stem cells, characterized by the ability to both self-renew and differentiate into various functional cell types, have been derived from the embryo and various sources of postnatal animals (Jaenisch and Young, 2008). MSCs have been isolated from bone marrow, adipose tissue, peripheral blood, fetal liver, lung, amniotic fluid, chorionic villi of the placenta and umbilical cord blood (Campagnoli et al., 2001; Erices et al., 2000; Gronthos et al., 2001; Igura et al., 2004; Tsai et al., 2004; Zvaifler et al., 2000). MSCs are promising tools for regenerative medicine. These cells can be differentiated into fibroblasts, adipocytes, osteoblasts, chondrocytes (Prockop, 1997), tendinocytes, ligamentocytes (Pittenger et al., 2002), cardiomyocytes (Makino et al., 1999), neuronal cell (Phinney and Isakova, 2005; Tropel et al., 2006); and other cells (Bhatia and Hare, 2005).

c-MYC and REX1 are two core transcription factors having critical role to maintain self renewal in embryonic stem cells (Cartwright et al., 2005; Rahl et al., ; Ben-Shushan et al., 1998). The c-MYC is a well known nuclear proto-oncogene having multiple functions in cell proliferation, differentiation, cellular transformation, apoptosis, as well as in cellular reprogramming (Singh and Dalton, 2009; Meyer and Penn, 2008). It is found in 20% of human cancers (Dang et al., 2006) and is also a critical factor for reprogramming of cells (Sridharan et al., 2009). REX1 is a well known embryonic stem (ES) cell marker (Ben-Shushan et al., 1998). It was identified for the first time in 1989, the expression level of REX1 decreased dramtically during differentiation of mouse F9 teratocarcinoma cells by retinoic acid (Hosler et al., 1989). It's expression is widely found in many stem cells both embryonic and adult stem cells (Mongan et al., 2006) as well as in placenta and spermatogenesis (Rogers et al., 1991).

Purpose of the study

From the literatures, it is found that the role of c-MYC and REX1 are studied in embryonic stem cells and cancers. Recently the study on the role of these transcription factors for cell proliferation and differentiation in adult stem cells was performed. For this, c-MYC and REX1, inhibition study was done by making small hairpin RNA (shRNA) for c-MYC and REX1 as well as c-MYC over-expression study was also performed.

Role in cell Proliferation

c-MYC is a global transcription regulator (Meyer and Penn, 2008). It can bind with 10-15% of human genome and regulate genes expression in different fields including cell cycle. c-MYC was reported to be well expressed in all proliferative cells. In mammalian cells, cell cycle enhances by the activation of cyclin dependent kinases and the regulatory cyclins (Zornig and Evan, 1996) and their expression level are the indicators of proliferation (Dang et al., 2006). Hyper-phosphorelated form of retinoblastoma (PpRb) protein can enhance cell cycle progression from G1 phase to S phase of cell cycle (Zornig and Evan, 1996; Steiner et al., 1995). Cell cycle progression/proliferation also depends on the expression level of cyclin dependent kinase inhibitors (p21, p27, and P57) proteins (Meyer and Penn, 2008; Obaya et al., 1999; Zornig and Evan, 1996). These inhibitors can bind the CDK/cyclins complex *in vitro* and inhibit the expression of CDKs, at the same time the expression of CDK inhibitors (p21, p27and p57) upregulated (Obaya et al., 1999; de Alboran et al., 2001; Xiong et al., 1993). Our present study indicated that the cell were arrested in G0/G1 phase as a result CDK4 and PpRb protein expression was found to be down regulated in c-MYC inhibited cells, however CDK inhibitors p21 and p27 were found to be up regulated. On the other hand in c-MYC over-expression cells the expression pattern was found to be vice versa than of c-MYC inhibited cells.

Cell proliferation status of hUCB-MSC was normal before knocked-down of REX1 in hUCB-MSC, which was dramatically arrested at G0/G1 phase of cells after REX1 knocked-down. For the continuation of cell cycle, activation of CDK and cyclins were required for G1/S transition ((Nigg, 1995; Murray, 2004). Cyclin E, in association with CDK2, is required for the G1/S transition. In our study, CDK2, CCND1 and CCNB1 down regulated in REX1 inhibited cells. Similar result was reported in REX1 double knock-out mES cells (Scotland et al., 2009). MKK3 is the upstream target of p38 activator, which was up-regulated after REX1 knocked-down in hUCB-MSC as a result over-expressoin of Pp38 was found in hUCB-MSC. Active form of p38 MAPK inhibits the cell cycle progression in G1/S phase (Molnar et al., 1997; Ono and Han, 2000) was already reported. Our studies showed the inverse relation of REX1 and MKK3 expression might play the influencing role on cell proliferation in human adult stem cells.

Role in cell differentiation

Differentiation ability is a fundamental characteristic of stem cells, which depends on the microenvironment of the stem cells. Genetic manipulation is also one of the influential factor for differentiation. c-MYC has inhibited the cell differentiation in varieties of cells (Selvakumaran et al., 1996; Canelles et al., 1997; van de Wetering et al., 2002; Cartwright et al., 2005). However, c-MYC has induced differentiation ability in epidermal stem cell (Frye et al., 2007) through histone modification. In hES cells in feeder

free culture condition, activation with c-MYC enhances the differentiation (Sumi et al., 2007) and v-MYC transfected hBM-MSC could differentiate into neural cells (Nagai et al., 2007). In some cancer cells c-MYC down regulation induce the differentiation (Meyer and Penn, 2008; Dang et al., 2006) and normal c-MYC expression enhances the cell proliferation. Our study showed in hUCB-MSC osteogenic and adipogenic differentiation ability was deteriorated in c-MYC knocked-down cells and improved in c-MYC over-expression cells. Based on the different studies, differentiation role of c-MYC is found variable case by case even in stem cells.

REX1 expression is regulated by the expression of other pluripotent markers genes Oct4, Sox2 and Nanog (Niwa et al., 2000; Shi et al., 2006). ESCs study from REX1 knock-out mice showed defect in the induction of a subset of marker genes of the visceral endoderm suggested that REX1 plays an important role in ESC differentiation (Masui et al., 2008). REX1 expression is found in undifferentiated mesenchymal stem cells (Lamoury et al., 2006). Osteogenic and adipogenic differentiation efficiency is increased in the presence of OCT4, REX1 and Gata-4, in human mesenchymal stem cells (Roche et al., 2007). Differentiation study was performed after REX1 inhibition in hUCB-MSC for osteogenesis and adipogenesis. hUCB-MSCs were differentiated into osteogenic cells but in REX1 inhibited cells it was deteriorated than control cells. However, REX1 inhibition showed slight improvement in the adipogenesis, it might be because of activated form of p38 MAPK (Engelman et al., 1998). It was already reported that neural cell

6

differentiation could be seen in REX1 inhibited/p38 activated hUCB-MSC cells (Morooka and Nishida, 1998). Activation of p38 MAPK is important for the differentiation of mouse ESCs (Chakraborty et al., 2009) and hMSCs (Platt et al., 2009). REX1 knockout mES cells differentiate in to parietal endoderm in the presence of retinoic acid (Thompson and Gudas, 2002) rather than primitive endoderm and visceral endoderm. Janus kinase (JAK) is highly inhibited by REX1 in mES cells which is the transducer and activator of STAT3 path way, can modulate the differentiation of F9 cells (Xu et al., 2008).

Conclusion:

In summary, the normal expression of c-MYC and REX1 is found in all proliferative stem cells. Lentivirus based knocked-down study revealed the dramatic reduction of their proliferative and differentiation status of c-MYC gene manipulated cells. However, over-expression of c-MYC could improve the cell proliferation in hUCB-MSC. REX1 inhibited cells also arrested same as c-MYC inhibited cells. Osteogenic and adipogenic differentiation ability of REX1 inhibited cells was found different than c-MYC gene manipulated cells. The differentiation potentialities of c-MYC and REX1 depend on the target lineages and source of stem cells.

CHAPTER I

The regulatory role of c-MYC on HDAC2 and PcG expression in human multipotent stem cells

1.1 INTRODUCTION

Stem cells, characterized by the ability to both self-renew and differentiate into various functional cell types, have been derived from the embryo and various sources of postnatal animals (Jaenisch and Young, 2008). MSCs are promising tools for regenerative medicine. MSCs have been isolated from bone marrow, adipose tissue, peripheral blood, fetal liver, lung, amniotic fluid, chorionic villi of the placenta and umbilical cord blood (Campagnoli et al., 2001; Erices et al., 2000; Gronthos et al., 2001; Igura et al., 2004; Tsai et al., 2004; Zvaifler et al., 2000). These cells can be differentiated into fibroblasts, adipocytes, osteoblasts, chondrocytes(Prockop, 1997), tendinocytes, ligamentocytes (Pittenger et al., 2002), cardiomyocytes (Makino et al., 1999), neuronal cell (Phinney and Isakova, 2005; Tropel et al., 2006) and other cells (Bhatia and Hare, 2005).

Myc is a transcription factor of the basic helix-loop-helix-leucine zipper (bHLH-LZ) family that can activate or repress gene expression. The c-MYC proto-oncogene has emerged as a critical regulator of cell growth and is one of the genes most frequently altered in cancer (Grandori et al., 2000). Myc has generally been associated with the promotion of cellular growth and proliferation, desensitization to growth-inhibitory stimuli, blockade of cell differentiation, cellular immortalization and oncogenic transformation (Adhikary and Eilers, 2005).The biochemical mechanism of Myc-mediated trans-activation has revealed a wide range of effects on chromatin and basal

transcription (Cowling and Cole, 2006). MYC proteins are also required for the widespread maintenance of active chromatin (Knoepfler et al., 2006). The activation of c-MYC in ESCs induces apoptosis and differentiation into extraembryonic endoderm and trophectoderm lineages while concomitantly reducing expression of OCT4 and NANOG (Sumi et al., 2007). Myc can positively regulate proliferation in normal cells and cause genomic instability in tumors by controlling DNA replication (Dominguez-Sola et al., 2007). The permanent and stable human MSC line generated by transfecting the v-myc gene can be differentiated into neural cell types, including neural stem cells, neurons, astrocytes and oligodendrocytes (Nagai et al., 2007). Over-expression of c-MYC strongly drives proliferation and growth but also sensitizes cells to apoptosis and senescence (Grandori et al., 2000).MYC suppresses expression of cell cycle/growth arrest genes gas1, p15, p21, p27 and others, directly, by at least two mechanisms (Gartel and Shchors, 2003). Decreased c-Myc binding to Sp1 transcriptional complexes in the p21 promoter results in reduced p21 repression (Wang et al., 2008).

Mammalian HDACs comprise a multiprotein family of zinc metallohydrolases that share a conserved catalytic center. There are four classes of HDACs in mammals: class I consist of proteins homologous to yeast Rpd3 (e.g., HDAC1, 2, 3 and 8) and class II (HDAC 4-7, 9 and 10) consists of proteins homologous to yeast Hda1. Class III consists of the homologs of Sir2 in the yeast S. cerevisiae and Class IV consists of HDAC11 (Gao et al., 2002). HDACs exist in multiprotein complexes with transcription

factors, DNA binding proteins and other chromatin modifying enzymes. Deacetylation of histones reseals the chromosomal package, leading to a repression of transcription (Wolffe, 1997). Class I HDACs 1, 2 and 3 interact with components of the p53 and RB tumor-suppressor pathways (Brehm et al., 1998; Wade, 2001), suggesting their direct involvement in growth control. The over-expression of class I HDACs is well correlated with cancer tissues including stomach, esophagus, colon, prostate, breast, ovary, lung, pancreas and thyroid (Nakagawa et al., 2007). Increased HDAC2 expression is associated with colon cancer depending on the Wnt pathway and c-Myc (Zhu et al., 2004). The activity of HDAC 1, 2 and 3 inhibits differentiation of ESCs to oligodendrocyte, astrocytes and neurons, respectively (Humphrey et al., 2008).The treatment of HDAC inhibitor suppresses c-MYC expression.

The Polycomb group (PcG) genes were initially identified as regulators of homeotic genes, master developmental regulators that participate in defining the blueprint for Drosophila's body plan. The identification of similar PcG genes and numerous paralogs in vertebrates raised the intriguing possibility that they may perform similar functions. In vertebrates, PcG proteins assemble into two discrete chromatin-associated complexes, which have been recently characterized (Kuzmichev et al., 2002; Valk-Lingbeek et al., 2004; Levine et al., 2002). In human, the first complex, referred to as Polycomb Repressive Complex 1 (PRC1), includes at least one paralog of the PCGFs, RING1, RING2, PHCs and CBXs components, whereas the second complex, named PRC2, which includes EED, EZHs and SUZ12. YY1, YY2

and SCML1 are PcG members which are not included in PRC1 and PRC2 groups. PcG genes are also implicated in regulation of stem cell self-renewal and in cancer development (Rajasekhar and Begemann, 2007). Myc-induced chromatin modifications play a major role in Myc-induced exit from the epidermal stem cell niche (Frye et al., 2007). c-MYC is structurally related to two other genes, l- and n-MYC, the expression of which has not been investigated in MSCs. The function of c-MYC has been extensively investigated in cancer cells but not in human adult stem cells, even though they have relatively high expression compared with normal cells and ESCs.

In this study, we hypothesized that c-MYC could regulate cell proliferation positively and differentiation negatively, not only by direct regulation of cell cycle regulating genes, but also by regulating chromosomal modification genes in human adult stem cells. To test this hypothesis, the transcriptional and translational changes of chromosomal modifying genes, controlled by c-MYC expression, were investigated using gene knock-down and over-expression techniques mediated by a lenti-viral vector system in hUCB-MSCs, hAD-MSCs and hBM-MSCs.

1.2 MATERIALS AND METHODS

1.2.1 hMSC isolation and culture and FACS analysis

hUCB-MSCs, hBM-MSCs and hAD-MSCs were isolated and cultured as previously described (Seo et al., 2009; Park et al., 2008; Gnecchi and Melo, 2009). In brief, two clones of hAD-MSCs were isolated from freshly excised mammary fat tissue acquired from the Ba-Ram plastic surgery hospital. Tissues were obtained from 20 to 30 year-old women during reduction mammoplasty. The hAD-MSCs were maintained in K-SFM medium, supplemented with 5% FBS, 2 mM N-acetyl-L-cysteine (Sigma-Aldrich, St. Louis, MO, USA) and L-ascorbic acid (0.2 mM, Sigma-Aldrich). hBM-MSCs were isolated from three healthy donors and were cultured in low glucose Dulbecco's Modified Eagle's Medium (DMEM) supplemented with 10 % fetal bovine serum (FBS) without any additional growth factors. hUCB-MSCs were obtained from umbilical cord blood immediately after full term delivery with written consent from 20 to 30 year-old mothers and the approval of the Boramae Hospital Institutional Review Board (IRB). The hUCB-MSCs were maintained in DMEM (Invitrogen, Carlsbad, USA) containing 10% FBS. The passages (p) of hMSCs used for the experiments were p5 in hUCB-MSCs, p5 in hAD-MSCs and p3 in hBM-MSCs. The isolation and research use of hAD-MSCs and hBM-MSCs were also approved by the Boramae Hospital IRB with written consent. All procedures were approved by the institutional review board of Seoul National University (UCB-MSC, #0603/001-002; AD-

MSC, #0600/001-001; BM-MSC, #0910/001-003). To analyze cell surface marker expression in hUCB-MSCs, Fluorescence-Activated Cell Sorting (FACS) Aria was used (Becton & Dickinson, Franklin Lakes, NJ). Antibodies were conjugated to CD29-phycoerythrin (PE), CD31-PE, CD33-PE, CD34-fluorescein isothiocyanate (FITC), CD44-PE, CD45-FITC, CD73-PE, CD90-PE, CD105-FITC, CD133-PE and HLA-DR-FITC (Abcam, Cambridge, UK).

1.2.2 Gene construction and production of lentivirus vectors

The lentivirus was generated using the ViraPowerTM Lentiviral Packaging Mix (Invitrogen, Carlsbad, CA, USA). Lipofectamine 2000 (Invitrogen) was used for transfection of small hairpin RNA of c-MYC (ShM1, TRCN0000039641; ShM3, TRCN0000039640) and vector control (SHC002) (Sigma, Saint Louis, MO, USA) to 293FT cells (Invitrogen). Cell culture medium was changed the day after transfection and the supernatant was harvested at 48 and 72 hours after transfection. The viral supernatant was filtered using 0.4μm pore filters (Invitrogen). Cells were transfected with lentivirus at a multiplicity of infection (MOI) of 10. Polybrene (Sigma) was added to the cell culture media at a final concentration of 6μg/ml. The cell culture medium was changed with fresh culture medium the day after transfection. For selection, puromycin was added to the cell culture medium at a final concentration of 10μg/ml for 3 days. The full coding region of c-MYC was cloned into the pLenti6/V5-D-TOPO vector (Invitrogen) and the lentivirus was made using the same protocol as in the inhibition study for c-

MYC over-expression. For selection, blasticidin was added to the cell culture media at a final concentration of 5µg/ml for 5 days.

1.2.3   Small interfering RNA (siRNA) transfection

Chemically synthesized siRNA of HDAC2 (cat. # L-003495-00) and vehicle control non-targeting RNA (cat. # D-001210-05) were purchased from Dharmacon RNA Technologies (Lafayette, CO, USA). Transfections were performed according to the manufacturer's instruction. In brief, cells were maintained in a culture dish at a confluence of 40-50%. Transfection complexes were prepared in serum and antibiotic-free medium and 20nM siHDAC2 was used for transfection. After transfection, cells were incubated in 5% CO_2 incubator at 37ºC for 48-96 hours for the RNA and protein expression studies.

1.2.4   Cell proliferation and cell cycle analyses

Three days after virus transduction, cells were seeded in 24-well plates and incubated for 2 days. After incubation, 20µl of 3-(4,5-dimethylthiazol-2-yl)-2,5-diphenyltetrazolium bromide (MTT) stock solution (5mg/ml, Sigma, St Louis, Missouri, USA) was added to each well and the plates were further incubated for 4 hours at 37°C. The supernatant was removed and 200µl of dimethyl sulfoxide was added to each well to solubilize the water-insoluble purple formazan crystals. The optical density was measured at a wavelength of 540nm in an enzyme-linked immunosorbent

assay plate reader (EL800, Bio-Tek Instruments Inc., Winooski, VT, USA). All measurements were performed in triplicate. For the cumulative population doubling level (CPDL) assay, 1×10^5 virus-infected cells were cultured in a T-75 flask and the cell numbers were counted after 4-5 days. Similarly for successive passages, the same numbers of cells as before were sub-cultured and counted after 4-5 days.

Cell cycle was detected using flow-cytometry. For this cells were washed twice with PBS and harvested by trypsinization 3 days after transfection. The cells were then washed again with PBS and fixed with 70% ethanol at -20°C for 1 day. The fixed cells were washed with ice cold PBS and stained with 50µg/ml of propidium iodide (Sigma) in the presence of 100µg/ml RNase A (Sigma) for 30 minutes. The cell cycle was analyzed using the FACS Calibur (Becton & Dickinson, NJ, USA).

1.2.5 RT-PCR

Total RNA was extracted with an easy-spin™ Total RNA Extraction Kit (iNtRON biotechnology, Sungnam, Korea) according to the manufacturer's instructions. cDNA synthesis was carried out using the SuperScript® III First-Strand Synthesis System for RT-PCR (Invitrogen) with 1µg total RNA and oligo dT. Primers for each gene are shown in the Table 1. Gene expression was also analyzed using real-time PCR with SYBR Green Master Mix reagents (Applied Biosystems, Foster City, CA, USA). The mRNA expression level of c-MYC and other genes were normalized with the

expression level of glyceraldehyde 3-phosphate dehydrogenase (GAPDH). Real-time RT-PCR was performed with a LightCycler 489 Real-Time PCR System (Roche, Indianapolis, IN, USA). In this study, three independent hUCB-MSCs clones isolated from three independent individuals were used.

Table 1 PCR primers used in c-MYC study

HUMAN MRNA	FORWARD (5'….3')	REVERSE (5'….3')
BMI1	TGCTGATGCTGCCAATGG	TTACTTTCCGATCCAATCTG
c-MYC	CAGCTGCTTAGACGCTGGATTT	ACCGAGTCGTAGTCGAGGTCAT
EED	CCAGACGGACACTCTGGTGG	CACCCAAAAGATCATAATCA
EED4	AACCATTGTTTGGAGTTCAG	GGATTTCTCCTTGTGAATGA
EZH1	CAATGAAGAATGGAAGAAGC	ATATTGCACAAAACCGTCTC
EZH2	ATTGGGACCAAAACATGTAG	TGTATCTTTCTGCAGTGTGC
GAPDH	GAGTCAACGGATTTGGTCGT	GACAAGCTTCCCGTTCTCAG
HDAC1	ATCGGTTAGGTTGCTTCA	TCATTCGTGTTCTGGTTAGTC
HDAC2	GACAGTGGAGATGAAGATGGA	TTCTGATTGGTTCCTTTGG
HDAC2 promoter	GAAAACTAGGCTACCAGGCAC	TCGTAGCCTTGGCGGTCT
HDAC3	CTGGCTTCTGCTATGTCAAC	ACATATTCAACGCATTCCCCA
HDAC4	TACATGTCCCTCCACCGCTAC	AGCCATGTTGACGTTGAAACC
HDAC5	GTAGCCATCACCCAAAACT	GTCCTCCACCAACCTCTTCA
HDAC6	CAACTGAGACCGTGGAGAG	CCTGTGCGAGACTGTAGC
HDAC8	ACGGGCCAGTATGGTGCAT	GCCCTCTTGGCTGACCTTCT
l-MYC	CCCAAAGTAGTGATCCTAAGCAA	TGTCCAGACTGTCCCACCATA
MEL18	GTACTTCATCGACGCACCACTATC	CTCGTCCTCGTACAGAACCTCCA
n-MYC	CCGATGCTTCTAACCCAG	CATCCAGAGGTCTTGTTCC
OCT4	TGTCTCCGTCACCACTCT	TTCCCAATTCCTTCCTTA
P21	TTAGCAGCGGAACAAGGAGT	AGCCGAGAGAAAACAGTCCA
P27	AGATGTCAAACGTCCGAGTG	GCGTGTCCTCAGAGTTAGCC
PHC1	CTATTGCAGGTAAACCGAAC	GTTGATTCCTTACTGCCAAG
PHC2	GAAACTCTGCCTCCAGCATC	GATAGGGCTCCTCCATCTCC
PHC3	CACTTCCTCCTCTCGAATGC	CTGCTTAAATGCTGCTGCTG
RING1	CGGGAACAAGGAGTGTCCTA	TCCTCCCGGCTAGGATAGAT
RING2	TCATCACAG CCCTTAGAAGT	TGAGTGCTTGCTGATTATTG
SCML1	CCTTTTGCATGGAAGAATAC	GAAGAAGAACCATACGTTGC
SOX2	CCTCCGGGACATGATCAG	TTCTCCCCCCTCCAGTTC
SUZ12	TGGGAGACTATTCTTGATGG	GGAGCCGTAGATTTATCATT
YY1	CAAGAAGTGGGAGCAGAAGC	CTGCCAGTTGTTTGGGATCT
YY2	AGACACAAGAGGAAGTGGTG	GGTTGATGTTGATGTTGATG

1.2.6 Immunofluorescence staining and western blot

Cells were fixed with 4% para-formaldehyde for 10 minutes at room temperature and incubated with blocking solutions (10% normal goat serum, Rockland Immunochemicals, Gilbertsville, PA, USA) overnight at 4°C. Cells were then incubated overnight at 4°C with a c-MYC (#sc-764, Santa Cruz Biotechnology, Delaware, CA, USA) and p27 (#sc-528, Santa Cruz) primary antibody at a 1:200 dilution in 5% blocking solution and then reacted with the Alexa Fluor anti-rabbit IgG secondary antibody (Invitrogen) for 1 hour. For nuclear counter-staining, Hoechst 33258 (1g/ml, Sigma) was diluted to 1:500 in PBS and incubated with the cells for 15 minutes at room temperature. Images were taken with a confocal microscope (Eclipse TE200, Nikon, Tokyo, Japan). For western blotting, cells were lysed with PRO-PREP (#17081, iNtRON biotechnology). Cell lysates were incubated on ice for 20 minutes followed by centrifugation (13,000 rpm, 15 minutes, 4°C) and supernatant collection. The protein concentrations of samples were determined using the Protein Assay Reagent (Bio-Rad laboratories, Hercules, CA, USA) according to the manufacturer's instructions. The protein (10-15 μg) was electrophoresed on a 10-12% SDS-polyacrylamide electrophoresis gel. The proteins were detected with primary antibodies for c-MYC (AF3696, R&D systems Inc., Minneapolis, MN, USA), HDAC1 (2E10, Millipore, Billerica, MA, USA), HDAC2 (3F3, Millipore), HDAC3 (3G6, Millipore), HDAC4 (sc-

48390, Santa Cruz), p21 (sc-32, Santa Cruz), p27(sc-528, Santa Cruz), p57 (06-556, upstate, Lake Placid, NY, USA), CDK4 (DCS156, Cell Signaling Inc, Danvers, MA, USA) and hyperphosphorylated Retinoblastoma (G3-245, BD Biosciences, San Jose, CA, USA). The antibodies were detected with the respective secondary antibody linked to horseradish peroxidase (Zymed Laboratories Inc., South San Francisco, CA, USA). Secondary horseradish peroxidase-conjugated antibodies were detected by the enhanced chemiluminescence reagent (ImageQuant 400, GE Healthcare, Piscataway, NJ, USA).

1.2.7   Chromatin Immunoprecipitation assay

The ChIP assay was carried out according to the manufacturer's protocol (cat. #17-295, upstate). Chromatin was cross-linked for 10 minutes, and then sonicated to shear DNA to a length of 200-1000 base pairs. The sonicated sample was diluted 10-fold with dilution buffer (1% of diluted solution was kept as input for quantification of the result). For a negative control, the sample was processed with normal IgG antibody (Santa Cruz). The rest of the sample was precipitated with the c-MYC mouse monoclonal antibody (1:200, Santa Cruz) for 48 hours at 4°C with gentle rotation. The chromatin-antibody complex was isolated by incubation with 60µl of salmon sperm DNA/Protein A agarose slurry for 1 hour at 4°C. The protein A agarose/antibody/histone complex pellet was isolated by gentle centrifugation (700-1000 rpm) and washed with a low-salt immune complex buffer, a high-

salt immune complex buffer, a LiCl immune complex buffer and TE buffer serially on a rotating platform at 4°C for each wash. Chromatin-antibody complexes were eluted from the protein A/antibody/histone/DNA complex bead by the addition of 1% SDS, 0.1M NaHCO3. Cross-linking was reversed by addition of a 0.05 volume of 5M NaCl and incubation of the eluted samples overnight at 65°C. The DNA was extracted with phenol-chloroform, precipitated with ethanol and dissolved in autoclaved distilled water. PCR analysis of the immunoprecipitated DNA was performed by using a PCR premix (Bioneer, Taejon, Korea). PCR of the genomic DNA (input, 1:20 dilution) was carried out along with the immunoprecipitated DNA. PCR products were visualized in a 2% agarose gel. PCR primer sequences are listed in Table 1.

1.2.8   Induction of differentiation and statistical analysis

To induce osteogenic differentiation, cells were seeded and maintained at 70-80% confluency, and incubated with DMEM low glucose medium (Gibco-Invitrogen), 10% FBS (Gibco-Invitrogen), 0.1 μM Dexamethasone (Sigma), 10mM beta-glycerophosphate (Sigma) and 50 μM ascorbate (Sigma) for 2-3 weeks (Okamoto et al., 2002). Osteogenic differentiation was determined by staining with Alizarin Red S (Sigma). For adipogenic differentiation, cells were seeded and maintained at 80-90% confluency, and incubated with DMEM low glucose medium (Gibco BRL), 10% FBS (Gibco BRL), 1μM□□ Dexamethasone (Sigma), 10 μg/ml insulin

(Sigma), 0.5mM 3-isobutyl-1-methylxanthine (Sigma) and 0.2mM indomethacin (Sigma) (Okamoto et al., 2002). Adipogenic differentiation was determined by staining with Oil Red O (Sigma).

Statistical analysis was performed with student t-test using Microsoft Excel and p-value was calculated.

1.3 RESULTS

1.3.1 The expression of c-MYC was found in hMSCs and cell proliferation was dramatically decreased after c-MYC knockdown

In this study, c-MYC expression was found in all hMSCs. The c-MYC in the hUCB-MSCs was specifically localized in the nucleus (Fig.1A). The RNA and protein expressions of c-MYC were relatively constant through passages (p) of hUCB-MSCs from p3 to p9 (Fig.1B). However, the expressions of l- and n-MYC were not constant in hUCB-MSCs throughout the passages (Fig.1B). FACS analysis was performed for the confirmation of hUCB-MSCs (Fig. 1C). Positive markers for hMSCs (CD29, CD44, CD73, CD90 and CD105) were well detected in hUCB-MSCs. To validate the function of c-MYC in hMSCs, a c-MYC knock-down experiment was performed using lentivirus vectors in hUCB-MSCs. c-MYC inhibition was confirmed with western blot and RT-PCR analysis (Fig.2A). The RNA expressions of cyclin-dependent kinase inhibitors 1A and 1B (p21 and p27) in c-MYC knocked-down hUCB-MSCs were increased and similar with the vehicle control infected hUCB-MSCs respectively (Fig. 2A). Real-time RT-PCR revealed that the expression of c-MYC was decreased by 60% in ShM1 and 80% in ShM3 lentivirus-infected hUCB-MSCs compared to vehicle control-infected hUCB-MSCs (Fig.2B). The expressions of n-Myc and l-MYC in hUCB-MSCs were not changed in c-MYC knocked-down hUCB-

23

MSCs (Fig. 2A). The expressions of SOX2 and OCT4 were decreased after c-MYC inhibition of hUCB-MSCs. Cell proliferation was significantly decreased in c-MYC knocked-down hUCB-MSCs compared to vehicle control-infected hUCB-MSCs, which was measured using CPDL (Fig.2C). The proliferation of c-MYC knocked-down cells decreased continuously from P1 to P3, it was assumed that the proliferation would reduce continuously in following passages too.
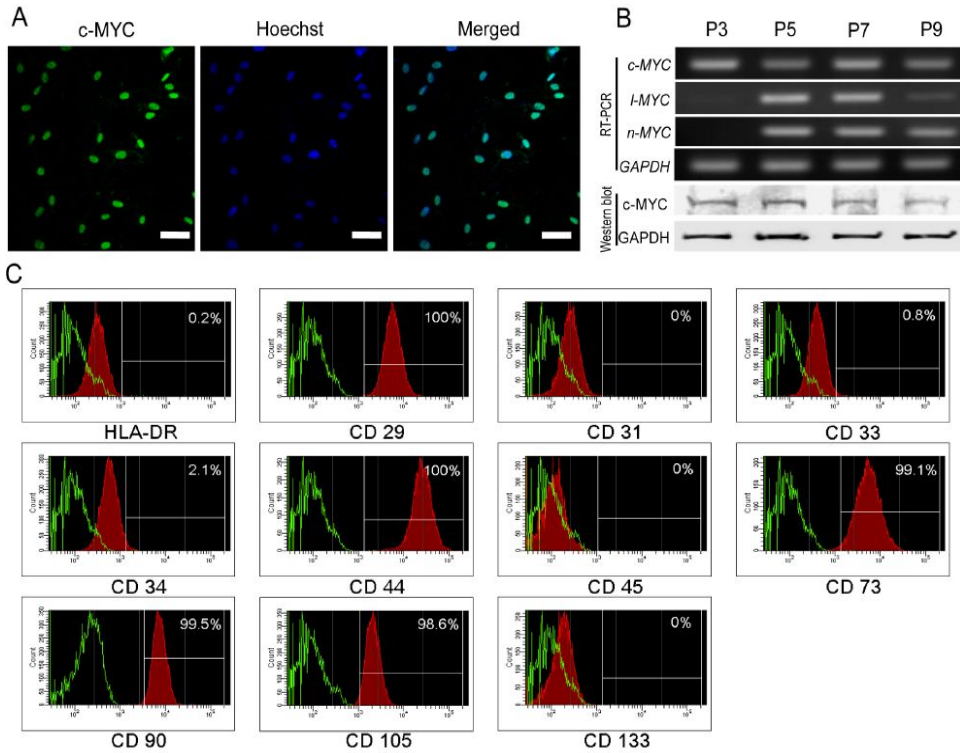
Figure 1 c-MYC expression in hUCB-MSCs.

(A) Immunostaining of c-MYC in p5 hUCB-MSCs. Nuclear localization of c-MYC is prominent. (B) MYC expression in hUCB-MSCs from p3 to p9. The expression of c-MYC is constant in hUCB-MSCs from p3 to p9. (C) FACS analysis of hUCB-MSCs. CD31 (EC/EPC marker); CD29, CD44, CD73, CD90, CD105 (MSC positive marker); CD34, CD45 (MSC Negative marker); CD31, CD34, CD133 (hematopoietic stem cell marker); HLA-DR (MHC class II, leukocyte marker). Scale bar represents 50 μm.
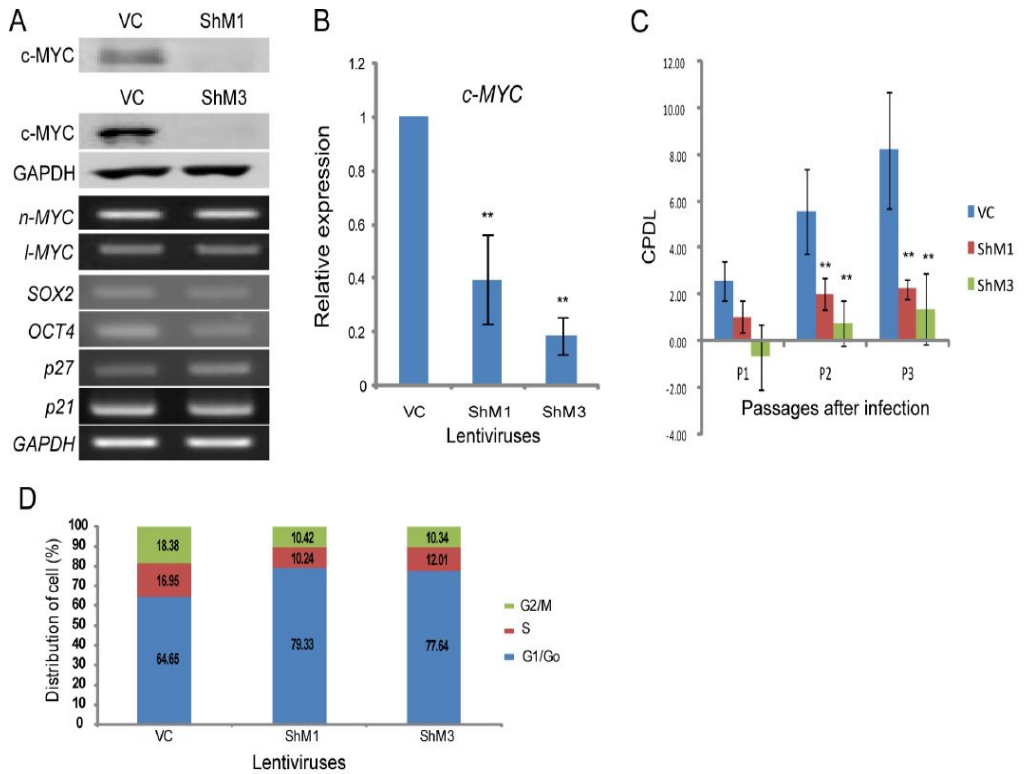
Figure 2 The knock-down of c-MYC results in growth retardation

(A) RNA and protein expression after c-MYC-inhibiting lentivirus infection. Two constructs of c-MYC-inhibiting lentivirus, ShM1 and ShM3, show effective inhibition in hUCB-MSCs. (B) Real-time RT-PCR after c-MYC inhibition in hUCB-MSCs. The expression of c-MYC was decreased by approximately 60% (ShM1) and 80% (ShM3) of the vector control-infected hUCB-MSCs. (C) Cell proliferation was measured with CPDL. c-MYC knocked-down hUCB-MSCs show severe growth retardation. (D) FACS analysis after c-MYC knock-down in hUCB-MSCs. G0/G1 cells are increased in c-MYC knocked-down hUCB-MSCs compared to those of the vehicle control-infected hUCB-MSCs. VC, vehicle control infected hUCB-MSCs. **, $p < 0.01$

1.3.2 The cell cycle was arrested in c-MYC knocked-down hUCB-MSCs

The cell cycle was measured in vehicle control-infected and c-MYC knocked-down hUCB-MSCs by FACS analysis (Fig. 2D). The number of cells in the G0/G1 phase was increased in c-MYC knocked-down hUCB-MSCs. Conversely, G2/M phase and S phase cells were decreased in c-MYC knocked-down hUCB-MSCs compared to the vehicle control-infected hUCB-MSCs. The expression of cyclin-dependent kinase-4 (CDK4), which is involved in the control of cell proliferation during the G1 phase (Lazarov et al., 2002), was decreased in c-MYC knocked-down hUCB-MSCs compared to that of vehicle control-infected hUCB-MSCs (Fig.3A). The protein expressions of p21 and p27, which are G1/S transition inhibitors (Sherr and Roberts, 1995), were increased in c-MYC knocked-down hUCB-MSCs compared to the levels in the vehicle control-infected hUCB-MSCs (Fig. 3A). The expression of hyperphosphorylated RB (PpRb), which is a G1/S transition accelerator (Ogawa et al., 2003) was significantly decreased in c-MYC knocked-down hUCB-MSCs compared to that of vehicle control-infected hUCB-MSCs (Fig. 3A). After c-MYC inhibition of hUCB-MSCs, the expression of class I and class II HDACs were compared at the RNA and protein levels. Among the HDAC family genes, the expressions of HDAC2, HDAC4 and HDAC5 in c-MYC knocked-down hUCB-MSCs were decreased compared to those of vehicle control-infected hUCB-MSCs at RNA

expression levels (Figs 3B-C). The protein expression levels of HDAC2 and HDAC4 were also decreased after c-MYC knockdown in hUCB-MSCs (Figs.3D and 6D). The localization of p27 is also an important factor for cell growth control (Slingerland and Pagano, 2000) and the levels of p27 are high in quiescent cells (Cheng et al., 1999). Therefore, immuno-cytochemical observation was performed after c-MYC knockdown. In vehicle-control infected hUCB-MSCs, the localization of p27 was almost confined in nucleus. However, the signal of p27 in ShM3 (c-MYC knocked-down hUCB-MSCs) was strong and broad, which was distributed not only in the nucleus but also in cytoplasm (Fig. 3E).
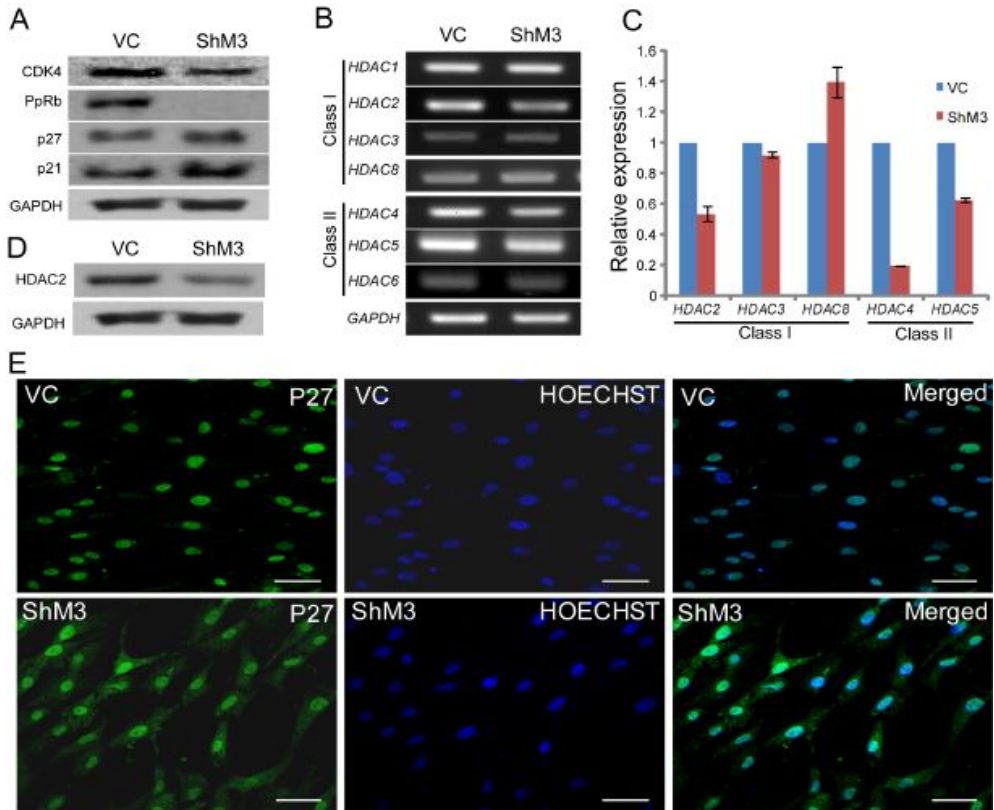
Figure 3 Gene expression changes after c-MYC inhibition in hUCB-MSCs.

(A) The expressions of CDK4 and PpRb are decreased after c-MYC inhibition. The expressions of p21 and p27 are increased after c-MYC inhibition. (B) The expressions of HDAC family genes. (C) The expressions of *HDAC2*, *HDAC4* and *HDAC5* are significantly decreased in real-time RT-PCR after c-MYC inhibition. (D) Western blot of HDAC2 after c-MYC inhibition. (E) Immunostaining of p27 after c-MYC knockdown. VC, vehicle control infected hUCB-MSCs; ShM3, c-MYC knocked-down hUCB-MSCs. Scale bar represents 50 µm.

1.3.3 The over-expression of c-MYC in hUCB-MSCs resulted in growth acceleration and up-regulation of HDAC2

To validate the function of c-MYC in hUCB-MSCs, over-expression study was performed using a lentivirus vector system. The expression of c-MYC was increased 3.5-fold in c-MYC over-expression lentivirus-infected hUCB-MSCs over the vehicle control-infected hUCB-MSCs in real-time RT-PCR analysis (Fig.4A). These results were confirmed by RT-PCR and western blot analysis (Fig.4B). The expressions of SOX2 and OCT4 were increased after c-MYC over-expression of hUCB-MSCs. c-MYC over-expressing hUCB-MSCs grew faster than vehicle control infected hUCB-MSCs, which was measured with MTT assay (Fig.4C). PpRB expression increased after c-MYC over-expression. The expressions of p21 and p27 were decreased in c-MYC over-expressing hUCB-MSCs compared with those of vehicle control-infected hUCB-MSCs (Fig.5A). Among class I and II HDACs, only HDAC2 and HDAC4 expression was significantly increased after c-MYC over-expression in hUCB-MSCs at RNA expression levels (Figs.5B-C). The increased expression of HDAC2 after c-MYC over-expression was confirmed at protein level (Fig. 5D). The expressions of other HDAC genes, except HDAC2 and HDAC4, were not significantly changed after c-MYC over-expression in hUCB-MSCs (Figs.5B-D). However, the protein expression pattern of HDAC4 differed from RNA expression pattern. The protein

expression of HDAC4 in c-MYC over-expressing hUCB-MSCs was not

increased compared with vehicle control infected hUCB-MSCs (Fig.6D).
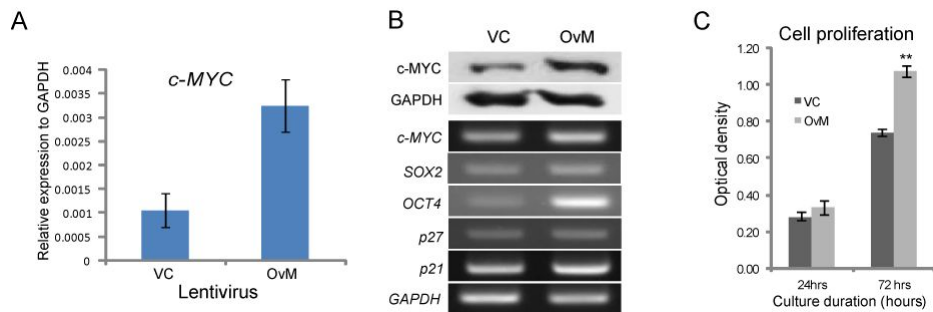
Figure 4 Over-expression of c-MYC in hUCB-MSCs

(A) c-MYC over-expressing lentivirus-infected hUCB-MSCs (OvM) showed a 3.5-folds increase in expression in real-time RT PCR. (B) RT-PCR and western blot analysis of c-MYC after c-MYC over-expressing lentivirus-treated hUCB-MSCs. (C) Cell proliferation is enhanced in c-MYC over-expressing hUCB-MSCs. VC, vehicle control infected hUCB-MSCs; OvM, c-MYC over-expressing hUCB-MSCs. **, $p < 0.01$.
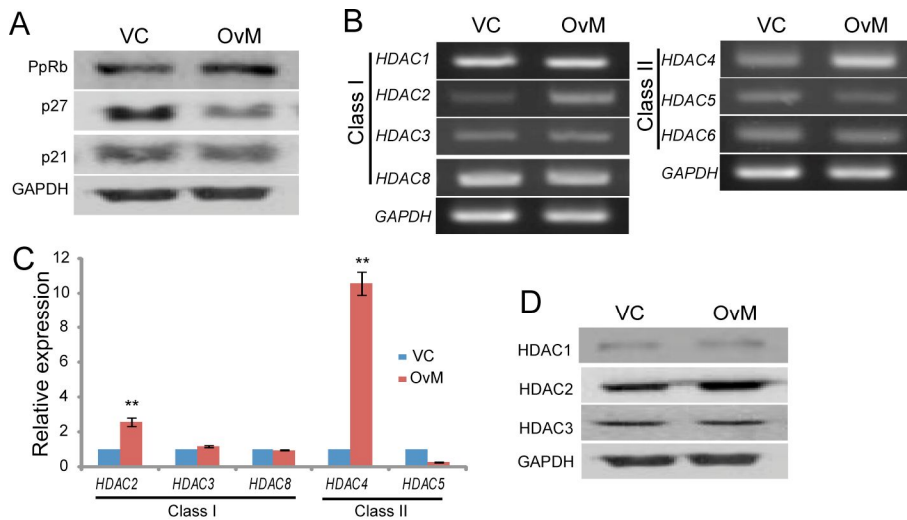
Figure 5 HDACs and cell cycle regulator expression after c-MYC over-expression in hUCB-MSCs.

(A) The expressions of cell cycle regulators. The expressions of p21 and p27 are down-regulated. The expression of PpRb is up-regulated in c-MYC over-expressing hUCB-MSCs. (B) The expressions of class I and II HDACs. HDAC2 and HDAC4 are up-regulated in c-MYC over-expressing hUCB-MSCs. (C) The expressions of class I and II HDACs in real time RT-PCR. (D) Western blot of HDAC 1, 2 and 3. VC, vehicle control lentivirus infected hUCB-MSCs; OvM, c-MYC over-expressing hUCB-MSCs. **, p<0.01.

1.3.4 The c-MYC binding site is present in the HDAC2 promoter region and HDAC2 regulation by c-MYC is related to cell growth of hUCB-MSCs

The expression pattern of HDAC2 was matched with that of the c-MYC expression pattern, implying a direct correlation between the expressions of the two genes. After c-MYC knockdown, the expression of HDAC2 was decreased (Figs.3C and 6D). However, the expression of HDAC2 was increased after c-MYC over-expression of hUCB-MSCs (Figs.5B-D and 6B-D). Therefore, we investigated c-MYC binding site to the HDAC2 promoter region. Only one putative c-MYC binding site was found in the HDAC2 promoter region, and c-MYC binding at this site was confirmed in hUCB-MSCs by performing a ChIP assay (Fig.6A). To evaluate the function of HDAC2 in c-MYC over-expressing hUCB-MSCs, HDAC2 was specifically inhibited with HDAC2 siRNA treatment in c-MYC over-expressing hUCB-MSCs (Figs.6B-D). The expressions of other HDACs were not significantly changed after HDAC2 siRNA treatment except for HDAC2 (Fig.6C). The down-regulated tumor suppression genes, p27 and p57, in c-MYC over-expressing hUCB-MSCs recovered after the HDAC2 siRNA treatment. However, over-expressed PpRb in c-MYC over-expressing hUCB-MSCs was down-regulated after HDAC2 siRNA treatment (Fig.6B). The expression of c-MYC in HDAC2 siRNA treated c-MYC over-expressing hUCB-MSCs was also restored to the normal expression level (Fig.6B). The

accelerated cell proliferation of hUCB-MSCs after c-MYC over-expression was down-regulated after HDAC2 siRNA treatment (data not shown).
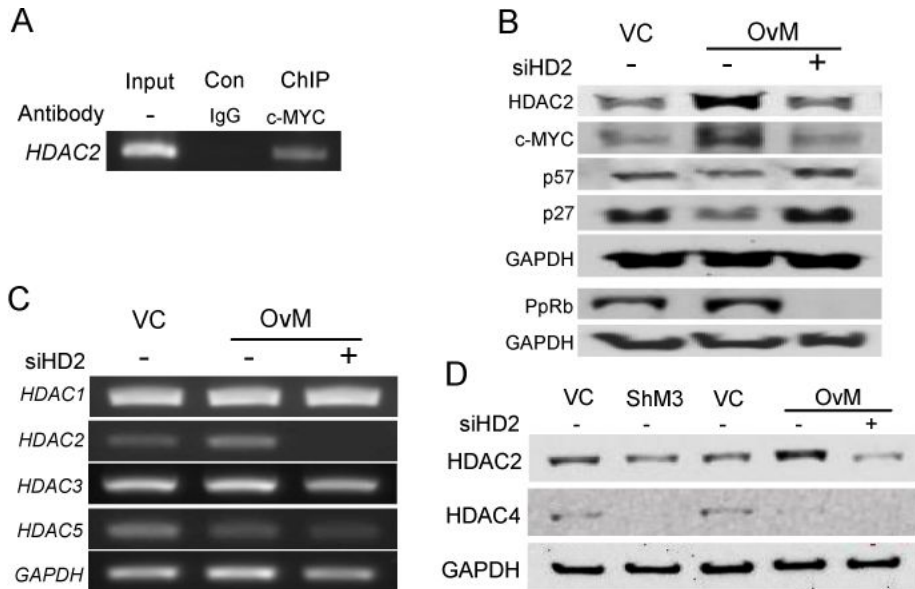
Figure 6 ChIP assay and mRNA & Protein expression after HDAC2 siRNA treatment in c-MYC over-expressing hUCB-MSCs.

(A) ChIP assay in hUCB-MSCs. The c-MYC binding site is present in the HDAC2 promoter region. (B) Western blot of HDAC2, p27, p57 and PpRb after HDAC2 siRNA treatment. The expression of HDAC2 is decreased after HDAC2 siRNA treatment. The expression of p27 and p57 is up-regulated but the expression of PpRb is down-regulated after HDAC2 siRNA treatment in c-MYC over-expressing hUCB-MSCs compared with those of control-treated c-MYC over-expressing hUCB-MSCs. (C) The expressions of HDACs after HDAC2 siRNA treatment in c-MYC over-expressing hUCB-MSCs. (D) Western blot of HDAC2 and HDAC4 in c-MYC knocked-down and over-expressed hUCB-MSCs before and after HDAC2 siRNA treatment. HDAC4 expression was decreased in both c-MYC knocked-down and over-expressed hUCB-MSCs without regarding to HDAC2 siRNA treatment. siHD2, HDAC2 siRNA treatment; VC, vehicle control lentivirus infected hUCB-MSCs; ShM3, c-MYC knocked-down hUCB-MSCs; OvM, c-MYC over-expressing hUCB-MSCs.

1.3.5 Differentiation ability was changed after c-MYC expression changes in hUCB-MSCs

The expression of c-MYC in hMSCs can affect stem cell differentiation, directly or indirectly. To evaluate the effect of c-MYC expression in hUCB-MSCs, a differentiation study was performed in c-MYC knocked-down and over-expressed hUCB-MSCs (Fig.7). In c-MYC knocked-down hUCB-MSCs, adipogenesis and osteogenesis were decreased after proper induction, which were confirmed with Oil-Red O and Alizarin Red S staining, respectively. However, adipogenesis and osteogenesis were similar or increased in c-MYC over-expressing hUCB-MSCs, compared with those of vehicle control-infected hUCB-MSCs after proper induction. The specific gene expressions of adipogenic and osteogenic differentiation after induction were confirmed by RT-PCR. The expressions of PPARγ and C/EBPδ, the markers of adipogenesis (Muruganandan et al., 2009), were decreased in c-MYC knocked-down hUCB-MSCs and increased in c-MYC over-expressing hUCB-MSCs, compared to vehicle control infected hUCB-MSCs. The expression of RUNX2, a marker of osteogenesis (Takada et al., 2007), was increased in c-MYC over-expressing hUCB-MSCs and the expression of RUNX1, the incomplete differentiation osteogenic marker (Yamashiro et al., 2004), increased in c-MYC knocked-down hUCB-MSCs after osteogenic induction.
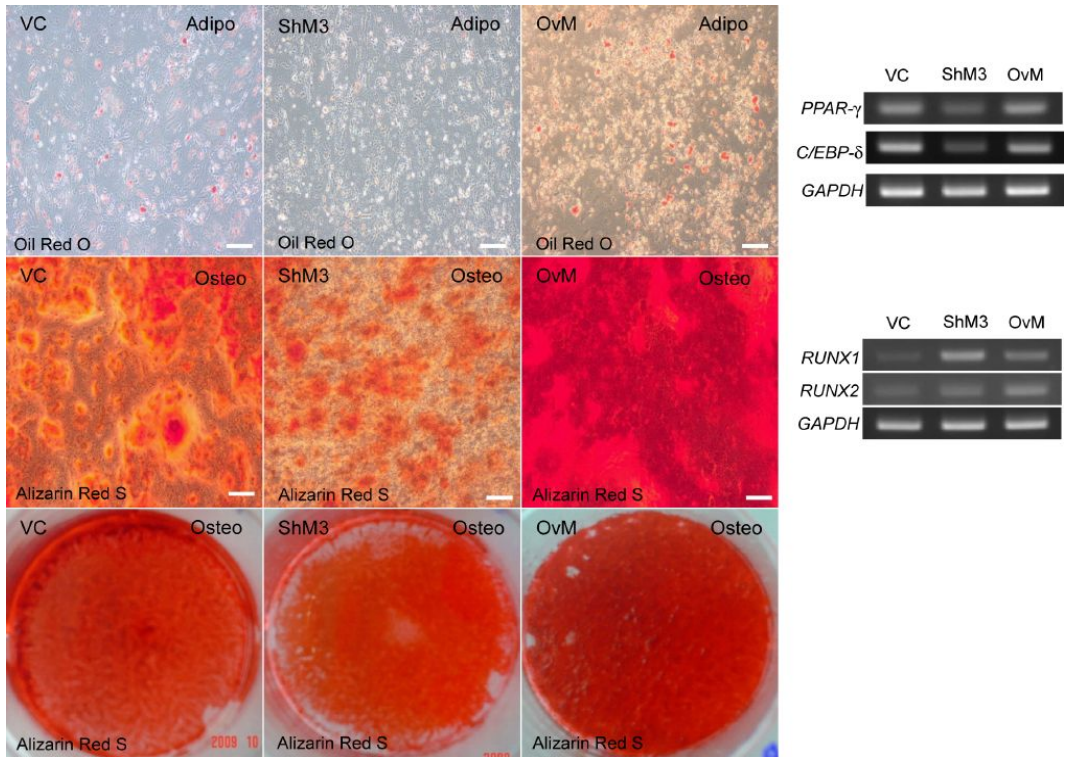
Figure 7 Differentiation study after c-MYC expression changes

Adipogenic cells are stained with Oil Red O and Osteogenic cells are stained with Alizarin Red S. After c-MYC knockdown, differentiation ability of hUCB-MSCs was decreased in both adipogenic and osteogenic differentiation study. The over-expression of c-MYC showed similar or enhanced induction of differentiation in both adipogenic and osteogenic. VC, vehicle control; shM3, c-MYC knockdown with ShM3 infection; OvM, c-MYC over-expression; Adipo, adipogenic differentiation; Osteo, osteogenic differentiation; Scale bars represents 50μm.

1.3.6 The influential role of c-MYC in PcG genes expression and the regulation of HDAC2 in hAD- and hBM-MSCs

The expressions of most PcG genes decreased after c-MYC knockdown but increased after c-MYC over-expression in hUCB-MSCs (Figs 8A-C). The increased PcG gene expressions in c-MYC over-expressing hUCB-MSCs were reduced after HDAC2 siRNA treatment, which was a similar pattern in most PcG complexes examined in the RT-PCR results (Figs 8A-C). A real-time RT-PCR was performed for detailed comparison in subtle changed genes. The expression of EDR2 was down-regulated after c-MYC inhibition and up-regulated after c-MYC over-expression but showed an up-regulation after HDAC2 siRNA treatment in c-MYC over-expressing hUCB-MSCs (Fig.8D). The expressions of EDR1, RING1 and EZH2 were not down-regulated after HDAC2 inhibition in c-MYC over-expressing hUCB-MSCs.

The expression of c-MYC in hAD-MSCs and hBM-MSCs was analyzed by western blot (Figs 8E-F). After c-MYC knocked-down, HDAC2 expression was significantly decreased in hAD-MSCs and hBM-MSCs respectively. The expressions of HDAC2 were increased after c-MYC over-expression in hAD-MSCs and hBM-MSCs. This expression pattern was similar to that observed in hUCB-MSCs. Therefore, it can be concluded that HDAC2 expression is positively regulated by c-MYC in three kinds of hMSCs which includes hUCB-MSCs, hAD-MSCs and hBM-MSCs.
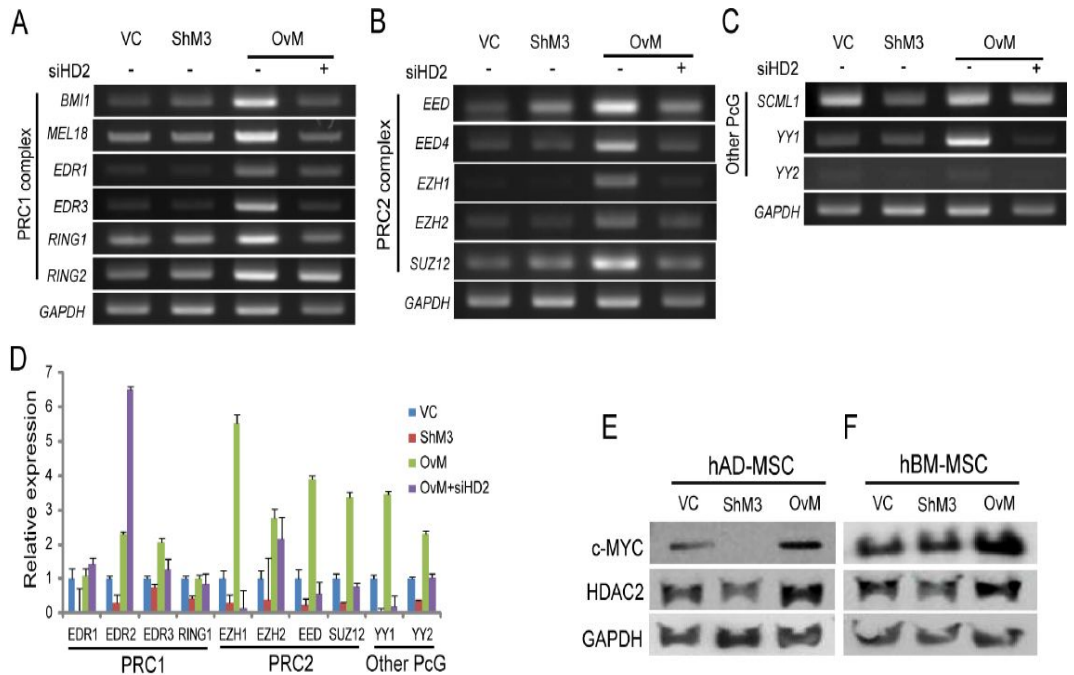
Figure 8 PcG gene expression after c-MYC expression changes and c-MYC/ HDAC2 expression in hAD-MSC and hBM-MSCs

(A-C) The expression changes of PcG complex genes after c-MYC expression changes with or without HDAC2 siRNA treatment. Most PcG genes expressions are increased after c-MYC over-expression and reduced after HDAC2 siRNA treatment. (D) Relative gene expression of PcG genes with real-time RT-PCR. PcG gene expressions are positively correlated with c-MYC and HDAC2 expression except of EDR1, EDR2 and RING1 expressions. (E, F) Western blot (E) The expression pattern of HDAC2 match that of c-MYC expression pattern in hAD-MSCs. (F) The expression of HDAC2 is down-regulated after c-MYC inhibition and up-regulated after c-MYC over-expression in hBM-MSCs. VC, vehicle control infected hMSCs; ShM3, c-MYC knocked-down hMSCs; OvM; c-MYC over-expressing hMSCs.

1.4 **DISCUSSION**

c-MYC is a nuclear onco-protein and has emerged as a critical regulator of cell growth and tumor generation (Adhikary and Eilers, 2005). Here in our study, we demonstrated that c-MYC is associated with cellular growth, proliferation and differentiation in adult stem cells. Previous reports indicate that HDAC2 expression is prominent in different cancers (Zhu et al., 2004; Humphrey et al., 2008), in accordance to this; in our c-MYC knocked-down study, when HDAC2 is down regulated, tumor suppression gene's expression increased there by reducing the cell proliferation. In contrary, when c-MYC over-expressed, the expression of HDAC2 is also up regulated as a result tumor suppresser genes' expression down-regulated there by promoting cell proliferation. Similarly, HDAC2 siRNA treatment in c-MYC over-expressing hUCB-MSCs, suppressed tumor suppressor genes reactivated and cell growth was reduced. The above finding indicates that c-MYC can regulate HDAC2 expression. In addition to this, the presence of c-MYC binding motif (CACGTG) in the promoter region of HDAC2 is confirmed by ChIP assay. This indicates the regulatory role of c-MYC on HDAC2 in hUCB-MSC. In other adult stem cells, hAD-MSCs and hBM-MSCs, HDAC2 expression was decreased after c-MYC inhibition and increased after c-MYC over-expression, which was a similar expression pattern to that of hUCB-MSCs.

c-MYC is a well known growth regulator, found particularly in tumors, that regulates numerous genes. The conserved core of high-affinity MYC target genes represents around 11% of all cellular promoters (Adhikary and Eilers, 2005). The response of any target gene following MYC activation depends on a variety of other factors and changes dramatically as a function of cell type and environment (Fernandez et al., 2003). Although the expression of c-MYC in adult stem cells has been reported previously (Studzinski, 1989; Seo et al., 2009), the expressions of n-MYC and l-MYC have not yet been illustrated. This study represents the first result confirming the expression patterns of these genes, which were not consistent throughout passages of hUCB-MSCs in culture. Only c-MYC expression was consistent from p3 until p9 of hUCB-MSCs culture. Chromosomal modification is one of most important regulatory mechanisms for maintaining the stemness of adult stem cells (Rajasekhar and Begemann, 2007). Therefore, this study investigated the role of c-MYC in human adult stem cells, particularly with respect to the regulation of chromosomal modification genes.

Among class I and II HDACs, only HDAC2 expression was significantly decreased after c-MYC inhibition and increased after c-MYC over-expression in hUCB-MSCs at the both of protein and RNA expression levels. c-MYC binding in the HDAC2 promoter region was evident from a ChIP assay in hUCB-MSCs. Therefore, we investigated cell growth changes as a function of HDAC2 expression that was regulated by c-MYC. The expression of cell growth regulators was changed after HDAC2 siRNA

treatment in c-MYC over-expressing hUCB-MSCs and cell growth was normalized. A correlation between c-MYC and HDAC2 expression was also found in hAD-MSCs and hBM-MSCs. Therefore, HDAC2 regulation by c-MYC in hMSCs is suggested as a common regulatory mechanism for cell growth control in adult stem cells. The expression of c-MYC itself was decreased after HDAC2 inhibition in c-MYC over-expressing hUCB-MSCs, which also implied that c-MYC expression could be regulated by HDAC2 expression conversely (Fig. 6C).

PcG genes are also important to epigenetic regulation of stem cells ((Rajasekhar and Begemann, 2007; Niessen et al., 2009), which is affected by c-MYC expression (Guney and Sedivy, 2006). Our data showed the expression PRC2 related genes were down-regulated in c-MYC and HDAC2 inhibited cells. c-MYC over-expression in hUCB-MSCs induces the expression of PcG complex genes, and most PcG genes were down-regulated after HDAC2 inhibition. However, the expression level of EDR1, EDR2, RING1 and EZH2 were not down-regulated after HDAC2 inhibition. This might indicate that these genes were not under the control of HDAC2 or c-MYC. Protein expression of PcG could not be checked because of the unavailability of a suitable antibody. Further study is necessary to explore individual PcG protein expression. Previous study reported that HDAC inhibitor treatment can reduce the expression of PcG gene expression (Kondo, 2009). In this report, it was also found that HDAC2 specific siRNA treatment reduced PcG expression in adult stem cells. Therefore, it is postulated that c-

43

MYC positively regulates most PcG expression in adult stem cells via HDAC2.

In conclusion, this study validated that c-MYC positively regulates HDAC2 expression at the transcriptional and translational level; this regulatory mechanism is found to be common in all three kinds of hMSCs. c-MYC binding site in the promoter region of HDAC2 was confirmed. c-MYC's regulatory role might also be able to regulate the expression of PcG gene expression via HDAC2 regulation. As a result, cell proliferation and differentiation of adult stem cells is affected. In addition, our data also indicates that c-MYC and HDAC2 have a mutual regulatory role.

CHAPTER II

REX1 Expression and p38 MAPK Activation Status Can Determine Proliferation/Differentiation Fates in Human Mesenchymal Stem Cells

2.1 INTRODUCTION

Embryonic stem cells (ESCs) are pluripotent stem cells that can self-renew and generate all the cell types of the body; however, they are not able to generate the extra embryonic trophoblast lineage (Rossant, 2008). The transcriptional regulatory network of ESCs that maintains pluripotency is well-established. Takahashi and Yamanaka reported critical transcription factors that are necessary for the induction of pluripotency (Takahashi and Yamanaka, 2006). The core transcription factors, including the Yamanaka factors, have been relatively well-defined in ESCs (Boyer et al., 2005; Wang et al., 2006). OCT4 (Boiani et al., 2002) and REX1 (Ben-Shushan et al., 1998) are transcription factors that are characteristic markers of pluripotent stem cells. Paradoxically, over- or under-expression of Oct4 leads to the down-regulation of Rex1 expression. Down-regulation of Oct4 and Rex1 triggers trophectoderm differentiation, while their up-regulation triggers primitive endoderm and mesoderm differentiation (Niwa et al., 2000). Rex1 (Zfp42) was first identified as a gene that is transcriptionally repressed by retinoic acid and encodes a zinc finger transcription factor that is expressed at high levels in F9 teratocarcinoma stem cells, embryonic stem cells, and other stem cells (Hosler et al., 1989; Mongan et al., 2006; Ramalho-Santos et al., 2002). REX1 is a member of the YY1 sub-family of transcription factors that can function as repressors, activators or transcription initiators depending on the sequence context of the YY1-binding sites with respect to other regulatory elements

(Mongan et al., 2006; Shi et al., 1997). Currently, REX1 is widely used as a stem cell marker, and Rex1 inhibits signaling via the Janus kinase (JAK)/STAT3 pathway during the differentiation of F9 teratocarcinoma stem cells (Xu et al., 2008). ESCs from Rex1 knock-out mice show defects in the induction of a subset of marker genes in the visceral endoderm, which suggests that Rex1 plays a role in ESC differentiation (Masui et al., 2008).

The family of Mitogen-Activated Protein Kinases (MAPKs) controls an enormous number of processes such as gene expression, metabolism, cell proliferation, division, differentiation, apoptosis and embryogenesis (Pearson et al., 2001; Johnson and Lapadat, 2002). Five different MAPK pathways have been described: the extracellular signal-regulated kinases (ERKs), the stress-activated protein kinases (SAPKs), the c-Jun N-terminal kinases (JNK), the ERK5/big MAP kinase 1 (BMK 1) and the p38 MAPK. The p38 MAPK pathway was initially described as being activated by different types of cellular stresses and cytokines. Numerous studies have reported the involvement of p38 MAPK pathways in the regulation of a wide spectrum of cellular processes including cell cycle arrest, apoptosis, senescence, regulation of RNA splicing, tumorigenesis and the growth/differentiation of specific cell types (Han and Molkentin, 2000; Zarubin and Han, 2005). In mammals, there are four p38 MAPKs: p38α, p38β, p38γ (SAPK3, ERK6) and p38δ (SAPK4). MAP kinase p38α is ubiquitously expressed whereas p38β, p38γ and p38δ□ have restricted expression patterns (Schieven, 2005). Two major MAPK kinases (MKKs), MKK3 and MKK6, are known to activate p38 MAPKs.

MKK6 activates all four p38 MAPKs and MKK3 activates p38α, p38γ and p38δ (Nebreda and Porras, 2000; Zarubin and Han, 2005).

Mesenchymal stem cells (MSCs) are promising tools in the field of regenerative medicine. MSCs have been isolated from bone marrow, adipose tissue, peripheral blood, fetal liver, lung, amniotic fluid, chorionic villi of the placenta and umbilical cord blood (Campagnoli et al., 2001; Erices et al., 2000; Gronthos et al., 2001; Igura et al., 2004; Tsai et al., 2004; Zvaifler et al., 2000). However, their ability to proliferate and differentiate differs depending on their parental tissue type and subsequent culture conditions. Roch et al. (Roche et al., 2007)described that OCT4, REX1 and GATA4 expression in human MSCs increases the differentiation efficiency of these cells. Furthermore, first-trimester human fetal MSCs express OCT4, NANOG and REX1 (Guillot et al., 2007); therefore, hMSCs originating from young tissue have a strong potential to obtain powerful multipotency and become large cell populations. In addition to the isolation method, the culturing method is another challenge in stem cell biology. Inhibition of p38 MAPK facilitates ex vivo expansion of skin epithelial progenitor cells (Peng et al., 2009), and several types of p38 MAPK inhibitors have been reported in the literature. In this report, we determined that the phosphorylation status of p38 MAPK and the expression of REX1 in hMSCs was an important regulatory machine that maintains ASCs via the direct regulation of MKK3.

2.2 MATERIALS AND METHODS

2.2.1 Isolation of hMSCs, Cell Culture and Ethics Statement

Human umbilical cord blood-derived MSCs (hUCB-MSCs) (Seo et al., 2009), human bone marrow derived MSCs (hBM-MSCs) (Pal et al., 2009) and human adipose tissue-derived MSCs (hAD-MSCs) (Park et al., 2008) were isolated and cultured as previously described. In brief, two clones of hAD-MSCs were isolated from freshly excised mammary fat tissue acquired from the Ba-Ram plastic surgery hospital. Tissues were obtained from 20 to 30 year-old women during reduction mammoplasty. The hAD-MSCs were maintained in K-SFM medium supplemented with 2 mM N-acetyl-L-cysteine (Sigma-Aldrich, St. Louis, MO, USA) and L-ascorbic acid (0.2 mM, Sigma-Aldrich). hBM-MSCs were isolated from three healthy donors and were cultured in low glucose Dulbecco's Modified Eagle's Medium (DMEM) supplemented with 10 % fetal bovine serum (FBS) without any additional growth factors. hUCB-MSCs were obtained from umbilical cord blood immediately after full term delivery with written consent from 20 to 30 year-old mothers and the approval of the Boramae Hospital Institutional Review Board (IRB). Three hUCB-MSC clones were used in this experiment. The hUCB-MSCs were maintained in DMEM (Invitrogen, Carlsbad, USA) containing 10% FBS. The passages (p) of hMSCs used for the experiments

were p5 in hUCB-MSCs, p5 in hAD-MSCs and p3 in hBM-MSCs. The isolation and research use of hAD-MSCs and hBM-MSCs were also approved by the Boramae Hospital IRB with written consent. All procedures were approved by the institutional review board of Seoul National University (UCB-MSC, #0603/001-002; AD-MSC, #0600/001-001; BM-MSC, #0910/001-003).

2.2.2 Cell proliferation and cell cycle analyses

To measure cell growth, CCK-8 (Dojindo Molecular Technologies Inc., San Diego, CA, USA) was used according to the manufacturer's protocol, and cells were measured at a wavelength of 540nm in an enzyme-linked immunosorbent assay plate reader (EL800, Bio-Tek Instruments Inc., Winooski, VT, USA).

The stages of the cell cycle were detected by FACS analysis. Briefly, the cells were washed twice with PBS and harvested by trypsinization after 3 days. The cells were then washed again with PBS and fixed with 70% ethanol at -20°C for 1 day. The fixed cells were washed with ice cold PBS and stained with 50μg/ml of propidium iodide (Sigma, St Louis, Missouri, USA) in the presence of 100μg/ml RNase A (Sigma) for 30 minutes. The cell cycle stages were analyzed using the FACS Calibur (Becton & Dickinson, NJ, USA).

2.2.3 The construction and production of lentiviral vectors

Lentiviruses were generated using ViraPowerTM Lentiviral packaging Mix (Invitrogen, Carlsbad, CA, USA). Lipofectamine 2000 (Invitrogen) was used for the transfection of 293FT cells (Invitrogen) with SHDNAC-TRCN0000107810 (REX1 knockdown-2, R2), SHDNAC-TRCN0000107812 (REX1 knockdown-4, R4) and SHC002 (VC, random sequence inserted) (Sigma, Saint Louis, MO, USA). Cell culture media was changed the day after transfection and the supernatant was harvested at 48 and 72 hours post transfection. The viral supernatant was filtered using 0.4μm pore filters (Invitrogen). Cells were transfected with REX1 shRNA-producing lentivirus at MOI (multiplicity of infection) of 5-10. Polybrene (Sigma) was added to the cell culture media at a final concentration of 6μg/ml. The cell culture medium was replaced with fresh culture medium the day after transfection. For selection, puromycin was added to the cell culture media at a final concentration of 10μg/ml for 3 days.

2.2.4 RT-PCR and ChIP assay

Total RNA was extracted with an easy-spin™ Total RNA Extraction Kit (iNtRON Biotechnology, Sungnam, Korea) according to the manufacturer's instructions. Synthesis of cDNA was carried out using the SuperScript® III First-Strand Synthesis System for RT-PCR (Invitrogen) with 1 μg total RNA and oligo dt and primers. The primers for each gene are shown in Table 2. Gene expression was also analyzed using real-time PCR

with SYBR Green Master Mix reagents (Applied Biosystems, Foster City, CA, USA). The expression level of REX1 was detected, and the real-time PCR values for gene expression were normalized to Glyceraldehyde 3-phosphate dehydrogenase (GAPDH) expression. Real time RT-PCR was performed with a LightCycler 480 Real-Time PCR System (Roche, Indianapolis, IN, USA). The chromatin immunoprecipitation (ChIP) assay was carried out according to the manufacturer's protocol (cat#17-295, Upstate Biotechnology, Billerica, MA, USA). PCR primers for the ChIP assay are listed in Table 2.

Table 2 RT- PCR primers sequences used REX1 Study.

Human mRNA	Forward (5'….3')	Reverse (5'….3')
AXIN1	TGATAACAATGGCATCGTGTC C	GTCCTGGTCACACTTCCATTC C
β-CATENIN	TCTGATAAAGGCTACTGTTGGATT GA	TCACGCAAAGGTGCATGATT
BMI1	TGCTGATGCTGCCAATGG	TTACTTTCCGATCCAATCTG
c-MYC	CAGCTGCTTAGACGCTGGATTT	ACCGAGTCGTAGTCGAGGTCAT
DKK1	AACCAGCTATCCAAATGCAG	TCACAGGGGAGTTCCATAAA
FZD2	CACGCCGCGCATGTC	ACGATGAGCGTCATGAGGTATTT
GAPDH	GAGTCAACGGATTTGGTCGT	GACAAGCTTCCCGTTCTCAG
JAG1	GCTGGCAAGGCCTGTACTG	ACTGCCAGGGCTCATTACAGA
LRP5	GACCCAGCCCTTTGTTTTGAC	TGTGGACGTTGATGGTATTGGT
MKK3	GTCCAAGCCACCCGCAC	CCTCAAAGTTTCTGTCTCCAATGG
MKK3 chip (Promoter)	GCCTGGTACATTCTGCCTTC	CAGTCTGCCCATCTGCATAA
MKK3 chip (1st intron)	CACAAGTGGTTCCATGTTGC	GGGATCCCCAGACTATCCAC
MKK3 chip (1st exon)	TGGAAACGAAAGGACCAATC	GACGGCGGTGGAGACTAAT
MKK6	GAACTGGGACGAGGTGCGTA	TTTACTGTGGCTCGGATCCG
NOTCH1	CGGGTCCACCAGTTTGAATG	GTTGTATTGGTTCGGCACCAT
NOTCH4	CGGCCTCGGACTCAGTCA	CAACTCCATCCTCATCAACTTCTG
p38α	GTGCCCGAGCGTTACCAGAAC	CTGTAAGCTTCTGACATTTC
p38β	CACCCAGCCCTGAGGTTCT	AATCTCCAGGCTGCCAGG
P38γ	ACATGAAGGGCCTCCCCG	TCTCCTTGGAGACCCTGG
P38δ	CCCAAGACCTACGTGTCCC	ACTGGATCTTCTCCTCACTG
REX1	GCGTACGCAAATTAAAGTCCAGA	CAGCATCCTAAACAGCTCGCAGAA T
SUZ12	TGGGAGACTATTCTTGATGG	GGAGCCGTAGATTTATCATT
ZNF281	ACGTAACAGCGCAGACAGAA	GTGTTGAAGCCCAAGTGGTT

2.2.5   Immunofluorescence staining

Cells were fixed with 4% paraformaldehyde for 20 minutes at room temperature, and incubated with blocking solution (10% normal goat serum, Rockland Immunochemicals, Gilbertsville, PA, USA) overnight at 4°C. The cells were then incubated overnight at 4°C with REX1 primary antibody diluted in blocking solution (ab50828, Abcam, Cambridge, MA, USA), following which the cells were treated with the Alexa Fluor anti-rabbit IgG secondary antibody (Invitrogen) for 1 hour. For nuclear counter-staining, Hoechst 33238 (1µg/ml, Sigma) was diluted to 1:500 in PBS and incubated with the cells for 15 minutes. Images were captured with a confocal microscope (Eclipse TE200, Nikon, Tokyo, Japan).

2.2.6   Western blotting

Cells were lysed with PRO-PREP (#17081, iNtRON Biotechnology). The cell lysates were then incubated on ice for 20 minutes followed by centrifugation (13,000 rpm, 15 minutes, 4°C) and supernatant collection. The protein concentrations of samples were determined using the Protein Assay Reagent (Bio-Rad laboratories, Hercules, CA, USA) according to the manufacturer's instructions. The protein samples (10-15µg) were electrophoresed using a 10-12% SDS-polyacrylamide electrophoresis gel. The proteins were detected with primary antibodies that recognize REX1 (ab50828, Abcam), CDK2 (#2546, Cell signaling Inc, Danvers, MA, USA),

CDK4 (#2906, Cell signaling Inc), Cyclin B1 (#4138, Cell signaling Inc), Cyclin D1 (#2926, Cell signaling Inc), p21 (sc-32, Santa Cruz Biotechnology, Santa Cruz, CA, USA), BAX (sc-493, Santa Cruz Biotechnology), pERK1/2 (V803A, Promega, Madison, WI, USA), ERK1/2 (V114A, Promega), pGSK3β (#9336, Cell signaling Inc), GSK3β (#9315, Cell signaling Inc), pSTAT3 (#9131, Cell signaling Inc), STAT3 (#9139, Cell signaling Inc), STAT5 (sc-835, Santa Cruz Biotechnology), MEK1/2 (#9122, Cell signaling Inc), pMEK1/2 (#9121, Cell signaling Inc), NFκB (#3034, Cell signaling Inc), HES1 (AB5702, Chemicon), Pp38 (#4631, Cell signaling Inc), p38 (#9212, Cell signaling Inc), MKK3 (#9232, Cell signaling Inc) and GAPDH (MAB374, Chemicon). Antibody recognition was detected with the respective secondary antibody linked to horseradish peroxidase (Zymed Laboratories Inc., South San Francisco, CA, USA). Secondary horseradish peroxidase–conjugated antibodies were detected by enhanced chemiluminescence (ImageQuant 400, GE Healthcare, Piscataway, NJ, USA). The relative quantities of each protein band, normalized to control cells, were quantified using Quantity One software (version 4.6.5, Bio-Rad Inc, Hercules, CA, USA).

2.2.7 ANNEXIN V staining for apoptosis

The apoptosis assay was performed with a two-color analysis of FITC-labeled ANNEXIN V binding and propidium iodide (PI) uptake using the ANNEXIN V–FITC Apoptosis Detection kit following the manufacturer's

instructions (Calbiochem, San Diego, CA, USA). Positioning of quadrants on ANNEXIN V/PI dot plots was performed, and live cells (ANNEXIN V–/PI–), early/primary apoptotic cells (ANNEXIN V+/PI–), late/secondary apoptotic cells (ANNEXIN V+/PI+), and necrotic cells (ANNEXIN V–/PI+) were distinguished.

2.2.8 Statistical analysis

The data are presented as mean value ± standard deviation obtained from three independent experiments in which hMSCs clones originated from three individuals. The student's t-test (Microsoft Excel) was used for statistical analysis. Data are considered statistically significant when $p < 0.01$.

2.3   RESULTS

2.3.1   The expression of REX1 is negatively correlated with the phosphorylation of p38 MAPK in hMSCs

REX1 is expressed in ESCs and MSCs. Among three well-characterized hMSCs, REX1 is strongly expressed in hUCB-MSCs and hAD-MSCs; however, REX1 is weakly expressed in hBM-MSCs when grown under previously reported culture conditions (Seo et al., 2009; Pal et al., 2009; Park et al., 2008). In hUCB-MSCs, REX1 expression was nearly five-fold greater than in hBM-MSCs (Fig. 9A). However, in three types of hMSCs, the levels of phosphorylated p38 MAPK (Pp38) was in inverse proportion to the expression of REX1 (Fig.9B). The level of Pp38 in hBM-MSCs was four-fold stronger than the level in hUCB-MSCs. The expression level of p38, itself, was similar between the three types of hMSCs (Fig.9B). The cell proliferation rates of these three types of hMSCs were quite different. In repeated experiments, hUCB-MSCs and hAD-MSCs grew faster than hBM-MSCs (Fig.9C). Therefore, the proliferation rates of hMSCs positively correlate with the REX1 expression level but inversely correlate with the level of Pp38 expression. REX1 was expressed in the majority of hUCB-MSCs, and the localization of REX1 was primarily confined to the nucleus of hUCB-MSCs as shown by immunocytochemistry (Fig.9D).
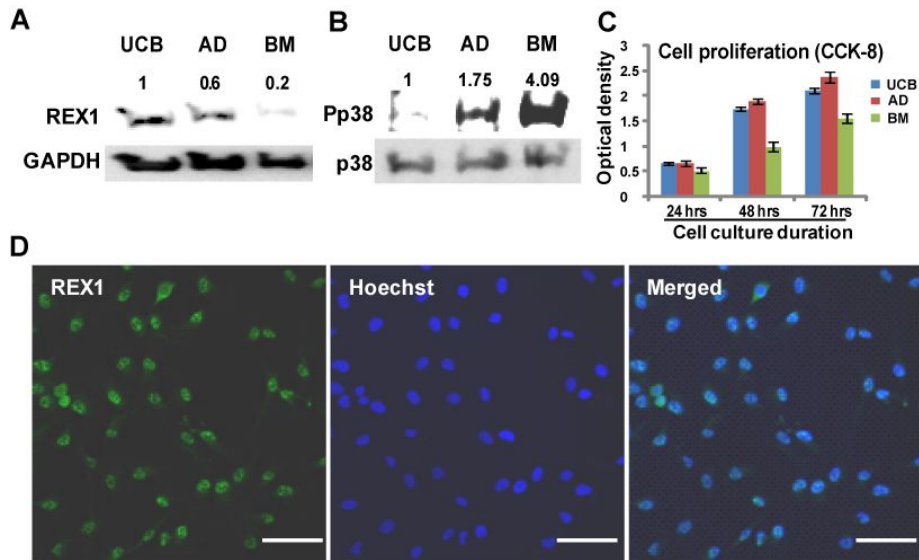
Figure 9 The expressions of REX1, p38 MAPK and the cell proliferation

of hMSC

(A) The expression of REX1 in hUCB-MSCs, hAD-MSCs and hBM-MSCs. hUCB-MSCs and hAD-MSCs have strong REX1 expression, but hBM-MSCs have very weak REX1 expression. (B) The expression of p38 and phosphorylated p38 (Pp38) in hUCB-MSCs, hAD-MSCs and hBM-MSCs. Expression levels of p38 was similar in three types of hMSCs. hBM-MSCs have the strongest expression level of Pp38 among the three types of hMSCs.

2.3.2 Knockdown of REX1 resulted in growth retardation of hUCB-MSCs

hUCB-MSCs grew faster than hBM-MSCs but at a similar pace as hAD-MSCs in *in-vitro* culture. The discrepancy in the proliferation speed may be potentially due to the difference in REX1 expression in the different cell types. Therefore, a REX1 knockdown experiment was performed in hUCB-MSCs, which had the highest expression of REX1 among the three types of hMSCs. Four different shRNA producing lentiviruses that target different REX1-regions were used for the experiment. Two lentiviruses construct, REX1-2 (R2) and REX1-4 (R4), showed specific inhibition of REX1 after puromycin selection (Fig.10A). After REX1 knockdown, cell growth severely decreased in hUCB-MSCs (Fig.10B and 10C). For detailed analysis of cell cycle progression, FACS analysis was performed with the hUCB-MSCs (Fig. 10D). The composition of the G0/G1 phase significantly increased and the composition of the S phase significantly decreased in REX1 knocked-down hUCB-MSCs compared to vehicle control-infected hUCB-MSCs. Western blot analysis of cell cycle regulators was performed using vehicle control-infected and REX1 knocked-down hUCB-MSCs. After REX1 knockdown, the expression levels of CDK2, Cyclin B1, CDK4 and Cyclin D1 decreased compared to the levels of vehicle control-infected hUCB-MSCs. However, the expression of p27 did not change when REX1 was knocked-down in hUCB-MSCs compared to vehicle control-infected hUCB-MSCs (Fig.10E).
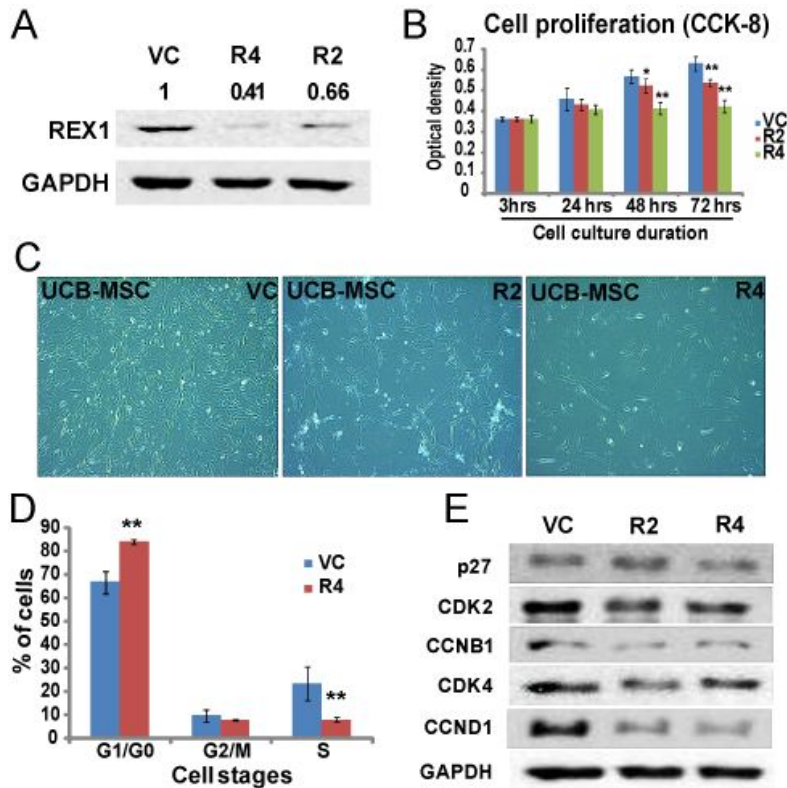
Figure 10 REX1 knockdown resulted in growth retardation of hUCB-MSCs.

(A) The expression of REX1 decreased after REX1-knockdown lenti-virus infection.(B) Cell proliferation of REX1 knocked-down hUCB-MSCs significantly decreased.(C) The morphology of cells on three days after culture. REX1 knocked-down cells are not growing well. (D) Cell cycle arrest was found in REX1 knocked-down hUCB-MSCs by using FACS analysis. (E) The expression levels of cyclins, CDK and cell cycle inhibitors. The expressions of CDK2, CCNB1, CDK4 and CCND1 decreased, but p27 did not change after REX1 knockdown. Error bars represent standard deviation from three independent experiments. **, $p<0.01$.

2.3.3 Phosphorylation of p38 MAPK significantly increased following the knockdown of REX1 in hUCB-MSCs

Among the detected MAPKs in hUCB-MSCs, p38 MAPK signaling significantly changed when REX1 was knocked-down. The expression level of p38 MAPK did not increase after REX1 knockdown; however, the level of Pp38 increased by more than fifty-fold after REX1 was knocked-down in hUCB-MSCs, which was verified in multiple experiments (Fig.11A). SB203580 and SB202190 are potent inhibitors of the p38α and p38β isoforms, respectively, and all p38 MAPK isoforms are inhibited by BIRB796 (Kuma et al., 2005). The hUCB-MSCs express all four types of p38 isoforms (Fig.11B); therefore, REX1 knocked-down hUCB-MSCs were treated with BIRB796. After p38 MAPK inhibitor treatment, the level of Pp38 in REX1 knocked-down hUCB-MSCs was not different compared to vehicle control-infected hUCB-MSCs (Fig.11C and 11E). After BIRB796 treatment, the cell proliferation defect of REX1 knocked-down hUCB-MSCs recovered, and the proliferation rate was similar to the rate in vehicle control-infected hUCB-MSCs (Fig.11D). Similarly, in hUCB-MSCs, 1 μM or 10 μM BIRB796 treatment repressed the phosphorylation of p38 MAPK (Fig.11E). In REX1 knocked-down hUCB-MSCs, the suppressed expression levels of CDK2 and CCND1 recovered after BIRB796 treatment (Fig.11F). The expression of p53 and hyper-phosphorylated RB (PpRB) did not change in REX1 knocked-down cells (Fig.11F). In hUCB-MSCs, the expression levels of ERK1/2 and

Mitogen-Activated Protein Kinase Kinase 1/2 (MAP2K1/2 or MEK1/2) did not change after the knockdown of REX1. The phosphorylation of MEK (pMEK1/2) and NFκB expression were not significantly different after the knockdown of REX1 in hUCB-MSCs compared to vehicle control-infected hUCB-MSCs (Fig.11G). REX1 inhibits signaling via the STAT pathway in F9 cells (Xu et al., 2008); however, the expression of STAT5 did not significantly change after REX1 knockdown in hUCB-MSCs. The expression levels of STAT3 and phosphorylated STAT3 increased after REX1 knockdown without regard to p38 MAPK inhibitor treatment (Fig.11H). After REX1 knockdown in hUCB-MSCs, the expression levels of the p38s did not significantly change (Fig.11I). In addition, BIRB 796 treatment did not influence REX1 expression in hUCB-MSCs (Fig.11J).
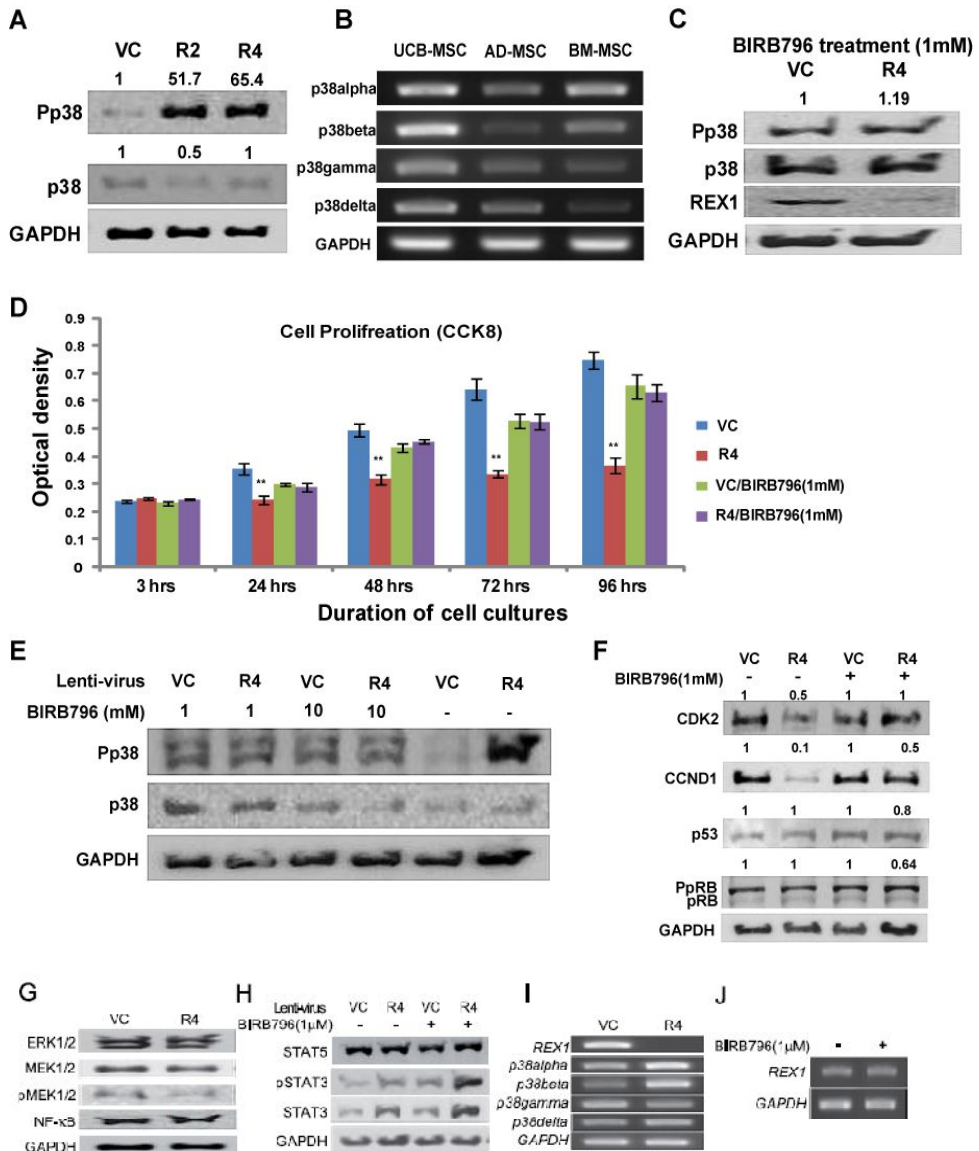
Figure 11 The levels of p38 MAPK, Cyclins and cell cycle inhibitors

changed after REX1 knockdown and p38 MAPK inhibitor treatment

(A) Significant phosphorylation of p38 MAPK (Pp38) was seen after REX1 knockdown in hUCB-MSCs.(B) hUCB-MSCs, hAD-MSCs and hBM-MSCs express all four types of p38 isoforms.(C) After p38 MAPK inhibitor treatment (1μM BIRB796), the phosphorylation of p38 MAPK was similar in REX1 knocked-down

hUCB-MSCs compared to vehicle control-infected hUCB-MSCs.(D) Cell proliferation was measured with CCK-8 for four days. The cell proliferation of REX1 knocked-down hUCB-MSCs was similar with vehicle control-infected hUCB-MSCs after BIRB796 (1μM) treatment. Without BIRB796, the proliferation of REX1 knocked-down hUCB-MSCs significantly decreased compared with vehicle control-infected hUCB-MSCs. **, p<0.01.(E) The p38 MAPK of REX1 knocked-down hUCB-MSCs was not activated after 1μM or 10μM BIRB796 treatment compared to those of vehicle control-infected hUCB-MSCs.(F) Changes in the expression of CDK and cell cycle inhibitors. The decreased expression of CDK2 and CCND1 recovered after p38 MAPK inhibitor treatment. (G) The expression levels of ERK1/2, MEK, phospho-MEK (pMEK1/2) and NFκB did not significantly change after REX1 knockdown in hUCB-MSCs. (H) The expression changes of STAT3 and STAT5. The expression levels of STAT3 and phospho-STAT3 were significantly increased after REX1 knockdown without regard to p38 MAPK inhibitor treatment. STAT5 expression did not change after the knockdown of REX1.(I) p38α and p38β were up-regulated but p38γ was down-regulated after REX1 knockdown in hUCB-MSCs.(J) REX1 expression of hUCB-MSCs did not change after BIRB796 (p38 MAPK inhibitor) treatment.Error bars represent the standard deviation from three independent experiments

2.3.4 MKK3 expression significantly increased after REX1 knockdown

In mammals, MKK3 and MKK6 are well known activators of p38 MAPK via the phosphorylation of p38 MAPK (Inoue et al., 2005). The expression of MKK6 did not significantly change after the knockdown of REX1, but the expression of MKK3 dramatically increased in REX1 knocked-down hUCB-MSCs (Fig.12A). The MKK3 RNA level increased approximately seven-fold as confirmed by real-time RT-PCR. The level of MKK3 protein expression also increased 3.4-fold (Fig.12B). In hMSCs, the expression of MKK3 was in inverse proportion to REX1 expression (Figs.9A and 12C). The expression level of MKK3 in hUCB-MSCs was 20-fold less than the level in hBM-MSCs. Therefore, the direct regulation of MKK3 by REX1 was investigated. The human genomic DNA sequences of MKK3 were analyzed for the presence of the REX1 binding motif. The DNA binding motif of REX1 contains the core sequences of GCAGCCAT or GCCATTA (Kim et al., 2007). In human genomic DNA, only three positions in MKK3 contain consensus sequences for REX1 binding. These consensus sequences are located 1 Kb upstream of the first exon (Promoter region), inside of the first exon (Exon 1) and inside of the first intron (Intron 1) (Fig. 12D). A ChIP assay was performed to confirm the direct binding of REX1 to MKK3, and REX1 specifically binds only to the first exon of MKK3 (Fig.12D). Other

regions of MKK3 did not contain REX1 binding motifs or a positive signal from the ChIP assay.
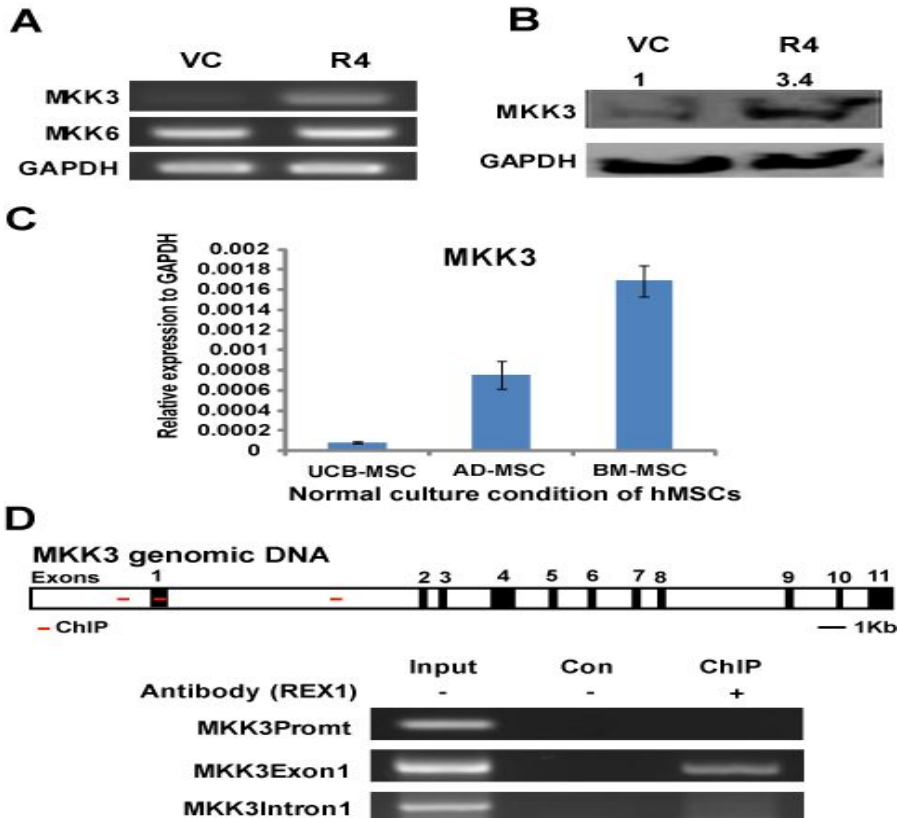
Figure 12 The expressions of ERK, MEK, STAT3/5 and p38s after REX1 knock-down

MKK3 expression significantly increased, but MKK6 did not significantly change after REX1 knockdown as shown by RT-PCR. (B) MKK3 increased after REX1 knockdown at the protein expression level. (C) The expression level of MKK3 in hUCB-MSCs was 20- fold less than the level in hBM-MSCs under normal culture conditions as shown by real-time RT-PCR. (D) The ChIP assay for REX1. Three regions have REX1 consensus sequences in the MKK3 genomic DNA. REX1 binds to the first exon region (MKK3Exon1) of MKK3. Abbreviations: MKK3Promt, MKK3 promoter region; MKK3Exon1, MKK3 exon 1 region; MKK3Intron1, MKK3 intron 1 region. Error bars represent the standard deviation from three independent experiments.

2.3.5 Alterations in the differentiation ability, and NOTCH and WNT signaling, of hUCB-MSCs following REX1 knockdown

The differentiation ability of hUCB-MSCs was investigated after the knockdown of REX1. The adipogenic potentiality in REX1 knocked-down hUCB-MSCs slightly increased or was similar to vehicle control-infected hUCB-MSCs after adipogenic differentiation as shown by Oil Red O staining. However, the osteogenic differentiation potential of REX1 knocked-down hUCB-MSCs visibly deteriorated after osteogenic induction as shown by Alizarin Red S staining (Fig.13A).

Notch signaling is important for the differentiation of MSCs (Grogan et al., 2008; Otto and Rao, 2004). JAGGED1 (JAG1) is a ligand of the NOTCH receptor and plays key roles in cell differentiation and morphogenesis (Guarnaccia et al., 2004). The expression of JAG1 was up-regulated in REX1 knocked-down hUCB-MSCs compared to vehicle control-infected hUCB-MSCs. NOTCH proteins are single-pass trans-membrane receptors that regulate cell fate decisions during development. The expression levels of NOTCH1 and NOTCH4 also increased in REX1 knocked-down hUCB-MSCs compared to vehicle control-infected hUCB-MSCs (Fig.13B). As a consequence, the expression of HES1, a NOTCH target molecule, was up-regulated in REX1 knocked-down hUCB-MSCs compared to vehicle control-infected hUCB-MSCs (Fig.13B).
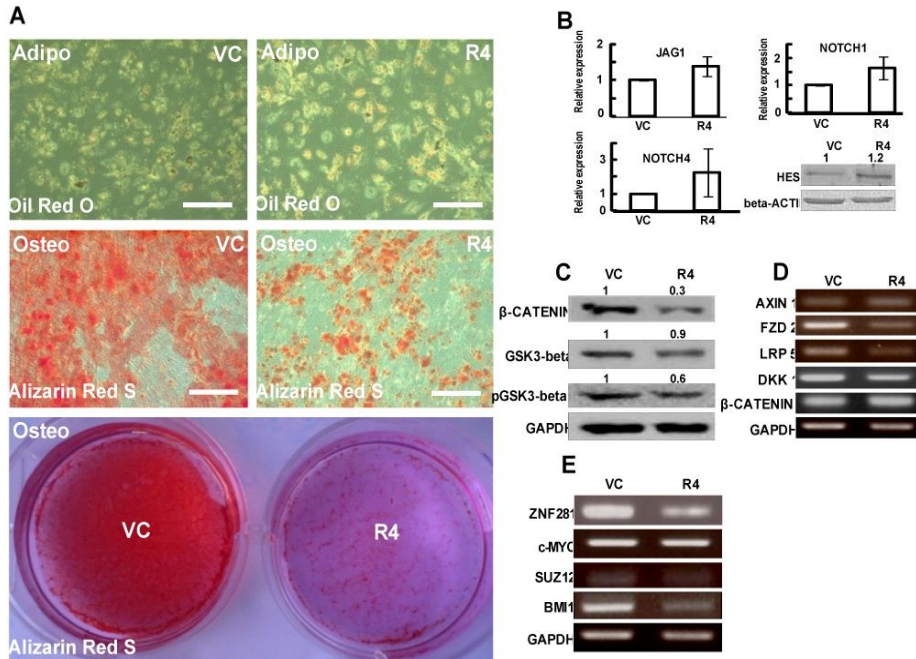
Figure 13 Differentiation study, NOTCH and WNT expression changes in REX1 knocked-down hUCB-MSCs

(A) Adipogenic and osteogenic differentiation of vehicle control and REX1 inhibited hUCB-MSCs. The number of adipogenic differentiated cells was found slightly more in REX1 knocked-down hUCB-MSCs. Osteogenesis was decreased in REX1 knocked-down hUCB-MSCs. (B) The expression changes of NOTCH signaling genes after REX1 knockdown. The expression levels of JAG1, NOTCH1 and NOTCH4 increased after REX1 knockdown. HES1 expression increased 1.2-fold after REX1 knockdown. (C) The expression levels of GSK3-β, pGSK3-β at serine-9 and β-CATENIN decreased in REX1 knocked-down hUCB-MSCs. (D) The expression levels of FZD2, LRP5 and DKK1 decreased after REX1 knockdown in hUCB-MSCs. (E) The expression levels of core transcription factors and PcG genes. The expression level of ZNF281, SUZ12 and BMI1 decreased after REX1 knockdown in hUCB-MSCs. The expression of c-MYC did not change after REX1 knockdown. Abbreviations: Adipo, adipogenic induction; Osteo, osteogenic induction. Error bars represent the standard deviation from three independent experiments. Scale bars represent 100 mm.

Canonical WNT/β-CATENIN signaling also plays an important role in regulating the differentiation of MSCs (Takada et al., 2009; Kawai et al., 2007).The expression levels of β-CATENIN, GSK3-β and phospho-GSK3-β at serine-9 decreased after REX1 inhibition in hUCB-MSCs (Fig.13C). The expression of a WNT signaling related gene, AXIN1, was not significantly different in REX1 knocked-down and vehicle control-infected hUCB-MSCs; however, the expression levels of FZD2, LRP5 and DKK1 decreased in REX1 knocked-down hUCB-MSCs compared to vehicle control-infected hUCB-MSCs (Fig.13D). The expression of ZNF281, a core transcription factor in stem cells that functions during hMSC osteogenesis (unpublished data), decreased in REX1 knocked-down hUCB-MSCs compared to the vehicle control-infected hUCB-MSCs (Fig.13E). The expression of c-MYC, another core transcription factor of stem cells, did not change significantly after REX1 knockdown in hUCB-MSCs. In order to evaluate the changes in expression of other polycomb group genes, the expression levels of two polycomb group genes that are important to maintenance and specification of stem cells (Rajasekhar and Begemann, 2007), SUZ12 and BMI1, were measured. The expression levels of SUZ12 and BMI1 decreased after REX1 knockdown in hUCB-MSCs (Fig.13E).

2.3.6 REX1 inhibition did not affect apoptosis of hUCB-MSCs and Pp38 level was not significantly altered after REX1 knockdown in hBM-MSCs

Apoptosis is influenced by p38 MAPK, which is also important to cell growth. ANNEXIN V is used as a probe in the ANNEXIN V assay to detect cells that express phosphatidyl serine on the cell surface, a feature found in apoptosis as well as other forms of cell death (Koopman et al., 1994; Vermes et al., 1995). ANNEXIN V staining was performed on three hUCB-MSCs clones derived from three different individuals (Fig.14A). The number of apoptotic cells (Q2 and Q4 fraction) or necrotic cells (Q1 fraction) of REX1 knocked-down hUCB-MSCs did not significantly differ from the vehicle control-infected hUCB-MSCs (Fig.14B). The expression of BAX, a marker protein of apoptosis, also did not increase in REX1 knocked-down hUCB-MSCs compared to vehicle control-infected hUCB-MSCs (Fig. 14C).

In hAD-MSCs, the level of Pp38 significantly increased after the knockdown of REX1 similar to hUCB-MSCs. However, in hBM-MSCs, the level of Pp38 increased slightly after REX1 knockdown (Fig. 14D). Basically, in hBM-MSCs, REX1 expression was very low (Fig.9A). Also, under normal culture conditions, the intrinsic Pp38 and MKK3 expression levels were much higher in hBM-MSCs than in hUCB-MSCs or in hAD-MSCs (Figs.9B, 12C and 14D). Therefore, the effect of the REX1 knockdown did not significantly influence Pp38 level in hBM-MSCs compared to other types of hMSCs.
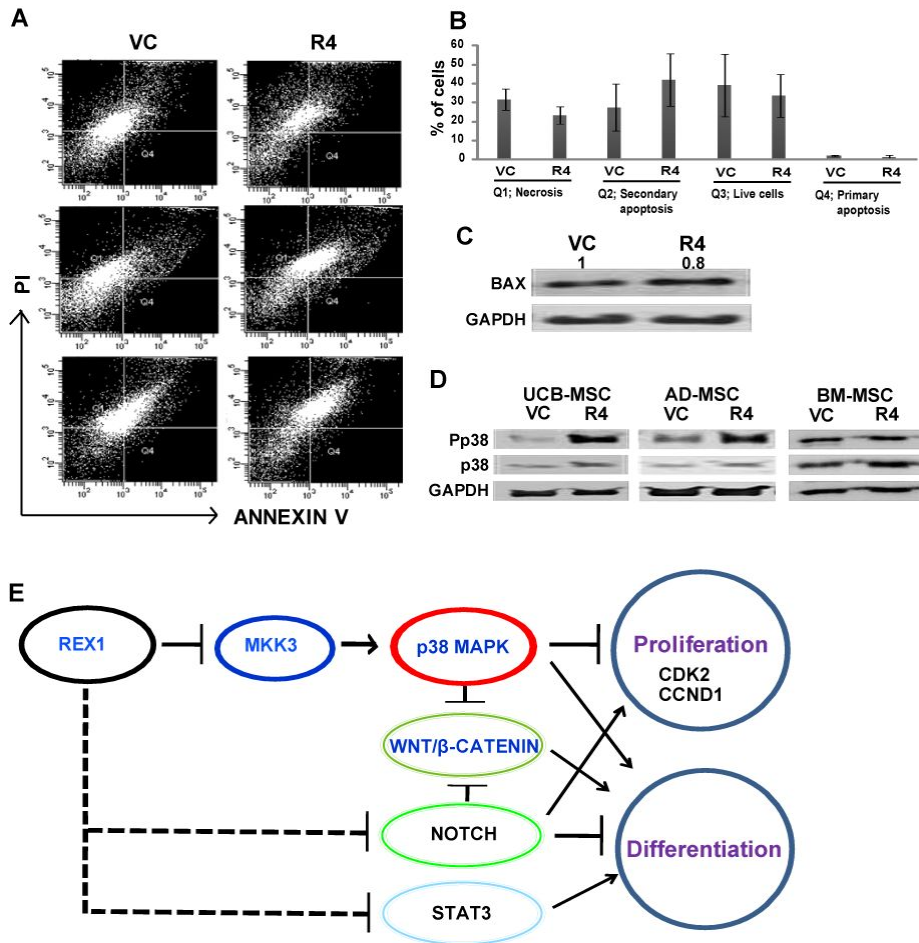
Figure 14 Apoptosis after REX1 knockdown in hUCB-MSCs and REX1

inhibition in hMSCs and the summary of the role of REX1 in stem cells

(A, B) Apoptotic cell death was not significantly different in REX1 knocked-down and vehicle control-infected hUCB-MSCs. (C) The expression of BAX did not change after REX1 knockdown in hUCB-MSCs. (D) Significant activation of p38 MAPK was observed after REX1 knockdown in hUCB-MSCs and hAD-MSCs but only slightly increased in hBM-MSCs. hBM-MSCs, which have low expression of REX1, have highly activated p38 MAPK (Pp38) in vehicle control-infected cells. (E) REX1 suppresses MKK3 expression, which activates p38 MAPK. REX1 also suppresses STAT3 expression and NOTCH signals. Error bars represent the standard deviation from three independent experiments.

2.4 DISCUSSION

The p38 MAPK is important for cell growth, apoptosis and differentiation in mammalian cells. Under specific culture conditions, in hUCB-MSCs, which strongly express REX1, p38 MAPK is suppressed. However, hBM-MSCs, which have weak REX1 expression, have activated p38 MAPK and a high expression level of MKK3 under normal culture conditions. REX1 expression was inversely correlated with p38 MAPK activation and positively correlated with the proliferation rates of the three types of hMSCs examined.

REX1, a pluripotent marker gene, was expressed in some types of hMSCs and cancer cells as well as ESCs. In hUCB-MSCs, the knockdown of REX1 resulted in severe growth retardation. The functions of p38α have been previously reported and p38α is a major component of p38 MAPK in the majority of cells. p38α can negatively regulate cell cycle progression at both the G1/S and G2/M transitions by several mechanisms such as, the down-regulation of Cyclins and the up-regulation of CDK inhibitors (Ambrosino and Nebreda, 2001). In REX1 knocked-down hUCB-MSCs, the cell cycle was arrested primarily in the G0/G1 stage, compared to vehicle control-infected hUCB-MSCs. Passage through the cell cycle requires the successive activation of different cyclin-dependent protein kinases (CDKs) and Cyclins (Nigg, 1995; Murray, 2004) . Cyclin E, in association with CDK2, is required for the G1/S transition (Knoblich et al., 1994; Ohtsubo and Roberts, 1993).

73

Both Cyclin A and the B-type Cyclins associate with CDC2 to promote entry into mitosis (King et al., 1994). The expression levels of CDK2, CCND1 and Cyclin B1 decreased in REX1 knocked-down hUCB-MSCs compared with the levels in vehicle control-infected hUCB-MSCs. The expression levels of CDK2 and CCND1 recovered after p38 MAPK inhibitor treatment in REX1 knocked-down hUCB-MSCs. However, the expression levels of CDK inhibitors, p53 and PpRB, did not change after p38 MAPK inhibitor treatment or REX1 knock-down in hUCB-MSCs. Although p38 MAPK was highly activated in REX1 knocked-down hUCB-MSCs, the cells grew slowly. Notch signaling, which increased in REX1 knocked-down hUCB-MSCs, also regulates stem cell number and has an opposite role of p38 MAPK (Androutsellis-Theotokis et al., 2006). Therefore, in REX1 knocked-down hUCB-MSCs, the growth inhibition signal by activated p38 MAPK was partially compensated by the cell proliferation signals from NOTCH activation.

Activation of p38 MAPK also contributes to chemically-induced cell death (Gills et al., 2007). The possibility of increasing apoptosis in REX1 knocked-down hUCB-MSCs was excluded because the results of the ANNEXIN V assay showed no significant difference between REX1 knocked-down and vehicle control-infected hUCB-MSCs. In addition, the expression of STAT3 increased in REX1 knocked-down hUCB-MSCs, which was also previously reported (Xu et al., 2008). After p38 MAPK inhibitor treatment and REX1 knockdown, the STAT3 activation patterns did not

change, suggesting that STAT3 suppression by REX1 is independent of p38 MAPK signaling.

Activation of p38 MAPK is important for the differentiation of mouse ESCs (Chakraborty et al., 2009) and hMSCs (Platt et al., 2009). The known up-stream regulators of p38 MAPK are MKK3 and MKK6, which are activated in response to many types of cell stresses (Cuenda and Rousseau, 2007; Mittelstadt et al., 2005). However, in stem cells, the transcriptional regulation of MKK3 and MKK6 was not previously reported. REX1 expression is specific to pluripotent stem cells, several types of hMSCs and cancer cells. REX1 is highly expressed in hUCB-MSCs, but MKK3 expression is approximately 20-fold lower in hUCB-MSCs, compared to hBM-MSCs, where REX1 expression is low under normal culture conditions. REX1 suppresses the expression of MKK3 in hMSCs, which was mediated by REX1 binding directly to the first exon of MKK3 (Fig.14E).

The Notch signaling pathway is implicated in the differentiation (Hiraoka et al., 2006; Li et al., 2006) and the immune-modulation of MSCs (Li et al., 2008). Notch signaling inhibits chondrogenesis of hMSCs (Grogan et al., 2008). Also, the expression of the NOTCH ligand and its receptors (JAG1, NOTCH1 and NOTCH 4) increased after the knockdown of REX1 in hUCB-MSCs. Therefore, osteogenic differentiation deformity was partially caused by NOTCH activation after REX1 knockdown in hUCB-MSCs. Notch signaling also has a role in adipogenesis, and in 3T3-L1 cells, the reduction of

Hes-1 inhibits adipogenic differentiation (Ross et al., 2004). The activation of p38 MAPK activates C/EBPβ, a transcription factor that has a critical role in adipogenesis (Ono and Han, 2000). Therefore, after REX1 knockdown in hUCB-MSCs, increased adipogenesis was potentially caused by both NOTCH and p38 MAPK activation. The expression level of HES1, a target molecule of NOTCH signaling, increased in REX1 knocked-down hUCB-MSCs; therefore, REX1 may suppress the NOTCH signaling pathways and maintains the undifferentiated state of hUCB-MSCs (Fig.14E).

In MSCs, Wnt/β-catenin (i.e., canonical) signaling is also important to maintain stemness and multipotency (Etheridge et al., 2004; Boland et al., 2004; Bennett et al., 2005) . β-CATENIN decreased after REX1 knockdown in hUCB-MSCs. The function of GSK3-β, which inactivates β-CATENIN, is inhibited by the phosphorylation of serine-9 (Stambolic and Woodgett, 1994). In REX1 knocked-down hUCB-MSCs, the expression level of GSK3-β decreased, and the level of phosphorylated GSK3-β at serine-9 also decreased. p38 MAPK down-regulates WNT/β-CATENIN signaling via GSK3-β□ (Bikkavilli et al., 2008), which was confirmed by our results. Notch1 over-expression inhibits osteoblastogenesis by suppressing Wnt/β-Catenin signaling (Deregowski et al., 2006), which correlated with osteogenic deformity in REX1 knocked-down hUCB-MSCs. The increased NOTCH signal also caused the suppression of WNT in REX1 knocked-down hUCB-MSCs. Several core transcription factors that have critical roles in ESCs were expressed in hUCB-MSCs. The effect of REX1 knockdown on these

transcription factors was different in each gene expression. The expression of ZNF281 decreased in REX1 knocked-down hUCB-MSCs compared to vehicle control-infected hUCB-MSCs, but the expression of c-MYC did not change when REX1 was knocked-down in hUCB-MSCs. REX1 is considered to be a member of the YY1 gene family which is a polycomb group gene. The expression levels of the polycomb group genes, SUZ12 and BMI1, were reduced in REX1 knocked-down hUCB-MSCs. Therefore, REX1 also has a role in modulating the chromatin structure of hUCB-MSCs, which needs to be further explored.

In conclusion, REX1 represses the expression of MKK3, which can activate p38 MAPK in hMSCs. The high expression level of REX1 in stem cells protects cell differentiation by suppressing p38 MAPK activation via MKK3 suppression and by suppressing NOTCH and STAT3 signaling. ASCs that highly express REX1 have more prominent cell-proliferation ability and multipotency than low REX1-expressing ASCs due to the p38 MAPK suppression in stem cells. Therefore, REX1 is a proper marker not only in ESCs but also in highly efficient multipotent human ASCs. Overall, the suppression of p38 MAPK is useful in the collection and culturing of multipotent human ASCs that do not have sufficient expression levels of REX1. This will be beneficial to the field of regenerative medicine.

CHAPTER III

The simplest Method for *in vitro* β-cell

Production from human adult stem cells

3.1 INTRODUCTION

Stem cell therapy represents a promising tool for the treatment of incurable diseases in the near future because of the unique characteristics of these cells related to the differentiation, regeneration, development, remodeling and replenishment of aged and diseased tissues. Stem cells derived from tissues other than embryos are referred to as adult stem cells. Tissues such as bone-marrow, blood, brain and placenta are sources of adult stem cells. The umbilical cord, umbilical cord blood and placenta become medical waste products following the birth of a baby, and these tissues represent rich sources of stem cells (Magatti et al., 2008; Murphy et al., 2011). Stem cells from these sources have the unique characteristics of being associated with a low risk of graft-versus-host diseases (GVHD), a lack of related ethical issues and easy availability (Zhao and Mazzone, 2011). In comparison, handling embryonic stem cells is more complex and is associated with ethical concerns. Because of the unique characteristics of stem cells from afterbirth byproduct origins, they have obtained a prominent position in the biomedical research field as limitless source of stem cells. Several clinical trials have already been performed in different diseases, including diabetes (Wei et al., 2003), spinal cord injuries (Kang et al., 2005), cardiac diseases (Copeland et al., 2009), lung injuries (Moodley et al.) and neural diseases (Seo et al., 2011), in animal models and in human trials.

Pancreatic β-cells are responsible for maintaining glucose homeostasis in the human body. Autoimmune destruction of β-cells causes diabetes mellitus (DM). It has been reported that 4-5% of world population suffers from DM (Shi et al., 2005). Therefore, there is an urgent need to develop reliable diabetes therapies. Testing blood glucose and injecting insulin represent life-saving therapies that have been practiced for a number of years. Other approaches, such as tissue- and cell-based therapies, have been employed to restore the functional β-cells. Among these methods, pancreatic islet transplantation is considered as a better means of treatment than insulin injection (Serup et al., 2001), but it is also associated with limitations of severe immunosuppression, a lack of sufficient numbers of islet donors and high economic costs. Current studies are focused on cell-based therapies, for which stem cells are the best option because of their therapeutic potential. In this regard, the development of limitless sources of stem cells represents a possible permanent way out for therapy of DM. Research in this field has been aimed at differentiating mouse embryonic stem cells (mES) (Shi et al., 2005; Lumelsky et al., 2001), human embryonic stem cells (hES) (Jiang et al., 2007b; Jiang et al., 2007a; D'Amour et al., 2006), umbilical cord blood (UCB) (Gao et al., 2008), umbilical cord-derived mesenchymal stem cells (UC-MSC) (Wang et al., 2011) and AE-SC (Wei et al., 2003) into insulin-producing cells. The time required for differentiation into insulin-producing cells (IPCs) is variable in every study according to the methods of differentiation and cell sources used. Shortening the time required for differentiation is important to

improve the efficiency of the differentiation process because it can save costs and diminish the possibilities of contamination. Because of their unique characteristics and the fact that they are abundantly available, UCB-MSC, Wharton's jelly-derived mesenchymal stem cells (WJ-MSC) and AE-SC were considered in the current study.

In the present study, we investigated whether the duration of differentiation of the most readily available and potentially unlimited source of stem cells in serum free culture conditions could be shortened for the purpose of making their production more economic, efficient and time and labor saving.

3.2 MATERIALS AND METHODS

3.2.1 Cell isolation and culture

Human amniotic tissue was obtained from Guro Korea Medical Hospital (Seoul, Korea) under informed consent, and isolation and culture were performed with the approval of the Seoul National University Institutional Review Board (IRB No. 0611/001-002). The amniotic tissue was washed several times with PBS to remove blood and incubated with 0.05% trypsin-EDTA (Invitrogen, Carlsbad, USA) for 1 hour. The amniotic epithelial cells were collected and suspended in standard culture media consisting of K-SFM (Keratinocyte-SFM) supplemented with 0.031 µg/µl human recombinant EGF, 12.4 mg/ml bovine pituitary extract (all from Invitrogen) and 10 % fetal bovine serum (FBS, Hyclone, Logan, UT, USA).

Human umbilical cord blood-derived MSC (hUCB-MSCs) collection, isolation and characterization was performed as described previously (Seo et al., 2009; Bhandari et al., 2011a; Bhandari et al., 2011b). For WJ-MSC isolation and culture, we followed the methods explained previously (Wang et al., 2004). In brief, after removing blood vessels from umbilical cord, mesenchymal tissues were scraped off with scalpel from the Wharton's jelly and centrifuged at 2,000 rpm for 5 min. at room temperature. The pellet was washed with serum free DMEM and resuspended in 10 ml of DMEM at 2,000 rpm for 5 min. at room temperature. Then, this pellet was resuspended in 15 ml of DMEM containing 0.2gm/ml of collagenase and incubated for 16 hours

at 37^0 C. Cells were washed , resuspended in 10 ml of DMEM containing 2.5 %

trypsin, incubated 30 min. at 37^0 C with agitation, washed and cultured in

DMEM-HG containing 10 %   FBS   in 5 % CO2 incubator. Cells were

passaged before 90 % confluency. After thawing, all UCB-MSC, WJ-MSC

and AE-SC were cultured in growth medium. Our growth medium contained

Endothelial Cell Basal Medium-2 (EBM-2) (#CC-4176, Lonza, Walkersville,

MD, USA) and the growth factor EGM-2 SingleQuots catalog# CC-4176

(Lonza) supplemented with 10% FBS (# 16000-044, Invitrogen). Cells were

detached with 1X 0.25% Trypsin EDTA (#25200-072, Invitrogen) incubated

for five minutes in an incubator and collected with phosphate buffered saline

(PBS), then spun down at the rate of 2,000 rpm for 5 minutes. The supernatant

was removed, and cells were resuspended with the above mentioned medium

and counted using a hemocytometer chamber. Subculturing was performed in

the same medium with 1 x 10^6 cells per 100-mm diameter NUNC cell culture

dish and cell were cultured until 60-70 % confluency.

3.2.2   In vitro differentiation of cells

All three cell lines, UCB-MSC, WJ-MSC and AE-SC, were grown to

60-70% confluency in growth medium with 10% FBS. Then the medium was

changed into differentiation medium. For differentiation, EBM-2 (Lonza)

supplemented with EGM2 (Lonza) was used as basal differentiation medium.

Our differentiation protocol is divided into two stages. Stage-1: The 70%

confluency cells were washed two times with PBS and cultured for 24 hours

in basal differentiation medium supplemented with 1 mM sodium butyrate (Sigma-Aldrich, St. Louis, MO, USA) and 50 ng/ml Activin A (R&D system). The next day, sodium butyrate was withdrawn. The medium was changed with fresh basal differentiation medium supplemented with 0.1-0.2% bovine serum albumin (Sigma Aldrich) and 50ng/ml Activin A for two more days. Stage-2: Basal differentiation medium was supplemented with 50ng/ml KGF/FGF7 and 1% BSA to prepare stage-2 medium. Before changing into stage-2 medium, cells were washed twice with PBS. Control cells were grown in basal differentiation medium supplemented with 10% FBS. Images of the cells were collected at the end of each stage using an Olympus CKX41 microscope (Olympus, Tokyo, Japan).

3.2.3 RT-PCR

Total RNA was extracted with an easy-spin™ Total RNA Extraction Kit (iNtRON biotechnology, Sungnam, Korea) according to the manufacturer's instructions. cDNA synthesis was performed using the SuperScript® III First-Strand Synthesis System for RT-PCR (Invitrogen) with 2g of total RNA and oligo dT. The primers used for each gene and the annealing temperatures and number of cycles are shown in Table 3. A Hot-Start Taq (#203603, Qiagen) kit was used for RT-PCR amplification. RT-PCR products were loaded into 1.5 to 2.5% agarose gels, stained with ethidium bromide and photographed under ultraviolet light in a Gene Flash (Syngene Bio Imaging, Cambridge, UK) machine.

Table 3 Primer sequences, RT-PCR conditions and product size

Human mRNA	Forward 5'—3'	Reverse 5'—3'
β-ACTIN	CGGCATCGTCACCAACTGGGA	CGTAGATGGGCACAGTGTGGG
CX36	AACGCCGCTACTCTACAGTC	TTGGCCGGGACACATAACAT
GCG	AGGCAGACCCACTCAGTGA	AACAATGGCGACCTCTTCTG
INSULIN	TTCTTCTACACACCCAAGAC	CTAGTTGCAGTAGTTCTCCA
NESTIN	AACAGCGACGGAGGTCTCTA	TTCTCTTGTCCCGCAGACTT
NGN3	CGAATGCACAACCTCAACTC	AGTCAGCGCCCAGATGTAGT
NKX6.1	ACACGAGACCCACTTTTTCCG	TGCTGGACTTGTGCTTCTTCAAC
PDX1	CTCCTACAGCACTCCACCTT	CCGAGTAAGAATGGCTTTAT
PPY	CTGCTGCTCCTGTCCACCTG	CTCCGAGAAGGCCAGCGTGT
SOX17	AGATTGAAAAAACACCCAGG	TTGTTCAGAGATTTGTTTCC

3.2.4 Immunofluorescence staining and quantification

For immunofluorescence staining, 3×10^4 to 5×10^4 cells/well were cultured on a 4-well chamber slide and differentiated according to the differentiation protocol. At the end of differentiation, cells were washed twice with PBS and fixed with 4% paraformaldehyde for 10 minutes at room temperature. After washing with PBS twice, cells were incubated with blocking solutions (10% normal goat serum in PBS) overnight at 4°C. Cells were washed two more times with PBS and then incubated with anti-mouse insulin antibodies (#ab8302, Abcam, Cambridge, MA, USA) at a 1:100 dilution and anti-rabbit C-Peptide (#4020-01, Linco) at a dilution of 1:200 in 5% blocking solution at room temperature for 2 hours 30 minutes. Subsequently, cells were treated with AlexaFluor anti-mouse and anti-rabbit IgG secondary antibodies (Invitrogen) at a dilution of 1:1,000 for 1 hour at room temperature. For nuclear counter-staining, Hoechst 33258 (1g/ml, Sigma) was diluted to 1:500 in PBS, and the cells were incubated with this solution for 15 minutes at room temperature. Images were collected with a confocal microscope (Eclipse TE200, Nikon, Tokyo, Japan).

For the quantification of differentiated (insulin and C-peptide) cells, confocal imaging of three different fields were performed for each cell lines. Total cells (Hoechst positive), insulin positive and C-peptide positive cells were counted using ImageJ version 1.4 (National Institute of Health-NIH)

software and percentage calculated. Clearly stained and almost full stained cells were counted to avoid counting error.

3.2.5 Measurement of extracellular and intracellular protein (insulin and C-peptide) using ELISA

At the end of each stage, the culture medium was collected and stored at -20°C until being assayed. For measurement of secreted insulin and C-Peptide, Ultrasensitive ELISA (#10-1132-01, #10-1141-01, Merocodia, Uppsala, Sweden) kits were used according to the manufacturer's instructions. A TMB substrate was used to read the absorbance at 450 nm. Unit used in this kit for insulin is mU/L and for C-peptide is pmol/L. According to the kit, conversion factor for insulin 1µg/l = 29 mU/L; 1mU/L = 6.0 pmol/L and for C-peptide 1µg/L corresponds to 331 pmol/L.

For intracellular insulin and C-peptide quantification, cells were harvested and lysed with PRO-PREP (#17081, iNtRON biotechnology). Cell lysates were incubated on ice for 20 minutes followed by centrifugation (13,000 rpm, 15 minutes, 4°C) and supernatant collection. The protein concentrations of samples were determined using the Protein Assay Reagent (Bio-Rad laboratories, Hercules, CA, USA) according to the manufacturer's instructions. Fifty microgram (µg) sample protein was used in each well of above mentioned ELISA kit for intracellular insulin and C-peptide quantification.

3.2.6   Glucose stimulation Test

At the end of each stage, cells were washed twice with PBS and cultured in 15 mM glucose containing DMEM and FBS for 2 hours. The medium was then collected and stored at -20°C until being assayed. The secreted C-peptide and insulin in the 15 mM glucose medium was measured according to the protocol of the Mercodia Ultrasensitive ELISA kit (Merocodia).

3.2.7   Statistical analysis

The results were presented as the mean ± standard deviation (SD). The statistical significance of the differences was tested with the Student's t-test in Microsoft Office Excel (2007). In all comparisons, values of $P<0.05$ (*) and $P<0.01$ (**) were considered statistically significant.

3.3 RESULTS

3.3.1 In vitro differentiation of adult stem cells into insulin-producing cells

After analyzing different protocols (Table 4) used for differentiating insulin-producing cells from various sources of stem cells, we designed the methods used here to obtain insulin-producing cells in as short duration as possible using adult stem cells. Thus, UCB-MSC, WJ-MSC and AE-SC were used in the present study. These cells were cultured in growth medium up to 60-70 % confluency, and the medium was then changed to stage-1 and stage-2 media, as per our differentiation protocol. Cell proliferation was continuous up to the 1st day of stage-1, and almost completely stopped thereafter. The maturation of UCB-MSC and WJ-MSC could be observed (Fig. 15). AE-SC became large and flattened in this stage. In stage-2, approximately 20-30 % of cells detached from the surface in each cell line. It was assumed that the differentiation medium became unfavorable for these cells. AE-SC became thicker epithelial cells, and some of the cells showed phenotypes of other lineages.
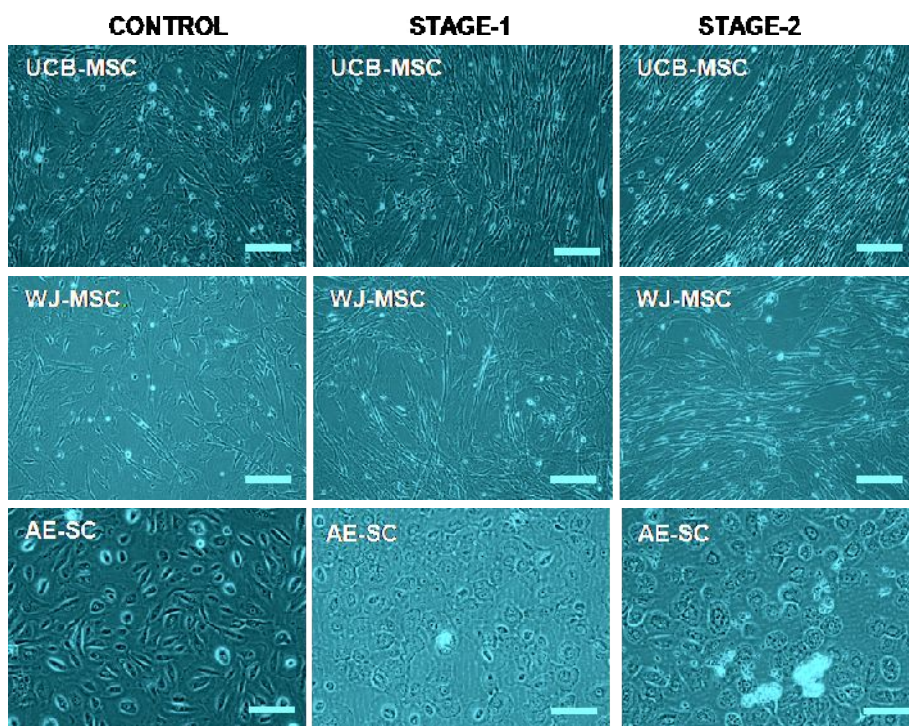
Figure 15 Phenotypes of cells during differentiation

Umbilical cord blood derived mesenchymal stem cells (UCB-MSC), Wharton's Jelly derived mesenchymal stem cells (WJ-MSC) and amniotic epithelial derived stem cells (AE-SC) cultured in basal medium (control), differentiating media (stage-1 and stage-2). Cell proliferation was continuous in all three different cell lines in stage-1. AE-SCs increased in size and became more flattened in stage-1. In stage-2 cell proliferation stopped, maturation of cell took place and some cells detached from the surface in all three different cell lines. AE-SCs became more thick epithelial and some of the cells showed phenotypes other lineages. Scale bar represents 50 µm.

Table 4 Comparison of duration for differentiation of stem cells' into

insulin producing cells (IPCs)

Duration (days)	Cells	Stage1	Stage2	Stage3	Stage4	Stage5	References
6	hUCB MSC, WJ-MSC and AE-SC	EBM2--- 3 days	EBM2--- 3days				N/A
24-27	mES	DMEM--- 2-3 days	DMEM--- 4 days	DMEM-- 6-7 days	DMEM--- 6 days	DMEM - 6 days	(Lumelsky et al., 2001)
7-12	mES	DMEM--- 1-2 days	DMEM--- 3-5days	DMEM/ F12---- 3-5 days			(Shi et al., 2005)
11-15 +	hES	RPMI--- 2-4 days	RPMI--- 2-4 days	DMEM-- 2-4 days	DMEM-- 2-3 days	CMRL-- 3+ days	(D'Amour et al., 2006)
36	hES	RPMI --- 7 days	RPMI--- 15 days	RPMI--- 7 days	RPMI--- 7 days		(Jiang et al., 2007a)
20	hES	CDM--- 2 days	CDM --- 4 days	CDM--- 4 days	DMEM/ F12--- 3days	DMEM/ F12--- 7 days	(Jiang et al., 2007b)
15	hUCB-MSC	DMEM-H --- 1 day	DMEM-H-- - 2 days	DMED-L ---- 6 days	DMEM-L----. 6 days		(Gao et al., 2008)
17	hUC-MSC	CMRL 1066 7 days	DMEM/F12 7 days	DMEM/ F12 3 days			(Wang et al., 2011)

N/A, Non-applicable

3.3.2 Pancreatic endocrine differentiation was confirmed by RT-PCR analysis

RT-PCR analysis was performed using marker genes for definitive endoderm (SOX17), pancreatic endoderm/pancreatic endocrine precursors (PDX1, NGN3, and NKX6.1) and pancreatic endocrine cells (INS, GCG, and PPY) (D'Amour et al., 2006). A suitable basal medium was also determined based on the gene expression pattern observed in the cells grown in three different media (EBM2, DMEM-LG and DMEM-HG). We used all three media supplemented with 1% BSA for the culture of control UCB-MSC until the end of the differentiation period. Gene expression was analyzed by RT-PCR (Fig. 16A). We did not detect the expression of insulin in any stage, although expression of SOX17 and PDX1 was observed. SOX17 and PDX1 were highly expressed in stage-1 and stage-2 in EBM2 medium, although they were only expressed in stage-1 in DMEM-LG and stage-2 in DMEM-HG medium, respectively (Fig. 16A). These data suggested that EBM2 is more suitable for our purposes than the other two types of media. All three different cell lines were positive for NESTIN from the beginning to the end of the differentiation process, except in stage-2 for AE-SCs (Fig. 16B). SOX17 was also expressed continuously up to stage-2 in UCB-MSC and AE-SC, but it was only clearly observable in stage-1 in WJ-MSC. PDX1 and NKX6.1 expression was maintained in all of the cells during the differentiation period. However, strong expression of NGN3 was observed in stage 2 in all cells,

except for WJ-MSC, in which weak expression was seen from the beginning of the experiment. The pancreatic endocrine marker genes INS, GCG and PPY were clearly detected in stage-2 in all cell lines. However, GCG was weakly expressed in the beginning of the experiment in WJ-MSC, but it was expressed at a considerable level in stage-1. Additionally, the β cell specific gap junction-related gene CX-36 was expressed well in all of our cells in stage-2.
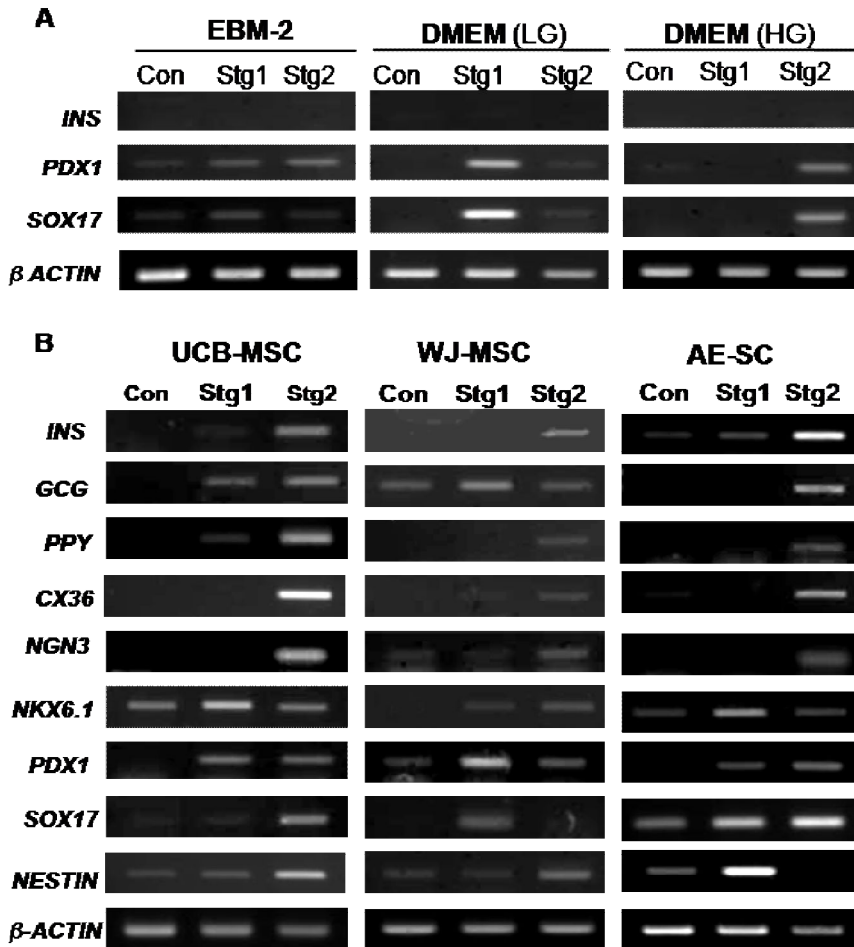
Figure 16 Gene expression pattern of three different types of cells during differentiation into insulin producing cells

(A) Gene expression pattern of UCB-MSC cells cultured in three different basal media during the total duration of differentiation. In all three basal media insulin was not expressed in full duration of differentiation. SOX17 and PDX1 expression was detected in early stage of differentiation in EBM-2 medium, which is better than other media. (B) Gene expression pattern of UCB-MSC, WJ-MSC and AE-SC cells cultured in basal medium (Con), stage-1 (Stg1) and stage-2 (Stg2) differentiation media.

3.3.3   Insulin and C-peptide protein expression were confirmed by Immunofluorescence analysis in differentiated cells

Double immunofluorescence staining (insulin and C-peptide) were performed for UCB-MSC, WJ-MSC and AE-SC in control, stage-1 and stage-2 conditions, respectively. Only stage-2 cells expressed insulin (red) and C-peptide (green) in all three different cell lines (Fig.17). Cytoplasmic localization of insulin and C-peptide was clear in UCB-MSC and AE-SC (Fig.17A and 17C), but it was not clearly seen in WJ-MSC (Fig.17B) because of the nucleus was located deeply inside of the WJ-MSC. Co-localization of insulin and C-peptide was confirmed (light yellow cells) in merged figures. Nuclei (blue) were counterstained with HOECHST. Quantification of insulin and C-peptide positive cells was performed (Fig.17D) using ImageJ software. 22.6%, 17.8% and 34.54 % insulin positive cells were found in UCB-MSC, WJ-MSC and AE-SC respectively. Similarly 25.5%, 18.0% and 37.1% C-peptide positive cells were found in above mentioned cell lines respectively.
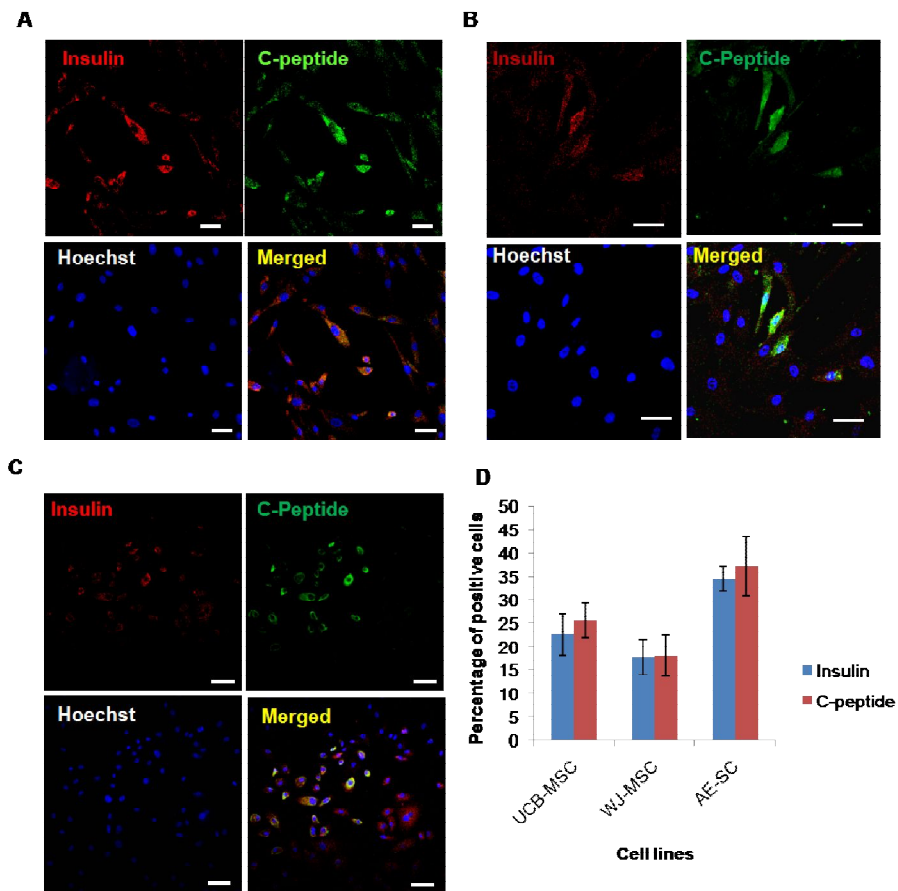
Figure 17 Immunofluorescence analysis of insulin (red) and C-peptide (green) expressing cells at stage-2 of differentiation

(A) Cytoplasmic localization of Insulin (red) upper left and C-peptide (green) upper right was detected in UCB-MSC. Counter staining of nucleus (blue) was done with Hoechst (lower left). Co-localization of insulin and C-peptide (light yellow) positive cells are shown in merged picture (lower right corner). Similar results were found in WJ-MSC (B) and AE-SC (C) respectively. (D) Percentage based quantification of differentiated insulin positive cells (blue bar) and C-peptide positive cells (red bar) of UCB-MSC, WJ-MSC and AE-SC respectively. Scale bar represents 50 µm.

3.3.4 Significant amounts of extracellular and intracellular Insulin and C-peptide were found in the differentiated cells

To determine the levels of secreted C-peptide and insulin in the culture media, media collected at each stage were subjected to ELISA tests. A significant difference was observed in the amount of C-peptide (14.98±0.63 pM/L) in differentiated UCB-MSC in comparison with undifferentiated cells (7.29±0.79 pM/L) (Fig. 18A). A clear difference also found in WJ-MSC (14.65±0.79 pM vs. 9.74±1.73 pM), although it was not statistically significant. The amount of C-peptide released from differentiated AE-SC was 16.46 ± 0.014 pM/L, which was significantly different than the undifferentiated cells (6.21± 1.2 pM/L).

Also the amount of insulin secreted (0.233±0.01 mU/L) from differentiated UCB-MSC was significantly different than secreted from (0.04±0.02 mU/L) control UCB-MSC. (Fig.18B). In WJ-MSC, the level of insulin (0.43±0.04 mU/L) in the medium of differentiated cells was found to be significantly different that of control cells (0.16±0.03 mU/L). AE-SC released 0.04±.01 mU/L insulin from differentiated cells, and undifferentiated cells also released very small amounts (0.005± 0.01 mU/L). The amount of secreted insulin in the medium seemed to be less in AE-SC, possibly due to degradation during storage.

In addition to secreted C-peptide and insulin, the intracellular C-peptide and insulin were also determined for further confirmatory test. Highly

significant amount of C-peptide was found (1.90±0.19µg/mg) in differentiated UCB-MSC and significant amount (3.84±0.8µg/mg, 1.73±0.24µg/mg) was found in differentiated WJ-MSC and AE-SC respectively (Fig.18C). However, C-peptide was not detected in control cells. Similarly significant amount of insulin was determined in differentiated cells compared to control cells; 122±12ng/mg vs 26.31±11.93ng/mg in UCB-MSC, 127.6±19.9ng/mg vs 6.62±15.92ng/mg in WJ-MSC and 133.24±11.94ng/mg vs 0.98±7.95 ng/mg in AE-SC cells   (Fig.18D).
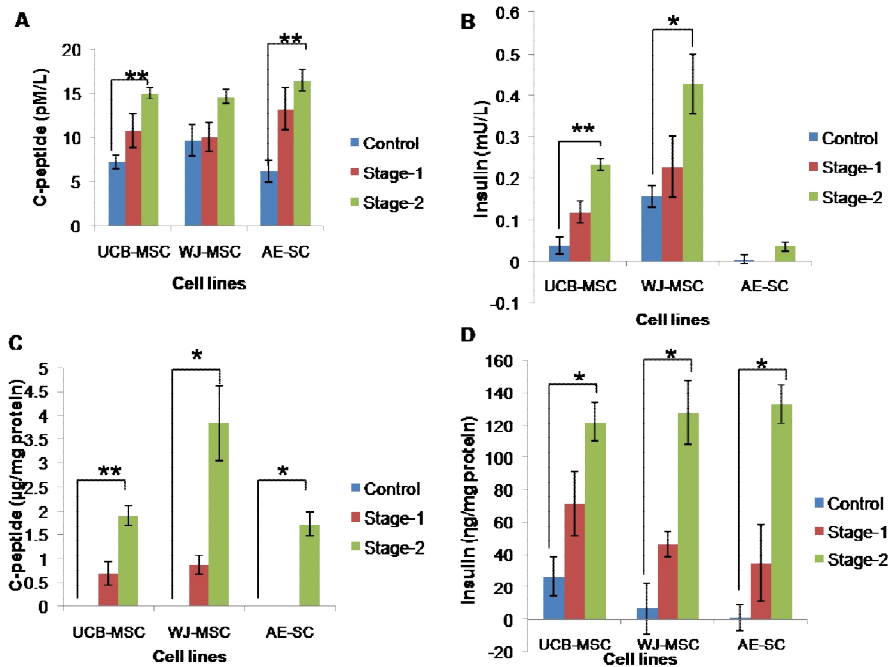
Figure 18 Quantification of secreted and intracellular C-peptide and insulin by ELISA

(A) Quantification of C-peptide released in cultured media (control, stage-1 and stage-2) during differentiation from UCB-MSC, WJ-MSC and AE-SC. Statistically significant amount of C-peptide was released in stage-2 cultured medium from UCB-MSC and AE-SC than in control medium. Numerically higher amount of C-peptide was found in WJ-MSC too. (B) Quantification of released insulin in cultured media during differentiation from the cells. Statistically significant amount of insulin was found in UCB-MSC and WJ-MSC in stage-2 medium than control medium. However, numerically higher amount of insulin was released in stage-2 cultured medium from AE-SC than control cells. (C) Quantification of intracellular C-peptide from each cell line, in which highly significant amount of C-peptide was found in UCB-MSC and significant amount was in WJ-MSC and AE-SC respectively in stage-2 versus control cells. (D) Quantification of intracellular insulin in each cell lines, statistically significant amount of insulin was detected in all there (UCB-MSC, WJ-MSC, AE-SC) stage-2 cells compared to control cells. *, $p < 0.05$; **, $p < 0.01$.

3.3.5 Differentiated cells showed a positive response to glucose stimulation tests

Differentiated (UCB-MSC) cells were cultured in serum-free medium with different glucose concentrations (5.5, 15, 25 mM) for 2 hours. Cells that were cultured in PBS for 2 hours were considered as 0 mM glucose. The amount of secreted C-peptide in the culture medium was measured with a Merocodia ultra-sensitive ELISA kit. Cells in 5.5 mM glucose secreted 15.90±0.19 pM/L C-peptide, and those in 15 mM glucose secreted 32.7±1.87 pM/L C-peptide. However, cells cultured in 0 mM glucose secreted 7.97±0.19 pM/L, and cells in 25 mM glucose secreted 7.17±0.9 pM/L C-peptide, respectively (Fig. 19A). The highest concentration of C-peptide (32.7 ± 1.87 pM/L) was obtained in 15 mM glucose-containing medium. Therefore, the 15 mM glucose concentration was considered to be the best concentration for subsequent experiments.

The amount of C-peptide secreted in response to 15 mM glucose is shown in Fig. 19B for all cell lines. Differentiated UCB-MSC were observed to secrete a significantly higher amount (17.55±0.47 pM/L) of C-peptide than undifferentiated cells (10.86±2.3 pM/L). A similar result was obtained in WJ-MSC, such that differentiated cells secreted 16.99±0.94 pM/L, and undifferentiated cells secreted 9.74±1.73 pM/L C-peptide. In the case of AE-SC, differentiated cells secreted a greater amount of C-peptide (21.23± 0.24 pM/L) than did undifferentiated cells (14.06±3.14 pM/L).

The results for the glucose (15 mM) challenge test and the amount of secreted insulin are shown in Fig. 19C. For UCB-MSC, the differentiated cells secreted 0.25 ± 0.04 mU/L, and the control cells secreted 0.07 ± 0.01 mU/L insulin. Similarly, differentiated WJ-MSC secreted 0.37 ± 0.04 mU/L, and the control cells secreted 0.25 ± 0.02 mU/L insulin. In the case of AE-SC, only differentiated cells responded to the glucose stimulation, secreting 0.26 ± 0.04 mU/L insulin. Thus, in this study, we observed that differentiated cells were able to secrete a statistically significantly greater amount of insulin than the undifferentiated cells. Three independent experiments were performed for the glucose stimulation tests for each cell line.
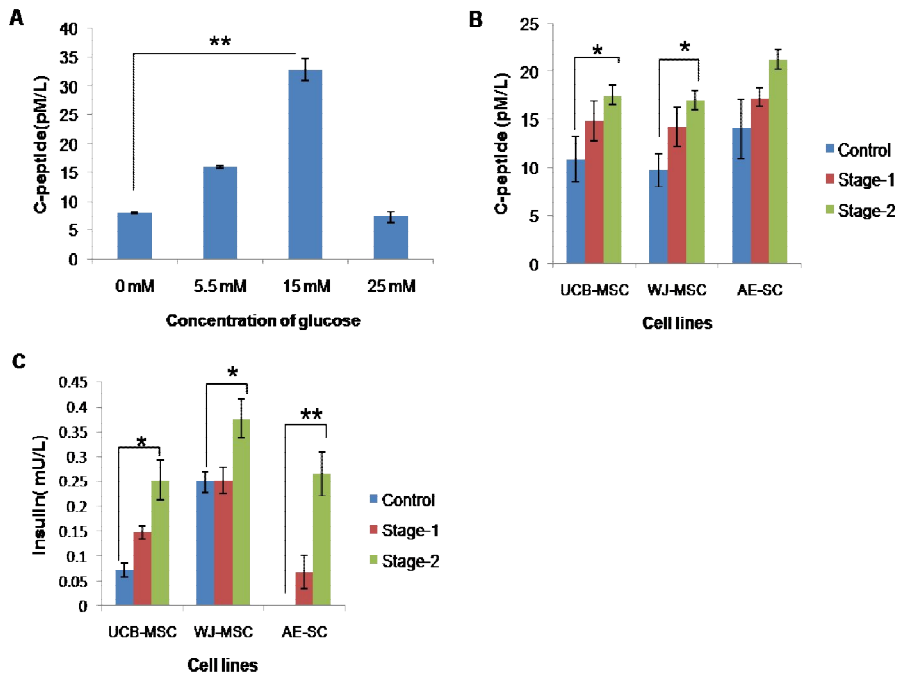
Figure 19 Quantification of released C-peptide and Insulin in cultured medium after glucose (15mM) stimulation test by ELISA

(A) Optimum concentration of glucose determination for glucose stimulation test. C-peptide was measured after two hours of incubation in differentiated UCB-MSC in four different concentrations (0, 5.5, 15 and 25 mM) of glucose containing medium. Statistically significant amount of C-peptide was detected in 15mM glucose containing medium. (B) Quantification of released C-peptide in 15 mM glucose containing DMEM from UCB-MSC, WJ-MSC and AE-SC. Statistically significant amount of C-peptide was released from UCB-MSC and WJ-MSC. (C) All three different cell lines (UCB-MSC, WJ-MSC and AE-SC) had released significant amount of insulin in stage-2 culture medium. *, $p < 0.05$; **, $p<0.01$.

3.4 **DISCUSSION**

An in vitro study of pancreatic β-cell production using the fastest and easiest method developed for this purpose to date was performed using adult stem cells, including UCB-MSC, WJ-MSC and AE-SC. Adult stem cells are readily available and are not associated with any ethical concerns. NESTIN-positive cells play a pivotal role in β-cell production (Treutelaar et al., 2003). Therefore, NESTIN-positive cells were used in this study. Based on a comparative analysis of different protocols (Table 4) and types of cells that have been used for differentiation into insulin producing cells, a new protocol was designed. In almost all studies, Activin-A has been considered to be the principle factor required for endoderm differentiation (Shi et al., 2005; Jiang et al., 2007a; Jiang et al., 2007b; D'Amour et al., 2006) leading to pancreatic progenitors cell differentiation. A combination of Activin A and sodium butyrate treatment can enhance endoderm differentiation into pancreatic endoderm in a short period in serum-free medium (Goicoa et al., 2006; Sulzbacher et al., 2009). In this study, we treated cells with a combination of Activin A (50 ng/ml) and sodium butyrate (1 mM) for 24 hours in serum-free medium, followed by treatment with Activin A alone for an additional 2 days in 0.1% bovine serum albumin in stage-1. This combination enhanced the expression of SOX17 and PDX1. Based on the previous report, growth factors play a critical role in terminal differentiation into pancreatic β-cells (Sulzbacher et al., 2009; Soria, 2001); including fibroblast growth factor

(FGF), epidermal growth factor (EGF), vascular endothelial growth factor (VEGF) and insulin-like growth factor-1 (IGF-1).These growth factors were included in the basal medium in this study. Insulin was not observed to be secreted from the cells in the basal medium. However, following the addition of keratinocyte growth factor (KGF)/fibroblast growth factor 7 (FGF7), insulin was detected in the stage-2 of the present study (Fig. 16). This finding is in accordance with the findings of previous studies (Movassat et al., 2003; Ye et al., 2005; Sulzbacher et al., 2009; Uzan et al., 2009) that noted the role of KGF/FGF 7 in β-cell differentiation. In addition to insulin, glucagon and pancreatic polypeptide were found to be well expressed in stage-2. Additionally, NGN3 was expressed in stage-2 in the entire cell types used in our study. Expression of the above-mentioned genes leads to functional beta cell production (Murtaugh, 2007; Mfopou et al., 2011).

Most reports mentioned in Table 4 have noted that islet-like clusters are a common phenomenon during pancreatic cell differentiation. However, the absence of islet-like clusters during the differentiation of umbilical cord-derived mesenchymal stem cells has also been reported (Wang et al., 2011). These clusters were not observed during the differentiation of cells in the present study. This could be due to differences in culture condition and the character of the cells used. During the differentiation process, a β-cell specific gene, CX36 was well expressed. The expression of CX36 has been reported to be correlated with insulin expression (Serre-Beinier et al., 2009; Le Gurun et al., 2003; Tai et al., 2003). In addition to our gene expression results, C-

peptide and insulin were clearly detected in immunofluorescence experiments (Fig.17A-C). Immunofluorescence quantification result had showed that more AE-SC cells (nearly 35%) were insulin and C-peptide positive than UCB-MSC (nearly 25%) and WJ-MSC (nearly18%) respectively (Fig.17D) which is improvement in terms of number of differentiated pancreatic β cell than previous studies (Lumelsky et al., 2001; D'Amour et al., 2006; Jiang et al., 2007b).

Extracellular C-peptide and insulin were detected in the culture media of differentiated cells, indicating that the cells are functional (Fig.18A-B). On the other hand intracellular C-peptide (> 1.7 µg/mg) and insulin (> 127ng/mg) content of this study (Fig.18C-D) showed the encouraging result compared to the published report mentioned in Table 4 (Shi et al., 2005; Jiang et al., 2007b). However, the intracellular insulin and C-peptide values were almost similar to the report by Lumelsky et al. (Lumelsky et al., 2001). In this study, it is revealed that number of differentiated cells (Fig.17D) and intracellular insulin/C-peptide concentration (Fig.18C-D) among the three different cell lines are quite different. It might be due to size and cytoplasmic volume of cells.

For further confirmation of this, glucose stimulation tests were performed in complete serum-free medium for 2 hours. The amounts of C-peptide and insulin secreted by differentiated cells were significantly higher than in control cells (Fig.19B and 19C). The average levels of C-peptide and

insulin secreted after glucose stimulation were calculated to be approximately 17 pM/L and 0.25 mU/L, respectively. The normal human blood serum range of C-peptide to be approximately 600 pM/L (Beischer et al., 1976; Gjessing et al., 1989; Wahren et al., 2000) and that of insulin to be 10 mU/L (Bristow and Das, 1988). The amounts of C-peptide and insulin found to be secreted in the present study were calculated to represent 1/34 parts and 1/40 parts of the normal ranges of these substances, respectively. Based on the number of cells investigated here ($1X10^6$ per 100 mm culture dish), this secreted amount is reasonable. Although the amount of secreted insulin and C-peptide was quite low, the differentiated cells had shown the physiological response with concentration of glucose, which encourage for further improvement for better results.

In summary, our protocol resulted in the production of pancreatic β-cells by the most-rapid means employed to date. This protocol can be considered to be efficient, economical and time saving. It also reduces the possibility of contamination and harmful effects on the cells. Additional studies are needed to demonstrate the applications of this finding for therapeutic purposes.

REFERENCES

Adhikary, S., and Eilers, M. (2005) Transcriptional regulation and transformation by Myc proteins. Nat Rev Mol Cell Biol 6:635-645.

Ambrosino, C., and Nebreda, A.R. (2001) Cell cycle regulation by p38 MAP kinases. Biol Cell 93:47-51.

Androutsellis-Theotokis, A., Leker, R.R., Soldner, F., Hoeppner, D.J., Ravin, R., Poser, S.W., Rueger, M.A., Bae, S.K., Kittappa, R., and McKay, R.D. (2006) Notch signalling regulates stem cell numbers in vitro and in vivo. Nature 442:823-826.

Beischer, W., Heinze, E., Keller, L., Raptis, S., Kerner, W., and Pfeiffer, E.F. (1976) Human C-peptide. Part II: Clinical studies. Klin Wochenschr 54:717-725.

Ben-Shushan, E., Thompson, J.R., Gudas, L.J., and Bergman, Y. (1998) Rex-1, a gene encoding a transcription factor expressed in the early embryo, is regulated via Oct-3/4 and Oct-6 binding to an octamer site and a novel protein, Rox-1, binding to an adjacent site. Mol Cell Biol 18:1866-1878.

Bennett, C.N., Longo, K.A., Wright, W.S., Suva, L.J., Lane, T.F., Hankenson, K.D., and MacDougald, O.A. (2005) Regulation of osteoblastogenesis and bone mass by Wnt10b. Proc Natl Acad Sci U S A 102:3324-3329.

Bhandari, D.R., Seo, K.W., Jung, J.W., Kim, H.S., Yang, S.R., and Kang, K.S. (2011a) The regulatory role of c-MYC on HDAC2 and PcG expression in human multipotent stem cells. J Cell Mol Med 15:1603-1614.

Bhandari, D.R., Seo, K.W., Roh, K.H., Jung, J.W., Kang, S.K., and Kang, K.S. (2011b) REX-1 expression and p38 MAPK activation status can determine proliferation/differentiation fates in human mesenchymal stem cells. PLoS One 5:e10493.

Bhatia, R., and Hare, J.M. (2005) Mesenchymal stem cells: future source for reparative medicine. Congest Heart Fail 11:87-91; quiz 92-83.

Bikkavilli, R.K., Feigin, M.E., and Malbon, C.C. (2008) p38 mitogen-activated protein kinase regulates canonical Wnt-beta-catenin signaling by inactivation of GSK3beta. J Cell Sci 121:3598-3607.

Boiani, M., Eckardt, S., Scholer, H.R., and McLaughlin, K.J. (2002) Oct4 distribution and level in mouse clones: consequences for pluripotency. Genes Dev 16:1209-1219.

Boland, G.M., Perkins, G., Hall, D.J., and Tuan, R.S. (2004) Wnt 3a promotes proliferation and suppresses osteogenic differentiation of adult human mesenchymal stem cells. J Cell Biochem 93:1210-1230.

Boyer, L.A., Lee, T.I., Cole, M.F., Johnstone, S.E., Levine, S.S., Zucker, J.P., Guenther, M.G., Kumar, R.M., Murray, H.L., Jenner, R.G., Gifford,

D.K., Melton, D.A., Jaenisch, R., and Young, R.A. (2005) Core transcriptional regulatory circuitry in human embryonic stem cells. Cell 122:947-956.

Brehm, A., Miska, E.A., McCance, D.J., Reid, J.L., Bannister, A.J., and Kouzarides, T. (1998) Retinoblastoma protein recruits histone deacetylase to repress transcription. Nature 391:597-601.

Bristow, A.F., and Das, R.E. (1988) WHO international reference reagents for human proinsulin and human insulin C-peptide. J Biol Stand 16:179-186.

Campagnoli, C., Roberts, I.A., Kumar, S., Bennett, P.R., Bellantuono, I., and Fisk, N.M. (2001) Identification of mesenchymal stem/progenitor cells in human first-trimester fetal blood, liver, and bone marrow. Blood 98:2396-2402.

Canelles, M., Delgado, M.D., Hyland, K.M., Lerga, A., Richard, C., Dang, C.V., and Leon, J. (1997) Max and inhibitory c-Myc mutants induce erythroid differentiation and resistance to apoptosis in human myeloid leukemia cells. Oncogene 14:1315-1327.

Cartwright, P., McLean, C., Sheppard, A., Rivett, D., Jones, K., and Dalton, S. (2005) LIF/STAT3 controls ES cell self-renewal and pluripotency by a Myc-dependent mechanism. Development 132:885-896.

Chakraborty, S., Kang, B., Huang, F., and Guo, Y.L. (2009) Mouse embryonic stem cells lacking p38alpha and p38delta can differentiate to endothelial cells, smooth muscle cells, and epithelial cells. Differentiation 78:143-150.

Cheng, M., Olivier, P., Diehl, J.A., Fero, M., Roussel, M.F., Roberts, J.M., and Sherr, C.J. (1999) The p21(Cip1) and p27(Kip1) CDK 'inhibitors' are essential activators of cyclin D-dependent kinases in murine fibroblasts. EMBO J 18:1571-1583.

Copeland, N., Harris, D., and Gaballa, M.A. (2009) Human umbilical cord blood stem cells, myocardial infarction and stroke. Clin Med 9:342-345.

Cowling, V.H., and Cole, M.D. (2006) Mechanism of transcriptional activation by the Myc oncoproteins. Semin Cancer Biol 16:242-252.

Cuenda, A., and Rousseau, S. (2007) p38 MAP-kinases pathway regulation, function and role in human diseases. Biochim Biophys Acta 1773:1358-1375.

D'Amour, K.A., Bang, A.G., Eliazer, S., Kelly, O.G., Agulnick, A.D., Smart, N.G., Moorman, M.A., Kroon, E., Carpenter, M.K., and Baetge, E.E. (2006) Production of pancreatic hormone-expressing endocrine cells from human embryonic stem cells. Nat Biotechnol 24:1392-1401.

Dang, C.V., O'Donnell, K.A., Zeller, K.I., Nguyen, T., Osthus, R.C., and Li, F. (2006) The c-Myc target gene network. Semin Cancer Biol 16:253-264.

de Alboran, I.M., O'Hagan, R.C., Gartner, F., Malynn, B., Davidson, L., Rickert, R., Rajewsky, K., DePinho, R.A., and Alt, F.W. (2001) Analysis of C-MYC function in normal cells via conditional gene-targeted mutation. Immunity 14:45-55.

Deregowski, V., Gazzerro, E., Priest, L., Rydziel, S., and Canalis, E. (2006) Notch 1 overexpression inhibits osteoblastogenesis by suppressing Wnt/beta-catenin but not bone morphogenetic protein signaling. J Biol Chem 281:6203-6210.

Dominguez-Sola, D., Ying, C.Y., Grandori, C., Ruggiero, L., Chen, B., Li, M., Galloway, D.A., Gu, W., Gautier, J., and Dalla-Favera, R. (2007) Non-transcriptional control of DNA replication by c-Myc. Nature 448:445-451.

Engelman, J.A., Lisanti, M.P., and Scherer, P.E. (1998) Specific inhibitors of p38 mitogen-activated protein kinase block 3T3-L1 adipogenesis. J Biol Chem 273:32111-32120.

Erices, A., Conget, P., and Minguell, J.J. (2000) Mesenchymal progenitor cells in human umbilical cord blood. Br J Haematol 109:235-242.

Etheridge, S.L., Spencer, G.J., Heath, D.J., and Genever, P.G. (2004) Expression profiling and functional analysis of wnt signaling mechanisms in mesenchymal stem cells. Stem Cells 22:849-860.

Fernandez, P.C., Frank, S.R., Wang, L., Schroeder, M., Liu, S., Greene, J., Cocito, A., and Amati, B. (2003) Genomic targets of the human c-Myc protein. Genes Dev 17:1115-1129.

Frye, M., Fisher, A.G., and Watt, F.M. (2007) Epidermal stem cells are defined by global histone modifications that are altered by Myc-induced differentiation. PLoS One 2:e763.

Gao, F., Wu, D.Q., Hu, Y.H., and Jin, G.X. (2008) Extracellular matrix gel is necessary for in vitro cultivation of insulin producing cells from human umbilical cord blood derived mesenchymal stem cells. Chin Med J (Engl) 121:811-818.

Gao, L., Cueto, M.A., Asselbergs, F., and Atadja, P. (2002) Cloning and functional characterization of HDAC11, a novel member of the human histone deacetylase family. J Biol Chem 277:25748-25755.

Gartel, A.L., and Shchors, K. (2003) Mechanisms of c-myc-mediated transcriptional repression of growth arrest genes. Exp Cell Res 283:17-21.

Gills, J.J., Castillo, S.S., Zhang, C., Petukhov, P.A., Memmott, R.M., Hollingshead, M., Warfel, N., Han, J., Kozikowski, A.P., and Dennis,

P.A. (2007) Phosphatidylinositol ether lipid analogues that inhibit AKT also independently activate the stress kinase, p38alpha, through MKK3/6-independent and -dependent mechanisms. J Biol Chem 282:27020-27029.

Gjessing, H.J., Matzen, L.E., Faber, O.K., and Froland, A. (1989) Sensitivity and reproducibility of urinary C-peptide as estimate of islet B-cell function in insulin-treated diabetes. Diabet Med 6:329-333.

Gnecchi, M., and Melo, L.G. (2009) Bone marrow-derived mesenchymal stem cells: isolation, expansion, characterization, viral transduction, and production of conditioned medium. Methods Mol Biol 482:281-294.

Goicoa, S., Alvarez, S., Ricordi, C., Inverardi, L., and Dominguez-Bendala, J. (2006) Sodium butyrate activates genes of early pancreatic development in embryonic stem cells. Cloning Stem Cells 8:140-149.

Grandori, C., Cowley, S.M., James, L.P., and Eisenman, R.N. (2000) The Myc/Max/Mad network and the transcriptional control of cell behavior. Annu Rev Cell Dev Biol 16:653-699.

Grogan, S.P., Olee, T., Hiraoka, K., and Lotz, M.K. (2008) Repression of chondrogenesis through binding of notch signaling proteins HES-1 and HEY-1 to N-box domains in the COL2A1 enhancer site. Arthritis Rheum 58:2754-2763.

Gronthos, S., Franklin, D.M., Leddy, H.A., Robey, P.G., Storms, R.W., and Gimble, J.M. (2001) Surface protein characterization of human adipose tissue-derived stromal cells. J Cell Physiol 189:54-63.

Guarnaccia, C., Pintar, A., and Pongor, S. (2004) Exon 6 of human Jagged-1 encodes an autonomously folding unit. FEBS Lett 574:156-160.

Guillot, P.V., Gotherstrom, C., Chan, J., Kurata, H., and Fisk, N.M. (2007) Human first-trimester fetal MSC express pluripotency markers and grow faster and have longer telomeres than adult MSC. Stem Cells 25:646-654.

Guney, I., and Sedivy, J.M. (2006) Cellular senescence, epigenetic switches and c-Myc. Cell Cycle 5:2319-2323.

Han, J., and Molkentin, J.D. (2000) Regulation of MEF2 by p38 MAPK and its implication in cardiomyocyte biology. Trends Cardiovasc Med 10:19-22.

Hiraoka, K., Grogan, S., Olee, T., and Lotz, M. (2006) Mesenchymal progenitor cells in adult human articular cartilage. Biorheology 43:447-454.

Hosler, B.A., LaRosa, G.J., Grippo, J.F., and Gudas, L.J. (1989) Expression of REX-1, a gene containing zinc finger motifs, is rapidly reduced by retinoic acid in F9 teratocarcinoma cells. Mol Cell Biol 9:5623-5629.

Humphrey, G.W., Wang, Y.H., Hirai, T., Padmanabhan, R., Panchision, D.M., Newell, L.F., McKay, R.D., and Howard, B.H. (2008) Complementary roles for histone deacetylases 1, 2, and 3 in differentiation of pluripotent stem cells. Differentiation 76:348-356.

Igura, K., Zhang, X., Takahashi, K., Mitsuru, A., Yamaguchi, S., and Takashi, T.A. (2004) Isolation and characterization of mesenchymal progenitor cells from chorionic villi of human placenta. Cytotherapy 6:543-553.

Inoue, T., Hammaker, D., Boyle, D.L., and Firestein, G.S. (2005) Regulation of p38 MAPK by MAPK kinases 3 and 6 in fibroblast-like synoviocytes. J Immunol 174:4301-4306.

Jaenisch, R., and Young, R. (2008) Stem cells, the molecular circuitry of pluripotency and nuclear reprogramming. Cell 132:567-582.

Jiang, J., Au, M., Lu, K., Eshpeter, A., Korbutt, G., Fisk, G., and Majumdar, A.S. (2007a) Generation of insulin-producing islet-like clusters from human embryonic stem cells. Stem Cells 25:1940-1953.

Jiang, W., Shi, Y., Zhao, D., Chen, S., Yong, J., Zhang, J., Qing, T., Sun, X., Zhang, P., Ding, M., Li, D., and Deng, H. (2007b) In vitro derivation of functional insulin-producing cells from human embryonic stem cells. Cell Res 17:333-344.

Johnson, G.L., and Lapadat, R. (2002) Mitogen-activated protein kinase pathways mediated by ERK, JNK, and p38 protein kinases. Science 298:1911-1912.

Kang, K.S., Kim, S.W., Oh, Y.H., Yu, J.W., Kim, K.Y., Park, H.K., Song, C.H., and Han, H. (2005) A 37-year-old spinal cord-injured female patient, transplanted of multipotent stem cells from human UC blood, with improved sensory perception and mobility, both functionally and morphologically: a case study. Cytotherapy 7:368-373.

Kawai, M., Mushiake, S., Bessho, K., Murakami, M., Namba, N., Kokubu, C., Michigami, T., and Ozono, K. (2007) Wnt/Lrp/beta-catenin signaling suppresses adipogenesis by inhibiting mutual activation of PPARgamma and C/EBPalpha. Biochem Biophys Res Commun 363:276-282.

Kim, J.D., Faulk, C., and Kim, J. (2007) Retroposition and evolution of the DNA-binding motifs of YY1, YY2 and REX1. Nucleic Acids Res 35:3442-3452.

King, R.W., Jackson, P.K., and Kirschner, M.W. (1994) Mitosis in transition. Cell 79:563-571.

Knoblich, J.A., Sauer, K., Jones, L., Richardson, H., Saint, R., and Lehner, C.F. (1994) Cyclin E controls S phase progression and its down-regulation during Drosophila embryogenesis is required for the arrest of cell proliferation. Cell 77:107-120.

Knoepfler, P.S., Zhang, X.Y., Cheng, P.F., Gafken, P.R., McMahon, S.B., and Eisenman, R.N. (2006) Myc influences global chromatin structure. EMBO J 25:2723-2734.

Kondo, Y. (2009) Epigenetic cross-talk between DNA methylation and histone modifications in human cancers. Yonsei Med J 50:455-463.

Koopman, G., Reutelingsperger, C.P., Kuijten, G.A., Keehnen, R.M., Pals, S.T., and van Oers, M.H. (1994) Annexin V for flow cytometric detection of phosphatidylserine expression on B cells undergoing apoptosis. Blood 84:1415-1420.

Kuma, Y., Sabio, G., Bain, J., Shpiro, N., Marquez, R., and Cuenda, A. (2005) BIRB796 inhibits all p38 MAPK isoforms in vitro and in vivo. J Biol Chem 280:19472-19479.

Kuzmichev, A., Nishioka, K., Erdjument-Bromage, H., Tempst, P., and Reinberg, D. (2002) Histone methyltransferase activity associated with a human multiprotein complex containing the Enhancer of Zeste protein. Genes Dev 16:2893-2905.

Lamoury, F.M., Croitoru-Lamoury, J., and Brew, B.J. (2006) Undifferentiated mouse mesenchymal stem cells spontaneously express neural and stem cell markers Oct-4 and Rex-1. Cytotherapy 8:228-242.

Lazarov, M., Kubo, Y., Cai, T., Dajee, M., Tarutani, M., Lin, Q., Fang, M., Tao, S., Green, C.L., and Khavari, P.A. (2002) CDK4 coexpression

with Ras generates malignant human epidermal tumorigenesis. Nat Med 8:1105-1114.

Le Gurun, S., Martin, D., Formenton, A., Maechler, P., Caille, D., Waeber, G., Meda, P., and Haefliger, J.A. (2003) Connexin-36 contributes to control function of insulin-producing cells. J Biol Chem 278:37690-37697.

Levine, S.S., Weiss, A., Erdjument-Bromage, H., Shao, Z., Tempst, P., and Kingston, R.E. (2002) The core of the polycomb repressive complex is compositionally and functionally conserved in flies and humans. Mol Cell Biol 22:6070-6078.

Li, H., Yu, B., Zhang, Y., Pan, Z., and Xu, W. (2006) Jagged1 protein enhances the differentiation of mesenchymal stem cells into cardiomyocytes. Biochem Biophys Res Commun 341:320-325.

Li, Y.P., Paczesny, S., Lauret, E., Poirault, S., Bordigoni, P., Mekhloufi, F., Hequet, O., Bertrand, Y., Ou-Yang, J.P., Stoltz, J.F., Miossec, P., and Eljaafari, A. (2008) Human mesenchymal stem cells license adult CD34+ hemopoietic progenitor cells to differentiate into regulatory dendritic cells through activation of the Notch pathway. J Immunol 180:1598-1608.

Lumelsky, N., Blondel, O., Laeng, P., Velasco, I., Ravin, R., and McKay, R. (2001) Differentiation of embryonic stem cells to insulin-secreting structures similar to pancreatic islets. Science 292:1389-1394.

Magatti, M., De Munari, S., Vertua, E., Gibelli, L., Wengler, G.S., and
Parolini, O. (2008) Human amnion mesenchyme harbors cells with
allogeneic T-cell suppression and stimulation capabilities. Stem Cells
26:182-192.

Makino, S., Fukuda, K., Miyoshi, S., Konishi, F., Kodama, H., Pan, J., Sano,
M., Takahashi, T., Hori, S., Abe, H., Hata, J., Umezawa, A., and
Ogawa, S. (1999) Cardiomyocytes can be generated from marrow
stromal cells in vitro. J Clin Invest 103:697-705.

Masui, S., Ohtsuka, S., Yagi, R., Takahashi, K., Ko, M.S., and Niwa, H.
(2008) Rex1/Zfp42 is dispensable for pluripotency in mouse ES cells.
BMC Dev Biol 8:45.

Meyer, N., and Penn, L.Z. (2008) Reflecting on 25 years with MYC. Nat Rev
Cancer 8:976-990.

Mfopou, J.K., Chen, B., Sui, L., Sermon, K., and Bouwens, L. (2011) Recent
advances and prospects in the differentiation of pancreatic cells from
human embryonic stem cells. Diabetes 59:2094-2101.

Mittelstadt, P.R., Salvador, J.M., Fornace, A.J., Jr., and Ashwell, J.D. (2005)
Activating p38 MAPK: new tricks for an old kinase. Cell Cycle
4:1189-1192.

Molnar, A., Theodoras, A.M., Zon, L.I., and Kyriakis, J.M. (1997) Cdc42Hs,
but not Rac1, inhibits serum-stimulated cell cycle progression at G1/S

through a mechanism requiring p38/RK. J Biol Chem 272:13229-13235.

Mongan, N.P., Martin, K.M., and Gudas, L.J. (2006) The putative human stem cell marker, Rex-1 (Zfp42): structural classification and expression in normal human epithelial and carcinoma cell cultures. Mol Carcinog 45:887-900.

Moodley, Y., Ilancheran, S., Samuel, C., Vaghjiani, V., Atienza, D., Williams, E.D., Jenkin, G., Wallace, E., Trounson, A., and Manuelpillai, U. Human amnion epithelial cell transplantation abrogates lung fibrosis and augments repair. Am J Respir Crit Care Med 182:643-651.

Morooka, T., and Nishida, E. (1998) Requirement of p38 mitogen-activated protein kinase for neuronal differentiation in PC12 cells. J Biol Chem 273:24285-24288.

Movassat, J., Beattie, G.M., Lopez, A.D., Portha, B., and Hayek, A. (2003) Keratinocyte growth factor and beta-cell differentiation in human fetal pancreatic endocrine precursor cells. Diabetologia 46:822-829.

Murphy, S., Rosli, S., Acharya, R., Mathias, L., Lim, R., Wallace, E., and Jenkin, G. (2011) Amnion epithelial cell isolation and characterization for clinical use. Curr Protoc Stem Cell Biol Chapter 1:Unit 1E 6.

Murray, A.W. (2004) Recycling the cell cycle: cyclins revisited. Cell 116:221-234.

Murtaugh, L.C. (2007) Pancreas and beta-cell development: from the actual to the possible. Development 134:427-438.

Muruganandan, S., Roman, A.A., and Sinal, C.J. (2009) Adipocyte differentiation of bone marrow-derived mesenchymal stem cells: cross talk with the osteoblastogenic program. Cell Mol Life Sci 66:236-253.

Nagai, A., Kim, W.K., Lee, H.J., Jeong, H.S., Kim, K.S., Hong, S.H., Park, I.H., and Kim, S.U. (2007) Multilineage potential of stable human mesenchymal stem cell line derived from fetal marrow. PLoS One 2:e1272.

Nakagawa, M., Oda, Y., Eguchi, T., Aishima, S., Yao, T., Hosoi, F., Basaki, Y., Ono, M., Kuwano, M., Tanaka, M., and Tsuneyoshi, M. (2007) Expression profile of class I histone deacetylases in human cancer tissues. Oncol Rep 18:769-774.

Nebreda, A.R., and Porras, A. (2000) p38 MAP kinases: beyond the stress response. Trends Biochem Sci 25:257-260.

Niessen, H.E., Demmers, J.A., and Voncken, J.W. (2009) Talking to chromatin: post-translational modulation of polycomb group function. Epigenetics Chromatin 2:10.

Nigg, E.A. (1995) Cyclin-dependent protein kinases: key regulators of the eukaryotic cell cycle. Bioessays 17:471-480.

Niwa, H., Miyazaki, J., and Smith, A.G. (2000) Quantitative expression of Oct-3/4 defines differentiation, dedifferentiation or self-renewal of ES cells. Nat Genet 24:372-376.

Obaya, A.J., Mateyak, M.K., and Sedivy, J.M. (1999) Mysterious liaisons: the relationship between c-Myc and the cell cycle. Oncogene 18:2934-2941.

Ogawa, T., Yogo, K., Ishida, N., and Takeya, T. (2003) Synergistic effects of activin and FSH on hyperphosphorylation of Rb and G1/S transition in rat primary granulosa cells. Mol Cell Endocrinol 210:31-38.

Ohtsubo, M., and Roberts, J.M. (1993) Cyclin-dependent regulation of G1 in mammalian fibroblasts. Science 259:1908-1912.

Okamoto, T., Aoyama, T., Nakayama, T., Nakamata, T., Hosaka, T., Nishijo, K., Nakamura, T., Kiyono, T., and Toguchida, J. (2002) Clonal heterogeneity in differentiation potential of immortalized human mesenchymal stem cells. Biochem Biophys Res Commun 295:354-361.

Ono, K., and Han, J. (2000) The p38 signal transduction pathway: activation and function. Cell Signal 12:1-13.

Otto, W.R., and Rao, J. (2004) Tomorrow's skeleton staff: mesenchymal stem cells and the repair of bone and cartilage. Cell Prolif 37:97-110.

Pal, R., Venkataramana, N.K., Bansal, A., Balaraju, S., Jan, M., Chandra, R., Dixit, A., Rauthan, A., Murgod, U., and Totey, S. (2009) Ex vivo-expanded autologous bone marrow-derived mesenchymal stromal cells in human spinal cord injury/paraplegia: a pilot clinical study. Cytotherapy 11:897-911.

Park, J.R., Jung, J.W., Lee, Y.S., and Kang, K.S. (2008) The roles of Wnt antagonists Dkk1 and sFRP4 during adipogenesis of human adipose tissue-derived mesenchymal stem cells. Cell Prolif 41:859-874.

Pearson, G., Robinson, F., Beers Gibson, T., Xu, B.E., Karandikar, M., Berman, K., and Cobb, M.H. (2001) Mitogen-activated protein (MAP) kinase pathways: regulation and physiological functions. Endocr Rev 22:153-183.

Peng, J., Li, W., Li, H., Jia, Y., and Liu, Z. (2009) Inhibition of p38 MAPK facilitates ex vivo expansion of skin epithelial progenitor cells. In Vitro Cell Dev Biol Anim 45:558-565.

Phinney, D.G., and Isakova, I. (2005) Plasticity and therapeutic potential of mesenchymal stem cells in the nervous system. Curr Pharm Des 11:1255-1265.

Pittenger, M., Vanguri, P., Simonetti, D., and Young, R. (2002) Adult mesenchymal stem cells: potential for muscle and tendon regeneration and use in gene therapy. J Musculoskelet Neuronal Interact 2:309-320.

Platt, M.O., Wilder, C.L., Wells, A., Griffith, L.G., and Lauffenburger, D.A. (2009) Multipathway kinase signatures of multipotent stromal cells are predictive for osteogenic differentiation: tissue-specific stem cells. Stem Cells 27:2804-2814.

Prockop, D.J. (1997) Marrow stromal cells as stem cells for nonhematopoietic tissues. Science 276:71-74.

Rahl, P.B., Lin, C.Y., Seila, A.C., Flynn, R.A., McCuine, S., Burge, C.B., Sharp, P.A., and Young, R.A. c-Myc regulates transcriptional pause release. Cell 141:432-445.

Rajasekhar, V.K., and Begemann, M. (2007) Concise review: roles of polycomb group proteins in development and disease: a stem cell perspective. Stem Cells 25:2498-2510.

Ramalho-Santos, M., Yoon, S., Matsuzaki, Y., Mulligan, R.C., and Melton, D.A. (2002) "Stemness": transcriptional profiling of embryonic and adult stem cells. Science 298:597-600.

Roche, S., Richard, M.J., and Favrot, M.C. (2007) Oct-4, Rex-1, and Gata-4 expression in human MSC increase the differentiation efficiency but not hTERT expression. J Cell Biochem 101:271-280.

Rogers, M.B., Hosler, B.A., and Gudas, L.J. (1991) Specific expression of a retinoic acid-regulated, zinc-finger gene, Rex-1, in preimplantation embryos, trophoblast and spermatocytes. Development 113:815-824.

Ross, D.A., Rao, P.K., and Kadesch, T. (2004) Dual roles for the Notch target gene Hes-1 in the differentiation of 3T3-L1 preadipocytes. Mol Cell Biol 24:3505-3513.

Rossant, J. (2008) Stem cells and early lineage development. Cell 132:527-531.

Schieven, G.L. (2005) The biology of p38 kinase: a central role in inflammation. Curr Top Med Chem 5:921-928.

Scotland, K.B., Chen, S., Sylvester, R., and Gudas, L.J. (2009) Analysis of Rex1 (zfp42) function in embryonic stem cell differentiation. Dev Dyn 238:1863-1877.

Selvakumaran, M., Liebermann, D., and Hoffman, B. (1996) The proto-oncogene c-myc blocks myeloid differentiation independently of its target gene ornithine decarboxylase. Blood 88:1248-1255.

Seo, K.W., Lee, S.R., Bhandari, D.R., Roh, K.H., Park, S.B., So, A.Y., Jung, J.W., Seo, M.S., Kang, S.K., Lee, Y.S., and Kang, K.S. (2009) OCT4A contributes to the stemness and multi-potency of human umbilical cord blood-derived multipotent stem cells (hUCB-MSCs). Biochem Biophys Res Commun 384:120-125.

Seo, Y., Yang, S.R., Jee, M.K., Joo, E.K., Roh, K.H., Seo, M.S., Han, T.H., Lee, S.Y., Ryu, P.D., Jung, J.W., Seo, K.W., Kang, S.K., and Kang, K.S. (2011) Human Umbilical Cord Blood-Derived Mesenchymal Stem Cells Protect against Neuronal Cell Death and Ameliorate Motor Deficits in Niemann Pick Type C1 Mice. Cell Transplant.

Serre-Beinier, V., Bosco, D., Zulianello, L., Charollais, A., Caille, D., Charpantier, E., Gauthier, B.R., Diaferia, G.R., Giepmans, B.N., Lupi, R., Marchetti, P., Deng, S., Buhler, L., Berney, T., Cirulli, V., and Meda, P. (2009) Cx36 makes channels coupling human pancreatic beta-cells, and correlates with insulin expression. Hum Mol Genet 18:428-439.

Serup, P., Madsen, O.D., and Mandrup-Poulsen, T. (2001) Islet and stem cell transplantation for treating diabetes. BMJ 322:29-32.

Sherr, C.J., and Roberts, J.M. (1995) Inhibitors of mammalian G1 cyclin-dependent kinases. Genes Dev 9:1149-1163.

Shi, W., Wang, H., Pan, G., Geng, Y., Guo, Y., and Pei, D. (2006) Regulation of the pluripotency marker Rex-1 by Nanog and Sox2. J Biol Chem 281:23319-23325.

Shi, Y., Hou, L., Tang, F., Jiang, W., Wang, P., Ding, M., and Deng, H. (2005) Inducing embryonic stem cells to differentiate into pancreatic beta cells by a novel three-step approach with activin A and all-trans retinoic acid. Stem Cells 23:656-662.

Shi, Y., Lee, J.S., and Galvin, K.M. (1997) Everything you have ever wanted to know about Yin Yang 1. Biochim Biophys Acta 1332:F49-66.

Singh, A.M., and Dalton, S. (2009) The cell cycle and Myc intersect with mechanisms that regulate pluripotency and reprogramming. Cell Stem Cell 5:141-149.

Slingerland, J., and Pagano, M. (2000) Regulation of the cdk inhibitor p27 and its deregulation in cancer. J Cell Physiol 183:10-17.

Soria, B. (2001) In-vitro differentiation of pancreatic beta-cells. Differentiation 68:205-219.

Sridharan, R., Tchieu, J., Mason, M.J., Yachechko, R., Kuoy, E., Horvath, S., Zhou, Q., and Plath, K. (2009) Role of the murine reprogramming factors in the induction of pluripotency. Cell 136:364-377.

Stambolic, V., and Woodgett, J.R. (1994) Mitogen inactivation of glycogen synthase kinase-3 beta in intact cells via serine 9 phosphorylation. Biochem J 303 (Pt 3):701-704.

Steiner, P., Philipp, A., Lukas, J., Godden-Kent, D., Pagano, M., Mittnacht, S., Bartek, J., and Eilers, M. (1995) Identification of a Myc-dependent step during the formation of active G1 cyclin-cdk complexes. EMBO J 14:4814-4826.

Studzinski, G.P. (1989) Oncogenes, growth, and the cell cycle: an overview. Cell Tissue Kinet 22:405-424.

Sulzbacher, S., Schroeder, I.S., Truong, T.T., and Wobus, A.M. (2009) Activin A-induced differentiation of embryonic stem cells into endoderm and pancreatic progenitors-the influence of differentiation factors and culture conditions. Stem Cell Rev 5:159-173.

Sumi, T., Tsuneyoshi, N., Nakatsuji, N., and Suemori, H. (2007) Apoptosis and differentiation of human embryonic stem cells induced by sustained activation of c-Myc. Oncogene 26:5564-5576.

Tai, M.H., Olson, L.K., Madhukar, B.V., Linning, K.D., Van Camp, L., Tsao, M.S., and Trosko, J.E. (2003) Characterization of gap junctional intercellular communication in immortalized human pancreatic ductal epithelial cells with stem cell characteristics. Pancreas 26:e18-26.

Takada, I., Kouzmenko, A.P., and Kato, S. (2009) Wnt and PPARgamma signaling in osteoblastogenesis and adipogenesis. Nat Rev Rheumatol 5:442-447.

Takada, I., Suzawa, M., Matsumoto, K., and Kato, S. (2007) Suppression of PPAR transactivation switches cell fate of bone marrow stem cells from adipocytes into osteoblasts. Ann N Y Acad Sci 1116:182-195.

Takahashi, K., and Yamanaka, S. (2006) Induction of pluripotent stem cells from mouse embryonic and adult fibroblast cultures by defined factors. Cell 126:663-676.

Thompson, J.R., and Gudas, L.J. (2002) Retinoic acid induces parietal endoderm but not primitive endoderm and visceral endoderm differentiation in F9 teratocarcinoma stem cells with a targeted deletion of the Rex-1 (Zfp-42) gene. Mol Cell Endocrinol 195:119-133.

Treutelaar, M.K., Skidmore, J.M., Dias-Leme, C.L., Hara, M., Zhang, L., Simeone, D., Martin, D.M., and Burant, C.F. (2003) Nestin-lineage cells contribute to the microvasculature but not endocrine cells of the islet. Diabetes 52:2503-2512.

Tropel, P., Platet, N., Platel, J.C., Noel, D., Albrieux, M., Benabid, A.L., and Berger, F. (2006) Functional neuronal differentiation of bone marrow-derived mesenchymal stem cells. Stem Cells 24:2868-2876.

Tsai, M.S., Lee, J.L., Chang, Y.J., and Hwang, S.M. (2004) Isolation of human multipotent mesenchymal stem cells from second-trimester amniotic fluid using a novel two-stage culture protocol. Hum Reprod 19:1450-1456.

Uzan, B., Figeac, F., Portha, B., and Movassat, J. (2009) Mechanisms of KGF mediated signaling in pancreatic duct cell proliferation and differentiation. PLoS One 4:e4734.

Valk-Lingbeek, M.E., Bruggeman, S.W., and van Lohuizen, M. (2004) Stem cells and cancer; the polycomb connection. Cell 118:409-418.

van de Wetering, M., Sancho, E., Verweij, C., de Lau, W., Oving, I., Hurlstone, A., van der Horn, K., Batlle, E., Coudreuse, D., Haramis, A.P., Tjon-Pon-Fong, M., Moerer, P., van den Born, M., Soete, G., Pals, S., Eilers, M., Medema, R., and Clevers, H. (2002) The beta-catenin/TCF-4 complex imposes a crypt progenitor phenotype on colorectal cancer cells. Cell 111:241-250.

Vermes, I., Haanen, C., Steffens-Nakken, H., and Reutelingsperger, C. (1995) A novel assay for apoptosis. Flow cytometric detection of phosphatidylserine expression on early apoptotic cells using fluorescein labelled Annexin V. J Immunol Methods 184:39-51.

Wade, P.A. (2001) Transcriptional control at regulatory checkpoints by histone deacetylases: molecular connections between cancer and chromatin. Hum Mol Genet 10:693-698.

Wahren, J., Ekberg, K., Johansson, J., Henriksson, M., Pramanik, A., Johansson, B.L., Rigler, R., and Jornvall, H. (2000) Role of C-peptide in human physiology. Am J Physiol Endocrinol Metab 278:E759-768.

Wang, H.S., Hung, S.C., Peng, S.T., Huang, C.C., Wei, H.M., Guo, Y.J., Fu, Y.S., Lai, M.C., and Chen, C.C. (2004) Mesenchymal stem cells in the Wharton's jelly of the human umbilical cord. Stem Cells 22:1330-1337.

Wang, H.S., Shyu, J.F., Shen, W.S., Hsu, H.C., Chi, T.C., Chen, C.P., Huang, S.W., Shyr, Y.M., Tang, K.T., and Chen, T.H. (2011) Transplantation

of insulin-producing cells derived from umbilical cord stromal mesenchymal stem cells to treat NOD mice. Cell Transplant 20:455-466.

Wang, J., Rao, S., Chu, J., Shen, X., Levasseur, D.N., Theunissen, T.W., and Orkin, S.H. (2006) A protein interaction network for pluripotency of embryonic stem cells. Nature 444:364-368.

Wang, L.G., Liu, X.M., Fang, Y., Dai, W., Chiao, F.B., Puccio, G.M., Feng, J., Liu, D., and Chiao, J.W. (2008) De-repression of the p21 promoter in prostate cancer cells by an isothiocyanate via inhibition of HDACs and c-Myc. Int J Oncol 33:375-380.

Wei, J.P., Zhang, T.S., Kawa, S., Aizawa, T., Ota, M., Akaike, T., Kato, K., Konishi, I., and Nikaido, T. (2003) Human amnion-isolated cells normalize blood glucose in streptozotocin-induced diabetic mice. Cell Transplant 12:545-552.

Wolffe, A.P. (1997) Histones, nucleosomes and the roles of chromatin structure in transcriptional control. Biochem Soc Trans 25:354-358.

Xiong, Y., Hannon, G.J., Zhang, H., Casso, D., Kobayashi, R., and Beach, D. (1993) p21 is a universal inhibitor of cyclin kinases. Nature 366:701-704.

Xu, J., Sylvester, R., Tighe, A.P., Chen, S., and Gudas, L.J. (2008) Transcriptional activation of the suppressor of cytokine signaling-3

(SOCS-3) gene via STAT3 is increased in F9 REX1 (ZFP-42) knockout teratocarcinoma stem cells relative to wild-type cells. J Mol Biol 377:28-46.

Yamashiro, T., Wang, X.P., Li, Z., Oya, S., Aberg, T., Fukunaga, T., Kamioka, H., Speck, N.A., Takano-Yamamoto, T., and Thesleff, I. (2004) Possible roles of Runx1 and Sox9 in incipient intramembranous ossification. J Bone Miner Res 19:1671-1677.

Ye, F., Duvillie, B., and Scharfmann, R. (2005) Fibroblast growth factors 7 and 10 are expressed in the human embryonic pancreatic mesenchyme and promote the proliferation of embryonic pancreatic epithelial cells. Diabetologia 48:277-281.

Zarubin, T., and Han, J. (2005) Activation and signaling of the p38 MAP kinase pathway. Cell Res 15:11-18.

Zhao, Y., and Mazzone, T. (2011) Human cord blood stem cells and the journey to a cure for type 1 diabetes. Autoimmun Rev 10:103-107.

Zhu, P., Martin, E., Mengwasser, J., Schlag, P., Janssen, K.P., and Gottlicher, M. (2004) Induction of HDAC2 expression upon loss of APC in colorectal tumorigenesis. Cancer Cell 5:455-463.

Zornig, M., and Evan, G.I. (1996) Cell cycle: on target with Myc. Curr Biol 6:1553-1556.

Zvaifler, N.J., Marinova-Mutafchieva, L., Adams, G., Edwards, C.J., Moss, J.,
Burger, J.A., and Maini, R.N. (2000) Mesenchymal precursor cells in
the blood of normal individuals. Arthritis Res 2:477-488.

GENERAL CONCLUSION

Adult stem cells are undifferentiated cell found in differentiated tissues; having selfrenewal capacity and can differentiate into different cells/tissunes based on the physiological or environmental conditions. There are different sources of hASCs, scientists have already confirmed the sources of adult stem cells from different tissues like barin, bone-marrow, peripheral blood, blood-vessels, teeth, heart, gut, skeletal muscles, ovarian epithelium, testis as well as umbilical cord/ umbilical cord blood. The current study basically focused on the adult stem cells isolated from human medical wastes e.g. umbilical cord, umbilical cord blood and placenta. These ASCs having unique characteristics of low risk of graft-versus-host-disease (GVHD), lack of related ethical issues as well as obtained from limitless sources.

c-MYC and REX1 are two core transctiption factors having critical role in embryonic stem cells. Here the mechanistic role for cell proliferation and differentiation were studied. On the other hand the possibility for clinical application of hASCs for diabetes mellitus was also performed.

c-MYC knock-down and over-expression studies have confirmed the regulatory role on HDAC2, as well as it is also found that c-MYC can regulate politively on PcG expression via HDAC2. Cell proliferation was deteriorated in c-MYC knocked-down cells and imporoved in over-expressed

cells. Similar result was found in osteogenic and adipogenic differentiation study with c-MYC knocked-down and over-expressing ASCs respectively.

Another transcription factor REX1 knock-down study confirmed that, the expression level of MKK3, which is an activator of p38MAPK in hMSCs. REX1 highly expressing cells have prominent proliferative ability and multipotency than low level of REX1 expressing cells, because of   p38 MAPK suppression in hASCs.

The potential ability for clinical application of of hASC was confirmed by in-vitro differentiation   into insulin producing cells with in a week both in tranciptional as well as translational level. Glucose stimulation test confirmed their functional ability of the hASCs. Thus, it can be concluded that hASCs have potentiality for clinical application. Further study is needed for confirmation.

국문 초록

성체줄기세포의 분화와 증식에관한 c-MYC 과 REX1 의

분자 생물학적 메커니즘 연구

서울대학교 대학원

수의학과 수의공중보건학 전공

Dilli Ram Bhandari

(지도교수 : 강 경 선)

전사인자인 c-MYC 과 REX1 은 배아 줄기세포에서 표지 유전자로 사료된다. 이들 유전자는 중간엽유래를 포함한 줄기세포에서 세포의 증식, 분화 및 변이 등 다양한 기능을 가지고 있다. 본인은 중간엽유래 줄기세포에서 c-MYC 의 histon 조절과 REX1 의 p38 MAPK 신호전달에 관련한 분자생물학적 기전 연구를 수행 하였다. c-MYC 과 REX1 의

유전자 발현저하 실험을 위해 lentivirus 를 사용하였으며, c-MYC 의 유전자 증강발현을 위해 역시 lentivirus 를 매개로 이용하였다. c-MYC 발현이 저하된 세포는 세포 증식과 분화가 현저하게 저하 되었으며, c-MYC 증강발현 시 개선 되었다. REX1 발현저하 세포는 c-MYC 과 유사하게 증식이 억제 되었으나, 지방분화는 증가 하였다. 반면, 골분화 세포는 현저하게 감소 하였다. RT-PCR 과 western blot 결과 c-MYC 의 HDAC2 와 PcG 유전자간의 조절역할이 규명 되었으며, REX1 연구에서는 REX1 과 p38 MAPK 의 상위 조절인자인 MKK3 의 반비례 발현이 규명 되었다. 최종적으로, 이들 유전자가 사람 중간엽유래 줄기세포의 증식과 분화에 결정적인 역할을 하는 것으로 확인 되었다. 염색체 면역 침강 실험에서는 c-MYC 이 HDAC2 에 그리고 REX1 이 MKK3 에 직접 결합하는 것을 확인 할 수 있었다. 이 연구로부터, 사람의 성체줄기 세포에서 c-MYC 은 염색체 조절을 통하여 세포증식 및 분화에 관여한다는 사실과 REX1 은 p38 MAPK 신호전달을 통하여 유사한 역할을 한다는 것을 확인할 수 있었다.

주요단어 : c-MYC, 분화, HDAC2, 증식, REX1, 줄기세포

학번 : 2007-30701